

Performance Limits and Robustness Issues in the Control of Flexible Link Manipulators

by

Carlos Eduardo Padilla Santos

B.S.E Princeton University (1986)

S.M. Massachusetts Institute of Technology (1989)


SUBMITTED TO THE DEPARTMENT OF
AERONAUTICS AND ASTRONAUTICS
IN PARTIAL FULFILLMENT OF THE REQUIREMENTS
FOR THE DEGREE OF
Doctor of Philosophy

at the

Massachusetts Institute of Technology

June, 1992

© Massachusetts Institute of Technology, 1992. All rights reserved.

Signature of Author _____
 Department of Aeronautics and Astronautics
May 18, 1992

Certified by _____
Professor Andreas H. von Flotow
Thesis Committee Chairman, Department of Aeronautics and Astronautics

Certified by _____
Professor Jean-Jacques E. Slotine
Department of Mechanical Engineering

Certified by _____
Professor Harold L. Alexander
Department of Aeronautics and Astronautics

Certified by _____
Professor Edward F. Crawley
Department of Aeronautics and Astronautics

Accepted by _____
Professor Harold Y. Wachman
Chairman, Department Graduate Committee

Aero
MASSACHUSETTS INSTITUTE
OF TECHNOLOGY

JUN 05 1992

LIBRARY

Performance Limits and Robustness Issues in the Control of Flexible Link Manipulators

by

Carlos Eduardo Padilla Santos

SUBMITTED TO THE DEPARTMENT OF AERONAUTICS AND ASTRONAUTICS
ON MAY 18, 1992, IN PARTIAL FULFILLMENT OF THE
REQUIREMENTS FOR THE DEGREE OF
DOCTOR OF PHILOSOPHY

In this thesis we consider fundamental principles and tradeoffs involved in the control of manipulators with distributed (structural) flexibility. In particular, we consider the end-point (angular) position control of flexible manipulators with joint actuation. The resulting nonlinear system exhibits a fundamental characteristic that has been termed nonminimum phase behavior in analogy with the terminology used for linear systems. This nonminimum phase character of the nonlinear system fundamentally limits the types of controllers that can be implemented, as well as the achievable performance. It is one of the main contributions of this thesis that an appropriate transient performance measure for nonlinear systems is defined which quantifies the limits on transient performance due to nonminimum phase characteristics. In addition, limits on the achievable benefits of feedback control are extended to the nonlinear setting and demonstrated with the feedback control of a two link flexible manipulator.

A very fundamental result for the control of flexible manipulators is the global asymptotic stability under independent joint proportional plus derivative (PD) control. A proof of this result using the full generality of the nonlinear partial differential equations of motion is presented here for the first time in the literature. Local exponential stability results are presented using full state feedback. By their local nature, these results are less robust. A quantitative analysis of the *local* character serves to highlight the tradeoffs between performance and robustness.

The transient performance measure is defined within the context of the nonlinear output regulation theory. This theory also helps to clearly elucidate the tradeoffs between the feedforward and the feedback control of flexible manipulators. After an extensive search of the current literature on the inverse dynamics and feedforward control of flexible manipulators, it is concluded that the nonlinear output regulation theory offers the best prospects for practical, high-performance control of nonminimum phase flexible manipulator systems in general.

Simulation results of a two-flexible-link manipulator are presented using the nonlinear output regulation theory. To the best of our knowledge, this constitutes the

first time that such a controller has been demonstrated for a two link manipulator with flexible links. For the feedforward controller, the regulator equations are solved using simplified models of the dynamics equations: linearized about the equilibrium; and nonlinear in rigid body coordinates and rates, but linear in flexible deformation coordinates and rates. Simulation results are surprisingly good for systems where the elastic deformations are required to remain small. This indicates both the robustness of the scheme and its practicality in the face of drastic design model simplifications. For the independently designed feedback controller, both the globally asymptotically stable robust controller and the locally exponentially stable controller are presented.

Thesis Committee: Professor Andreas H. von Flotow
Associate Professor of Aeronautics and Astronautics
Professor Jean-Jacques E. Slotine
Department of Mechanical Engineering
Professor Harold L. Alexander
Department of Aeronautics and Astronautics
Professor Edward F. Crawley
Department of Aeronautics and Astronautics

Acknowledgements

It has been a pleasure and a privilege to have worked with Prof. Andy von Flotow. His unerring intuition, quick insight, and solid hold on reality have been a source of inspiration, frustration, and, ultimately, of knowledge. My thanks go to the other members of my committee, who to varying degrees have left their mark on this work. I would like to thank Prof. Slotine in particular, for having supported me in my fledgling theoretical endeavors.

I would like to thank all my friends who have made my time in school enjoyable and memorable. I look forward to many more years of sowing the seeds and reaping the fruits of enduring friendships.

I would not have been able to endure all these years without the love and support of my family. My mother's prayers, my father's advice, my brother's encouragement and enthusiasm, and my sister's happiness. To my wife to be, Amy, I owe my sanity and my perspective, not to mention quite a bit of editing. I cannot express how deeply indebted I am for your love, patience, and unyielding faith.

I dedicate this thesis to my father, Eduardo Padilla:

Papi, te dedico esta tesis con todo mi amor por todo el apoyo y el cariño que tú me has dado durante estos veintiocho años de mi vida. Todo lo que he logrado hasta hoy se los debo a ustedes. Espero que sigamos creciendo siempre juntos en nuestro amor y nuestra fé y que sigamos más unidos que nunca.

Contents

1	Introduction	15
1.1	Open Issues in Flexible Manipulator Control	16
1.2	Thesis Outline	20
2	Dynamics	23
2.1	Manipulator with One Flexible Link	23
2.1.1	Exact Formulation—Undamped Beam	23
2.1.2	Approximate Formulation	28
2.2	Manipulators with Multiple Flexible Links	30
2.2.1	General Form of the Equations of Motion	30
2.2.2	Equations of Motion for Flexible-Link Manipulators	31
3	Nonminimum Phase Systems and Limits of Feedback Performance	35
3.1	Linear Systems	35
3.1.1	Sensitivity Theory	35
3.1.2	Structure of the Feedback System	36
3.1.3	Nonminimum Phase Systems	42
3.2	Nonlinear Systems	50
3.2.1	Zero Dynamics	53
4	Inverse Dynamics and Feedforward Control	57
4.1	Nonlinear Feedback Linearization	58
4.2	Inverse Dynamics Problem	61
4.2.1	Chains of Rigid Bodies	61

4.2.2	Chains of Flexible Bodies	62
4.2.3	Summary	70
5	Output Regulation Theory and Limits of Performance	73
5.1	Output Regulation Theory	74
5.1.1	Linear Regulator Theory	77
5.1.2	Nonlinear Output Regulation Theory	79
5.2	Performance Measure	83
5.2.1	Stability of the Center Manifold	84
5.2.2	Frequency Domain Heuristics	86
5.2.3	On the Local Nature of Results	87
5.3	Application to Flexible Robotics	89
5.3.1	Joint Actuation	90
5.3.2	Other Actuators	98
6	Robustness vs. Performance in Feedback Control	101
6.1	Mathematical Preliminaries	101
6.1.1	Dynamical Systems in Banach Spaces	103
6.1.2	An Invariance Principle	103
6.2	Joint PD Control	107
6.2.1	One Flexible Link Arm	107
6.2.2	Manipulators with Multiple Flexible Links	116
6.3	Full State Feedback	116
6.3.1	Trajectory Tracking	116
6.3.2	Higher Performance Feedback Control	117
7	Control of a Two Link Manipulator with Flexible Links	121
7.1	Output Regulation Control of the Two-Flexible-Link Arm	122
7.1.1	Set-point Regulation	124
7.1.2	Sinusoidal Exosystem	128
7.2	MIMO Sensitivity Analysis	136

7.3	Some Practical Considerations	140
8	Conclusions	147
8.1	Recommendations for Future Work	151
A	Some Results from Center Manifold Theory	153
A.1	Preliminaries	153
A.2	Existence of a Center Manifold	154
A.3	Stability of the Center Manifold	155
A.4	Reduction Principle	156
A.5	Approximation of the Center Manifold	156
B	Gronwall's Inequality	159
C	Cantilevered-Loaded Mode Shapes	161
C.1	Code Listing	163
D	Solution of the Nonlinear Regulator Equations via Polynomial Ex-	
	pansion	169
D.1	Code Listing	169
	References	179

List of Figures

2.1	Single Flexible Link Arm	24
2.2	Manipulator with Two Flexible Links	32
3.1	Definitions for Feedback Control Theory	36
3.2	Single Degree of Freedom Feedback Configuration	37
3.3	Two Degree of Freedom Feedback Configuration	39
4.1	Feedback Linearization — Original System	60
4.2	Feedback Linearization — Transformed System	60
4.3	Feedforward Inversion Control	71
5.1	Output Regulation Control	82
5.2	Output of One-flexible-link Arm: Set Point Regulation; $\mu = 1 \times 10^{-7}$	94
5.3	Output of One-flexible-link Arm: Sinusoidal Regulation; $\mu = 1 \times 10^{-7}$, A = 45°, $\omega = 6$ r/s.	96
5.4	Output of One-flexible-link Arm: Sinusoidal Regulation; $\mu = 1 \times 10^{-7}$, A = 5°, $\omega = 60$ r/s.	97
5.5	Output of One-flexible-link Arm: Set Point Regulation; $\mu = 1 \times 10^{-5}$	100
7.1	Output of Two-flexible-link Arm: Set-point Regulation; Independent Joint PD; $\mu = 1 \times 10^{-6}$	127
7.2	Output of Two-flexible-link Arm: Set-point Regulation; Independent Joint PD; $\mu = 1 \times 10^{-4}$	128
7.3	Output of Two-flexible-link Arm: Set-point Regulation; $\mu = 1 \times 10^{-4}$	130
7.4	Output of Two-flexible-link Arm: Sinusoidal Regulation; $\mu = 1 \times 10^{-4}$	132

7.5	Output of Two-flexible-link Arm: Sinusoidal Regulation; $\mu = 1 \times 10^{-4}$.	133
7.6	Output of Two-flexible-link Arm: Sinusoidal Regulation; $\mu = 1 \times 10^{-4}$.	134
7.7	Output of Two-flexible-link Arm: Sinusoidal Regulation; $\mu = 0.1$.	135
7.8	Output of Two-flexible-link Arm: Sinusoidal Regulation; $\mu = 1 \times 10^{-4}$.	136
7.9	Definition of MIMO Sensitivity Transfer Function	137
7.10	SISO Sensitivity Plots: $\mu = 1 \times 10^{-4}$.	139
7.11	MIMO Sensitivity Plot: $\mu = 1 \times 10^{-4}$.	140
7.12	MIMO Sensitivity Plot: $\mu = 1 \times 10^{-8}$.	141
7.13	Sinusoidal Output Disturbance: $\mu = 1 \times 10^{-4}$.	142
7.14	Sinusoidal Output Disturbance: $\mu = 1 \times 10^{-4}$.	143
7.15	Open Loop Sinusoidal Output Disturbance: $\mu = 1 \times 10^{-4}$.	144
7.16	MIMO Sensitivity Plot: $\mu = 1 \times 10^{-2}$.	145
7.17	Sinusoidal Output Disturbance: $\mu = 1 \times 10^{-2}$.	146
C.1	Cantilevered-Loaded Beam	161

List of Tables

5.1	Parameters for the One-flexible-link Manipulator	91
5.2	Open Loop Poles and Zeros for the One-flexible-link Manipulator . .	91
5.3	Closed-Loop Poles for the One-flexible-link Manipulator; $\mu = 1 \times 10^{-7}$.	92
5.4	Closed-Loop Poles for the One-flexible-link Manipulator; $\mu = 1 \times 10^{-5}$.	99
7.1	Parameters for the Two-flexible-link Manipulator: Link 1	123
7.2	Parameters for the Two-flexible-link Manipulator: Link 2	123
7.3	Open Loop Poles for the Two-flexible-link Manipulator	124
7.4	Open Loop Zeros for the Two-flexible-link Manipulator	124
7.5	Closed-Loop Poles for the Two-flexible-link Manipulator; $\mu = 1 \times 10^{-4}$.	129

Chapter 1

Introduction

The reasons for the study of manipulators with flexibility are manifold. For industrial earth-bound robots, light-weight manipulators with reduced arm to payload weight ratios would result in higher performance and in safer workplaces. Higher speeds and lightweight manipulators inevitably result in joint compliance and link flexibility becoming significant effects. For large, space-based manipulators required to handle massive payloads the flexibility of the manipulator effectively sets the performance limits. As an example, the shuttle remote manipulator system (SRMS) has its lowest natural frequency, with joints locked, between 0.04 and 0.4 Hz, depending on the payload [51, 63]. For this reason, joint speeds cannot exceed about 6 deg/min [74] at maximum loading.

End-point control of a one-link flexible manipulator was first suggested in Ref. [19]. In Ref. [78] the benefits of end-point control are described in detail, and the results of implementing such a control on an experimental one-flexible-link arm are demonstrated: a bandwidth four times higher than that achievable with a standard joint PID controller was achieved. This was done assuming a linear model and solving the H_2 control problem (LQR or LQG). For a two-link manipulator with compliant drives a similar result has been shown in Ref. [40]. In this case, an LQR/Constant-Gain-Extended-Kalman-Filter (LQR/CGEKF) controller was implemented using results [77] that show under certain conditions a suitable linear plant can be found such that the regulator and estimator gains obtained from solving this linear problem

will stabilize the nonlinear plant. This *suitable* linear plant is found by Hollars [40] through Monte Carlo search.

The work of Hollars is extended by Uhlik [89] through the use of nonlinear feedback input/output linearization and gain/scheduled LQR/CGEKF for a two-link manipulator with joint compliance. Celia Oakley [64] extends some of these results to the control of a two-link flexible manipulator. In particular, she implements tracking control through the use of an LQR-based feedback controller designed using the linearization of the plant about an equilibrium configuration.

The control of manipulators with joint and distributed link flexibility has been the subject of much research in recent years. An explosion of papers of a highly theoretical nature has unfortunately not been followed by more practical results. As a consequence, there has been a widening gap between theoretical results and engineering applications to real manipulators. It is one of the main aims of this work to aid in the bridging of this gap by marrying theory to practical engineering considerations.

1.1 Open Issues in Flexible Manipulator Control

The following are some of the unresolved issues in the control of manipulators with distributed link flexibility. Invariably, the control designer for practical systems must confront the modelling problem. Systems with distributed parameters have corresponding mathematical models that are infinite dimensional. In particular, the system description involves partial differential equations whose solution is much more complex than the more desirable ordinary differential equations. While for some distributed linear systems the mathematical tools exist to deal analytically with some problems of stability [61], and even control synthesis [75, 6], the problem becomes much more intractable when we consider nonlinear systems [91].

For this reason, engineers turn to assumed modes [60] or finite element formulations [46] in order to discretize the system and thus obtain a finite number of ordinary differential equations. The order of the approximate finite order system, and in the

case of assumed modes, the choice of mode shapes that yield an accurate representation of the actual system, seem to depend both on the system and on the control task. The selection of these for a given system and task is still mostly a trial and error process and is thus an open issue in manipulator control.

The next important issue, and one that is most easily understood in the case of linear plants, is the nonminimum phase issue. It has been known for some time [14,41] that linear plants with nonminimum phase zeros exhibit limitations on the achievable performance. In particular, it has more recently been shown [33] that nonminimum phase zeros limit the ability of a controller to shape the sensitivity function. Generally speaking, this limits the bandwidth of a feedback controller to be well below the frequency of the first nonminimum phase zero in the plant. The reason this is a concern in flexible manipulator control is that the transfer function from joint torque input to tip position output of the linearized system is nonminimum phase. Thus these results from the linear theory place ultimate bandwidth limitations on any closed-loop control.

The performance bounds derived in the single-input single-output (SISO) case from sensitivity theory (see Chapter 3) are a direct consequence of properties of linear time-invariant systems: properties of analytic functions lead to Bode gain-phase type relations through complex variable theory. All of these properties are extended to distributed, unstable, multi-input multi-output (MIMO) systems by Boyd and Desoer [15] through the use of subharmonic functions. In the MIMO case, we are concerned with nonminimum phase transmission zeros in particular. Kwakernaak and Sivan [52] point out that a regulator cannot achieve perfect tracking if the plant has nonminimum phase zeros, in the context of linear-quadratic regulator (LQR) optimal control. (Recall that state feedback cannot change zero locations.) More generally, Cheng and Desoer [21] show that for a two degree-of-freedom configuration linear system (see Fig. 3.3) which could be distributed, if the closed-loop system is exponentially stable, every zero in the closed right-half plane is necessarily a zero of the closed-loop transfer function from input to output.

The concept of a nonminimum phase system has been extended to the nonlinear

case. A system with relative degree less than its order will exhibit internal dynamics. If the output is constrained to be zero for all time, the internal dynamics that results are termed the zero dynamics. It turns out that for the control of the tip of a flexible manipulator, using only joint actuation, the zero dynamics are unstable. This is the nonlinear equivalent of the notion of a nonminimum phase zero. In the literature, the study of the stability of the zero dynamics has been used mostly in relation to finding solution to the inverse dynamics problem. The reader is referred to Chapter 4 for a detailed discussion.

The undesirable characteristics of nonminimum phase systems have prompted researchers to try to find ways to circumvent this stumbling block. Park and Asada [72] use a cable transmission mechanism to change the torque along the beam. This results in the transfer function from torque to tip position being minimum phase over a wider frequency range as the torque location approaches the tip. Wang and Vidyasagar [92] propose a redefinition of the output that results in a system with a well-defined relative degree (they note that the standard *arc-length* output for the one flexible link system has an ill-defined relative degree as the number of modes increases). The new output function, which consists of the difference between the arc-length due to the rigid body hub angle and the tip deflection in the moving frame, is minimum phase for the number of modes considered (three). Furthermore, in some instances the new transfer function is passive, depending on the ratio of beam inertia to hub inertia. In this case, they point out, it is possible to invoke the Passivity Theorem [81] in order to stabilize the system through the use of a strictly passive, finite gain controller which can be model independent.

In the context of large space structures (LSS), Williams [94] suggests the use of low authority control (LAC) utilizing a different sensor/actuator set than that reserved for high authority control (HAC). In this way, the zero locations can be set with the LAC portion of the control scheme and then the HAC strategy can proceed with a new set of zeros. This is possible because the LAC strategy is not equivalent to state feedback, as far as the HAC portion is concerned, since it uses a different set of actuators and sensors.

An issue of concern when developing model-based control schemes is that of parameter uncertainty. This issue has been resolved satisfactorily for the tracking control of rigid manipulators through the use of Sliding Controllers and Adaptive Controllers [81]. Similar results have been extended to manipulators with flexible joints and even to linear flexible structures. Lozano-Leal and Brogliato [55] use adaptive control on manipulators with flexible joints. Global asymptotic stability is assured regardless of joint stiffness value. The approach is similar to that of Slotine and Li [81]. The passivity properties of manipulators with flexible joints are exploited. Elmali and Olgac [29] investigate robust output tracking of nonlinear MIMO systems via sliding mode control. Kao and Sinha [50] present a sliding mode control solution to the control of vibration in flexible structures using estimated states. To our knowledge, similar results have not been extended to manipulators with multiple flexible links.

Finally, there is the practical engineering issue of what kinds of simplifications are possible in the control design when a manipulator is limited to *slow enough* maneuvers. This leads to questions of model simplifications [68, 71, 65] as well as to issues of controller simplification. On the controller side, spectral separation arguments (whereby the system is split into slow and fast subsystems that can be controlled separately) are appealing, while on the modelling side the correct choice of *slow* and *fast* variables could influence the effectiveness of the controller.

Some work has been carried out along these lines in the fields of singular perturbation and integral manifold control [86, 80, 79]. The basic philosophy is to control the slow variables separately after the fast variables, treated as a perturbation, have decayed to the slow manifold. The success of the approach in every case depends on the slow variables being slow enough. In practice, this means keeping the bandwidth of the controller well below the first flexible modal frequency. Comparatively good results are obtained when feedforward terms are added to the slow control. This is not surprising, especially when the controller schemes are compared to LQR-based feedback controllers that do not include feedforward terms, as in Ref. [79].

In this work we delve into the fundamental principles and tradeoffs involved in flex-

ible manipulator control. In the process, we succeed in bringing flexible manipulator control within the grasp of the classical theories for an important class of systems in which flexible deformations remain small. In so doing we provide formal justification for what has been commonly carried out in an *ad hoc* manner in the interest of practical implementations. Moreover, we provide clear and in many instances quantifiable descriptions of the fundamental tradeoffs between feedback control and feedforward control; and between global robust control and local high performance control in a nonlinear context.

We have tried to harvest from the more theoretical results practical fruits that enhance our understanding of the control of flexible link manipulators. For this purpose we have identified from the nonlinear topological control field a *transient performance measure* that evidences the fundamental performance limits due to the nonminimum phase nature of our system. Empowered and emboldened this way, we have conjectured that locally linear sensitivity theory limits also apply in our nonlinear setting. In the final analysis, we test our results with the simulated control of a two-flexible-link arm.

1.2 Thesis Outline

In Chapter 2 we derive the nonlinear partial differential equations of motion for a planar one-link manipulator attached to a rotating base with mass and inertia and with end-effector mass and inertia. The most general form of the equations contains Rayleigh damping as well as foreshortening effects. To our knowledge, this is the first time these equations have been presented. These equations are discretized in space using an assumed modes procedure. The form of the equations of motion of general multibody chains in discretized form is then given, and from these we specialize to the equation of motion of a two-link manipulator to be used for control design and evaluation in later chapters.

In Chapter 3 we delve into the linear sensitivity theory, both for classical and multivariable settings. Specifically, we investigate the limits on performance and

the achievable benefits of feedback imposed by nonminimum phase characteristics on linear systems. It turns out that these represent fundamental limits for nonlinear nonminimum phase systems as well. The chapter concludes with extensions of the concepts of zero and nonminimum phase systems to the nonlinear multivariable case.

In Chapter 4 we examine the state of the art in inverse dynamics and feedforward control of flexible manipulators. After some background on nonlinear control theory, we examine the relative merits and drawbacks of schemes proposed in the recent literature. We draw some conclusions which lead naturally to the consideration of the developments in Chapter 5.

In Chapter 5 we introduce in detail the nonlinear output regulation theory. This theory provides a framework within which we can clearly elucidate the tradeoffs between feedback and feedforward control. Furthermore, it is within this framework that we identify and define a *performance* measure for nonlinear finite dimensional systems. With this performance measure we are able to examine fundamental limits to the achievable performance of flexible link manipulators with joint actuation and tip sensing. Illustrations are made with a one-flexible-link example, and it is pointed out how the results are not limited to finite dimensional systems.

Chapter 6 is the most theoretical of the chapters. In it we provide a proof of the global asymptotic stability of a one link flexible arm under joint PD control. This fundamental and perhaps intuitive result is carried out for the nonlinear partial differential equations developed in Chapter 2. To our knowledge this is the first time such a result has been presented. The chapter continues with proofs of locally exponentially stable joint tracking control using full state feedback. More than anything, these results on joint tracking serve to point out the limit of achievable globally stable controls through the use of feedback inversion techniques of the type presented in Chapter 4. We then explore the tradeoff between loss of robustness and globality when compared to the PD case on the one side, vs. the increased local performance. Finally, suggestions are made as to how to extend these results to the multiple link case.

In Chapter 7 we bring the results and insights of the previous chapters into focus

by considering the control of a two flexible link manipulator. In the first part of the chapter we implement a controller based on the results of the output regulation theory. We solve the regulator equations for the feedforward control and the steady state manifold, which we use as part of the feedback control. We then implement various feedback schemes to elucidate the themes of robustness vs. performance. In the last part we revisit the fundamental limitations to the achievable benefits of feedback through sensitivity analysis of the nonlinear system.

Chapter 2

Dynamics

2.1 Manipulator with One Flexible Link

In this section we develop the equations of motion for the system depicted in Fig. 2.1. The system consists of: a rigid hub which is free to rotate in the plane; a flexible link attached to the hub in a cantilevered way; and, a tip mass with inertia attached to the tip of the flexible link, also in a cantilevered way. This system represents one of the simplest *manipulators* which exhibit both distributed flexibility and nonlinear dynamic and kinematic behavior.

In what follows, we shall derive both exact and approximate equations of motion for the one-flexible-link manipulator. We will also consider the cases where the flexible link does and does not exhibit material damping.

2.1.1 Exact Formulation—Undamped Beam

It will be convenient for the developments in later chapters to refer to the system's kinetic and potential energies. For this reason, we subscribe to a Lagrangian approach in order to determine the system's equations of motion. We will, in effect, make use of Hamilton's Principle [73]. Because at this point we are only interested in deriving equations of motion, we do not need to concern ourselves with the difference between

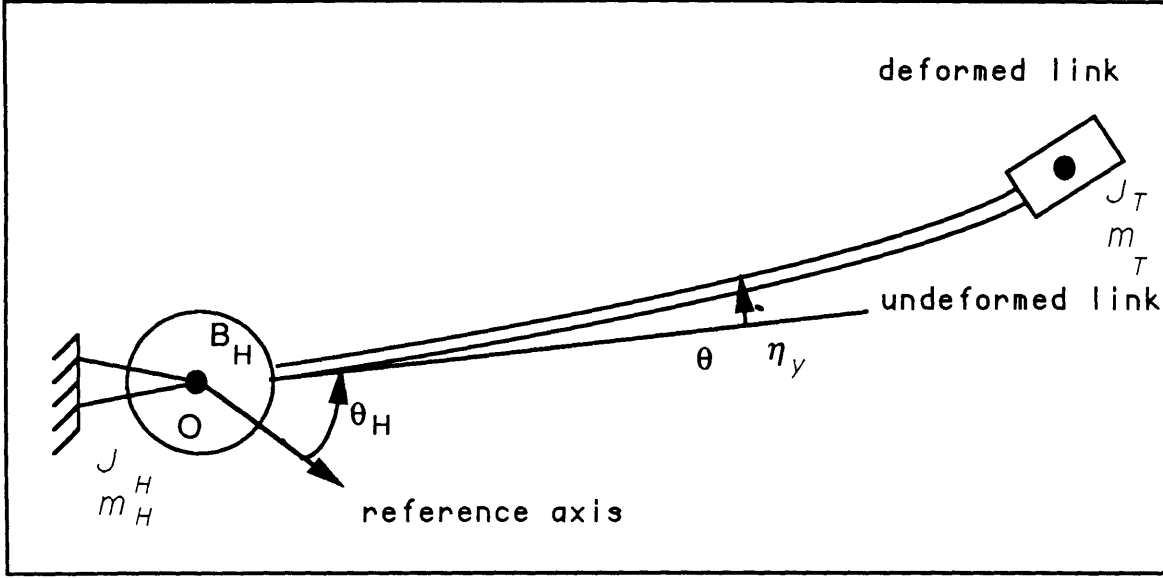


Figure 2.1: Single Flexible Link Arm

Hamilton's Principle and Hamilton's Law. The interested reader is referred to [4] for a thorough discussion of this topic.

Kinetic and Potential Energies

Referring to Fig. 2.1, we can immediately write down the kinetic energy of the one flexible link arm as

$$\begin{aligned}
 T &= \frac{1}{2} J_H \dot{\theta}_H^2(t) + \frac{1}{2} m_T \left\| {}^N \mathbf{v}^T \right\|_2^2 + \frac{1}{2} J_T (\dot{\theta}_H(t) + \dot{\eta}'_y(l, t))^2 \\
 &+ \frac{1}{2} \int_0^l \rho (\dot{\eta}_x(x, t) - \dot{\theta}_H(t) \eta_y(x, t))^2 dx \\
 &+ \frac{1}{2} \int_0^l \rho (\dot{\eta}_y(x, t) + \dot{\theta}_H(t) (x + b_H + \eta_x(x, t)))^2 dx \quad (2.1)
 \end{aligned}$$

where

$$\begin{aligned}
 {}^N \mathbf{v}^T &= {}^H \mathbf{v}^T + {}^N \boldsymbol{\omega}^H \times \mathbf{p}^{OT} \\
 &= \left[\dot{\eta}_x(l, t) - \dot{\theta}_H(t) (\eta_y(l, t) + b_T \sin \beta(t)) \right] \hat{\mathbf{a}}_1 \\
 &\quad + \left[\dot{\eta}_y(l, t) + \dot{\theta}_H(t) (b_H + l + \eta_x(l, t) + b_T \cos \beta(t)) \right] \hat{\mathbf{a}}_2 \\
 \beta(t) &= \eta'_y(l, t).
 \end{aligned}$$

As is customary, the following convention has been used $\partial(\cdot)/\partial \mathbf{x} = (\cdot)'$ and $\partial(\cdot)/\partial t = (\cdot)\dot{}$. The constants J_H , m_T , and J_T represent, respectively, the moment

of inertia of the hub body, and the mass and the moment of inertia of the tip body. The mass per unit length of the beam is given by ρ . The constant length b_H is the distance between the hinge axis in the hub body, represented in Fig. 2.1 as the point O , and the point of attachment of the link to the hub. Notice that we are assuming that the hinge point O coincides with the center of mass of the hub body. On the tip body, b_T is the distance between the point of attachment of the tip body to the link and the center of mass of the tip body along the extension of the beams' neutral axis.

Following the notation established by Kane in [47], the vector ${}^N\mathbf{v}^T$ represents the velocity of the point T in the inertial reference frame. The vector ${}^H\mathbf{v}^T$ is the velocity of T with respect to the reference frame attached to the hub and represented by the orthogonal unit vectors $\{\hat{\mathbf{a}}_1, \hat{\mathbf{a}}_2\}$. The vector ${}^N\boldsymbol{\omega}^H$ is the angular velocity of the body-fixed frame $\{\hat{\mathbf{a}}_1, \hat{\mathbf{a}}_2\}$ with respect to the inertial frame; \mathbf{p}^{OT} is the distance vector between the hinge point O and the point T . Finally, the time-varying quantities $\theta_H(t)$, $\eta_x(x, t)$, $\eta_y(x, t)$ represent, respectively, the angular position of the hub-attached frame with respect to the inertial frame, and the link deflections in the $\hat{\mathbf{a}}_1$ (x -) direction and in the $\hat{\mathbf{a}}_2$ (y -) direction.

If we now further assume the link can be modelled as an undamped Bernoulli-Euler beam [87], the potential energy can be written as

$$V = \frac{1}{2} \int_0^l EI (\eta_y''(x, t))^2 dx + \frac{1}{2} \int_0^l EA (\eta_x'(x, t))^2 dx \quad (2.2)$$

The quantities EI and EA , assumed constant for simplicity, represent the flexural rigidity and the axial stiffness of the beam, respectively.

Correct Linearization

We are ultimately interested in deriving exact nonlinear equations of motion for the system of Fig. 2.1, which are nonetheless linearized with respect to the (expected) small elastic deflections. In order to do this properly, we must have the correct energy expressions at least to second order in the small quantities (see for example Ref. [68, Appendix A]). Eqs. 2.1 and 2.2 are actually exact, for a Bernoulli-Euler

beam. However, for simplicity, we would like to ignore axial extensions of the beam since these are negligible in comparison to bending deflections.

In order to do this properly, however, we must take into account the correct nonlinear strain-displacement relations [71, 49] in the formulation of the energy expressions. This is so because the axial extensions are not independent and in fact depend on the transverse displacement in a nonlinear way. In fact

$$\eta_x(x, t) = - \int_0^x \frac{1}{2} \left(\frac{\partial \eta_y(\sigma, t)}{\partial \sigma} \right)^2 d\sigma.$$

Equations of Motion

Substituting for $\eta_x(x, t)$ using the relation given above, and proceeding with Hamilton's Principle, we obtain the equations of motion for our system: nonlinear in rigid body motions, but linear in small elastic deflections.

$$\begin{aligned} J_H \ddot{\theta}_H(t) + \int_0^l \rho \left[(x + b_H)(\ddot{\eta}_y(x, t) + (x + b_H)\ddot{\theta}_H(t)) \right] dx \\ + m_T \left[(b_H + l + b_T)(\ddot{\eta}_y(x, t) + (b_H + l + b_T)\ddot{\theta}_H(t)) \right] \\ + J_T(\ddot{\theta}_H(t) + \ddot{\beta}(t)) = \tau(t) \end{aligned} \quad (2.3)$$

$$\begin{aligned} EI \eta_y''''(x, t) + \rho \ddot{\eta}_y(x, t) + \rho(x + b_H)\ddot{\theta}_H(t) \\ - \rho \dot{\theta}_H^2(t) \left(\eta_y(x, t) - (x + b_H)\eta_y'(x, t) + \left(\frac{x^2}{2} + b_H x + b_H + \frac{1}{2} \right) \eta_y''(x, t) \right) \\ - m_T \dot{\theta}_H^2(t)(b_H + l + b_T)\eta_y''(x, t) = 0 \end{aligned} \quad (2.4)$$

$$\begin{aligned} m_T \dot{\theta}_H^2(t)\eta_y(l, t) - m_T \ddot{\eta}_y(l, t) - m_T(b_H + l + b_T)\ddot{\theta}_H(t) \\ - m_T(b_H + l)\dot{\theta}_H^2(t)\beta(t) + EI \eta_y''''(l, t) = 0 \end{aligned} \quad (2.5)$$

$$\begin{aligned} J_T(\ddot{\theta}_H(t) + \ddot{\beta}(t)) + EI \eta_y''(l, t) - m_T b_T \dot{\theta}_H^2(t)(\eta_y(l, t) + b_T \beta(t)) \\ + m_T b_T (b_H + l + b_T) \dot{\theta}_H^2(t) \beta(t) = 0 \end{aligned} \quad (2.6)$$

In addition, the following boundary conditions must be satisfied:

$$\eta_y(0, t) = \eta_y'(0, t) = 0$$

Nondimensionalized Equations The above equations can be made more tractable for ease of manipulation by nondimensionalizing. Let displacements be measured in units of $[l]$ and time be measured in units of $[\sqrt{\rho l^4/EI}]$. If we further remove the tip body, the equations of motion become

$$I\ddot{\theta}_H(t) + \int_0^1 [(x+b)(\ddot{\eta}_y(x,t) + (x+b)\ddot{\theta}_H(t))] dx = \hat{\tau}(t) \quad (2.7)$$

$$\begin{aligned} &\eta_y''''(x,t) + \ddot{\eta}_y(x,t) + (x+b)\ddot{\theta}_H(t) \\ &- \dot{\theta}_H^2(t) \left(\eta_y(x,t) - (x+b)\eta_y'(x,t) + \left(\frac{x^2}{2} + bx + b + \frac{1}{2}\right)\eta_y''(x,t) \right) = 0 \end{aligned} \quad (2.8)$$

where we have defined the following quantities:

$$\begin{aligned} I &= \frac{J_H}{\rho l^3} \\ b &= \frac{b_H}{l} \\ \hat{\tau}(t) &= \frac{\tau(t)}{EI/l}. \end{aligned}$$

The following additional boundary conditions apply in the absence of a tip body:

$$\eta_y''(1,t) = \eta_y'''(1,t) = 0$$

The nondimensionalized energy expressions become:

$$\begin{aligned} T &= \frac{1}{2}I\dot{\theta}_H^2(t) \\ &+ \frac{1}{2}\int_0^1 \left[\left(\dot{\theta}_H(t)\eta_y(x,t) \right)^2 + \left(\dot{\eta}_y(x,t) + \dot{\theta}_H(t)(x+b+\eta_x(x,t)) \right)^2 \right] dx \end{aligned} \quad (2.9)$$

$$V = \frac{1}{2}\int_0^1 \left(\eta_y''(x,t) \right)^2 dx \quad (2.10)$$

Notice that in Eq. 2.9 we have included the term $\eta_x(x,t)$. Omitting this term would result in incorrectly (or inconsistently) linearized equations. Of course, $\eta_x(x,t)$ should be replaced by its expression in terms of $\eta_y(x,t)$. We have not done so above in the interest of clarity.

2.1.2 Approximate Formulation

In order to carry out numerical integration of the equations of motion, it is necessary to convert the partial differential equations obtained above into ordinary differential equations. This is done by discretizing the flexible degrees of freedom, represented above by the flexible beam transverse displacement $\eta_y(x, t)$. Traditionally, this is achieved either by a finite element formulation [46], where the beam is broken down into a finite series of elements with their own mass and stiffness, or by an assumed modes approach [60], where the transverse displacement is represented as a finite sum of time-dependent generalized coordinates weighted by space-dependent mode shapes.

We choose the assumed modes method and represent the transverse beam displacement as

$$\eta_y(x, t) = \sum_{i=1}^n \phi(x) q_i(t).$$

In this case the dependent axial extensions become

$$\eta_x(x, t) = -\frac{1}{2} \sum_{i=1}^n \sum_{j=1}^n \int_0^x \phi'_i(\sigma) \phi'_j(\sigma) d\sigma q_i q_j.$$

Substituting these relations into the kinetic and potential energy expressions and then proceeding with Hamilton's principle, we obtain the following set of ordinary differential equations which are an approximation to the equations of motion for our system.

$$I_{Tot} \ddot{\theta}_H(t) + \sum_{i=1}^n m_i \ddot{q}_i(t) = \tau \quad (2.11)$$

$$m_j \ddot{\theta}_H(t) + \sum_{i=1}^n G_{ij} \ddot{q}_i(t) + \sum_{i=1}^n H_{ij} q_i(t) = -\dot{\theta}_H^2(t) \sum_{i=1}^n K_{ij}^g q_i(t), \quad (j = 1, \dots, n) \quad (2.12)$$

where we have made the following definitions:

$$\begin{aligned} I_{Tot} &= J_H + I_B + b_H^2 m_B + 2eb_H + m_T(b_H + l)^2 + J_T \\ m_i &= b_H E_i + F_i + m_T(b + l) \phi_i(l) + J_T \phi'_i(l) \\ G_{ij} &= g_{ij} + m_T \phi_j(l) \phi_i(l) + J_T \phi'_j(l) \phi'_i(l) \\ K_{ij}^g &= b_H \mu_{ij} + \eta_{ij} - g_{ij} + m_T(b + l) \beta_{ij}(l) - m_T \phi_j(l) \phi_i(l) \end{aligned}$$

and following Kane *et al.* [48] we have defined

$$\begin{aligned} m_B &= \int_0^l \rho dx, & e &= \int_0^l x \rho dx, & I_B &= \int_0^l x^2 \rho dx \\ H_{ij} &= \int_0^l EI \phi_i''(x) \phi_j''(x) dx, & E_i &= \int_0^l \phi_i(x) \rho dx, & F_i &= \int_0^l x \phi_i(x) \rho dx \\ & & g_{ij} &= \int_0^l \phi_i(x) \phi_j(x) \rho dx \end{aligned}$$

and we have further defined

$$\beta_{ij}(x) = \int_0^x \phi_i'(\sigma) \phi_j'(\sigma) d\sigma, \quad \mu_{ij} = \int_0^l \rho \beta_{ij}(x) dx, \quad \eta_{ij} = \int_0^l x \rho \beta_{ij}(x) dx.$$

For future reference, we recast Eqs. 2.11–2.12 into matrix form.

$$M \begin{bmatrix} \ddot{\theta}_H(t) \\ \ddot{\mathbf{q}}(t) \end{bmatrix} + D_t \begin{bmatrix} \dot{\theta}_H(t) \\ \dot{\mathbf{q}}(t) \end{bmatrix} + K \begin{bmatrix} \theta_H(t) \\ \mathbf{q}(t) \end{bmatrix} = -\dot{\theta}_H^2(t) K_t^g \begin{bmatrix} \theta_H(t) \\ \mathbf{q}(t) \end{bmatrix} + B\tau \quad (2.13)$$

where

$$M = \begin{bmatrix} I_{Tot} & \mathbf{m}^T \\ \mathbf{m} & G \end{bmatrix}, \quad D_t = \begin{bmatrix} 0 & 0 \dots 0 \\ 0 & \\ \vdots & D \\ 0 & \end{bmatrix}, \quad K = \begin{bmatrix} 0 & 0 \dots 0 \\ 0 & \\ \vdots & H \\ 0 & \end{bmatrix}$$

$$K_t^g = \begin{bmatrix} 0 & 0 \dots 0 \\ 0 & \\ \vdots & K^g \\ 0 & \end{bmatrix}, \quad B = \begin{bmatrix} 1 \\ 0 \\ \vdots \\ 0 \end{bmatrix}, \quad \mathbf{q}(t) = \begin{bmatrix} q_1(t) \\ \vdots \\ q_n(t) \end{bmatrix}$$

and we have defined the following vectors and matrices: \mathbf{m} is the n -vector whose i -th component is m_i ; D is a matrix of Rayleigh damping; H is an $n \times n$ matrix with ij -th component H_{ij} ; and, K^g is an $n \times n$ matrix whose ij -th component is K_{ij}^g .

It is now an easy matter to set Eq. 2.13 in state space form by inverting the mass matrix and defining a state vector such as, e.g.,

$$\mathbf{x} = \begin{bmatrix} \theta_H(t) \\ \mathbf{q} \\ \dot{\theta}_H(t) \\ \dot{\mathbf{q}} \end{bmatrix}.$$

2.2 Manipulators with Multiple Flexible Links

In this section we present the equations of motion for open chains of flexible bodies, of which the equations for flexible manipulators form a subset. We circumscribe ourselves to approximate equations so that we will end up with finite sets of ordinary differential equations.

2.2.1 General Form of the Equations of Motion

The equations of motion of an open chain of elastic bodies can be expressed quite generally as [42]

$$\begin{bmatrix} M_{RR}(\boldsymbol{\theta}, \mathbf{q}) & M_{RE}(\boldsymbol{\theta}, \mathbf{q}) \\ M_{ER}(\boldsymbol{\theta}, \mathbf{q}) & M_{EE}(\boldsymbol{\theta}, \mathbf{q}) \end{bmatrix} \begin{bmatrix} \ddot{\boldsymbol{\theta}} \\ \ddot{\mathbf{q}} \end{bmatrix} = \begin{bmatrix} \mathbf{f}_R \\ \mathbf{f}_E \end{bmatrix} + \begin{bmatrix} \mathbf{F}_R(\boldsymbol{\theta}, \mathbf{q}, \dot{\boldsymbol{\theta}}, \dot{\mathbf{q}}) \\ \mathbf{F}_E(\boldsymbol{\theta}, \mathbf{q}, \dot{\boldsymbol{\theta}}, \dot{\mathbf{q}}) \end{bmatrix} \quad (2.14)$$

where $\boldsymbol{\theta}$ is a vector of rigid body generalized coordinates; \mathbf{q} is a vector of the elastic generalized coordinates; M_{RR} , M_{RE} , M_{ER} , and M_{EE} form the configuration dependent mass matrix; \mathbf{f} is a vector of control forces (as in joint-torque actuators in a manipulator); and \mathbf{F} is a vector of nonlinear (e.g., inertial, elastic) forces.

Small Deformations Assumption

It is of great interest to model in particular the important class of systems for which the elastic deformations remain small so it is possible to ignore terms of second order in the $q_i(t)$ and $\dot{q}_i(t)$. If we also assume linear elastic relations, it is possible to expand Eq. 2.14 into a form which is reminiscent of the form of Eq. 2.13 for the one-flexible link arm:

$$M(\boldsymbol{\theta}, \mathbf{q}) \begin{bmatrix} \ddot{\boldsymbol{\theta}} \\ \ddot{\mathbf{q}} \end{bmatrix} + D \begin{bmatrix} \dot{\boldsymbol{\theta}} \\ \dot{\mathbf{q}} \end{bmatrix} + K \begin{bmatrix} \boldsymbol{\theta} \\ \mathbf{q} \end{bmatrix} + G(\boldsymbol{\theta}, \mathbf{q}) = -C(\boldsymbol{\theta}, \mathbf{q}, \dot{\boldsymbol{\theta}}, \dot{\mathbf{q}}) + B\boldsymbol{\tau} \quad (2.15)$$

where D is a constant matrix of Rayleigh damping; K is a constant stiffness matrix; $C(\boldsymbol{\theta}, \mathbf{q}, \dot{\boldsymbol{\theta}}, \dot{\mathbf{q}})$ is a vector of inertial (coriolis and centripetal) forces; $G(\boldsymbol{\theta}, \mathbf{q})$ is a non-linear vector of position dependent gravity forces; and we have set $\mathbf{f} = B\boldsymbol{\tau}$ where B is the control distribution matrix and the control vector $\boldsymbol{\tau}$ has in general many fewer elements than the number of degrees of freedom.

As was the case with Eq. 2.13, it is an easy matter to rewrite Eq. 2.15 in state space form by defining the state vector

$$\mathbf{x} = \begin{bmatrix} \theta \\ \mathbf{q} \\ \dot{\theta} \\ \dot{\mathbf{q}} \end{bmatrix}.$$

2.2.2 Equations of Motion for Flexible-Link Manipulators

The equations presented in the previous section are quite general and include among others the equations of motion of three-dimensional, flexible-link (and flexible joint) manipulators, with revolute and/or prismatic joints, operating in a gravity field. In this work we limit ourselves to the study of planar (i.e., two-dimensional), revolute, flexible-link manipulators that do not form closed chains and that operate in a plane perpendicular to the action of gravity (i.e., so that the G term in Eq. 2.15 is zero). A two-link example is shown in Fig. 2.2

To model the links, we assume as for the one link case that we are dealing with flexible beams undergoing small deflections so that the Bernoulli-Euler beam theory applies. We further use the assumed modes method to discretize the continuous (in the spatial variables) displacements. We can then identify the components $q_i(t)$ of \mathbf{q} with the time-dependent generalized coordinates. We can also take the components $\theta_i(t)$ of θ to be the relative joint angles between the links. We then see that Eq. 2.15 is indeed a more general version of Eq. 2.13, where now the matrix terms contain in general spatial integrals of functions of the modeshapes of the individual links.

Specifically, referring to Fig. 2.2 we identify

$$\theta(t) = \begin{bmatrix} \theta(t) \\ \beta(t) \end{bmatrix}, \quad \mathbf{q}(t) = \begin{bmatrix} q_1(t) \\ \vdots \\ q_n(t) \\ p_1(t) \\ \vdots \\ p_m(t) \end{bmatrix}$$

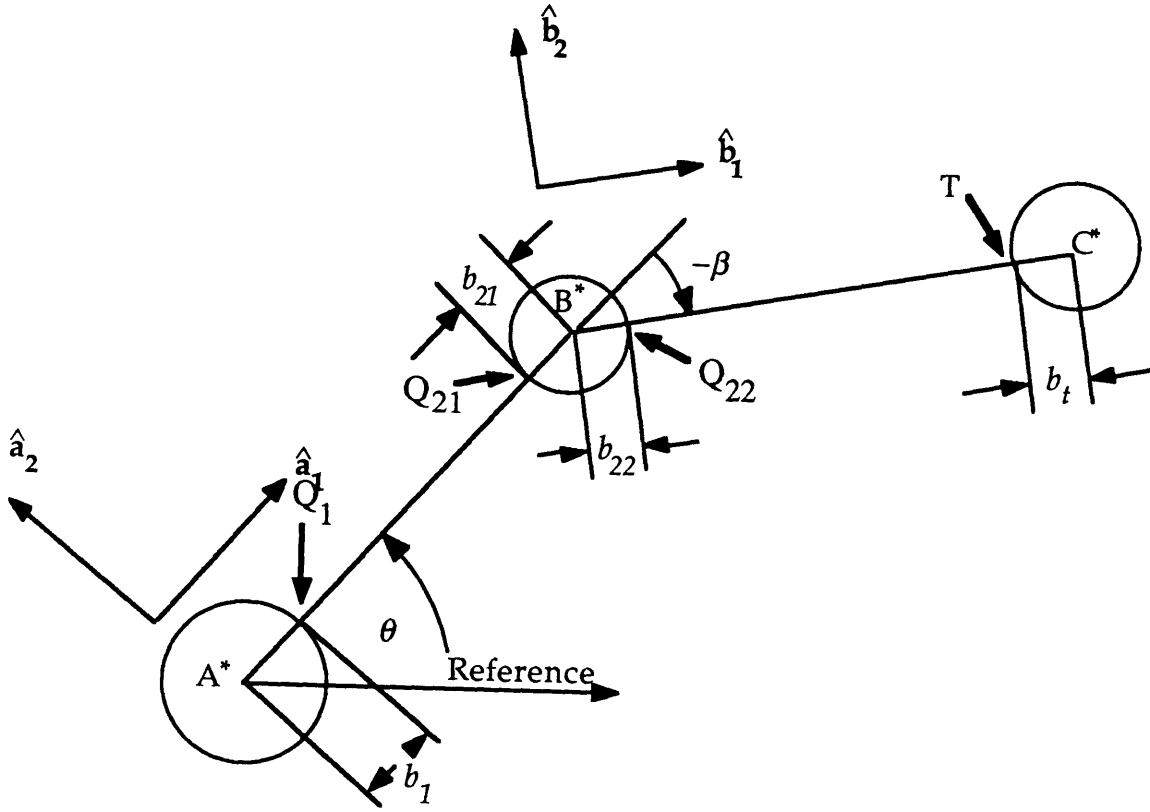


Figure 2.2: Manipulator with Two Flexible Links

where, following the assumed modes method procedure, we represent each link's transverse displacement respectively as

$$\eta_{y_1}(x_1, t) = \sum_{i=1}^n \phi_i(x_1)q_i(t)$$

$$\eta_{y_2}(x_2, t) = \sum_{i=1}^m \psi_i(x_2)p_i(t).$$

As can be seen from Fig. 2.2, $\theta(t)$ represents the (inertial) shoulder angle, while $\beta(t)$ is the relative angle between the stator and the rotor at the elbow joint.

The shoulder body A is hinged at its center of mass and has mass m_A and inertia J_A . link 1 is attached to body A in a cantilevered way at a distance b_1 of the hinge point. Link 1 has mass per unit length ρ_1 , length l_1 , and flexural rigidity EI_1 .

The elbow consists of two rigid bodies. Body B_1 is the stator and is attached to link 1 in a cantilevered way. Body B_1 is attached to body B_2 , the rotor, at the elbow hinge point. Body B_i has mass m_{B_i} and inertia J_{B_i} , for $i = 1, 2$. The mass centers of the bodies $B_i, i = 1, 2$, are offset from the hinge point. The distance between the

point of attachment of body B_1 to link 1 and the hinge point at the elbow is given by b_{21} . Notice that b_{21} is chosen to coincide with the extension of the slope of link 1 at the tip ($x_1 = l_1$).

The location of the mass center of body B_1 is then given by the radial distance b from the elbow hinge point and the angle β_{12} that it makes with the extension of line b_{21} . The distance between the elbow hinge point and the point of attachment of link 2 is given by b_{22} , which is chosen to coincide with the extension of the undeformed neutral axis of link 2. The location of the mass center of body B_2 is now given by the radial distance b' from the elbow hinge point and the angle β'_{12} that it makes with the extension of line b_{22} .

Notice that the joint relative angle $\beta(t)$ is exactly the angle made between the extension of the line b_{22} and that of line b_{21} . Link 2 is attached to body B_2 in a cantilevered way. The mass per unit length of link 2 is given by ρ_2 , its length by l_2 , and its flexural rigidity by EI_2 .

Finally, the tip body C_1 is attached to link 2 in a cantilevered way. The distance from the point of attachment of link 2 to the center of mass of body C_1 is given by b_t , where we assume b_t coincides with the extension of the slope of link 2 at the tip ($x_2 = l_2$). Body C_1 has mass m_{C_1} and inertial J_{C_1} .

If we take cantilevered mode shapes as the assumed modes, then the control distribution matrix assumes a very simple form

$$\begin{bmatrix} 1 & 0 \\ 0 & 1 \\ 0 & 0 \\ \vdots & \vdots \\ 0 & 0 \end{bmatrix}$$

where the actuators are taken to be joint torquers.

The general form of Eq. 2.15 is quite satisfactory for the developments in future chapters. In Chapter 7, digital simulation results are presented using the specific example of a planar two-link manipulator. The reader is referred to [68] for the detailed equations of motion in this case. In Appendix C the subject of mode shape

selection for the assumed modes expansion is addressed for both the one and two-link manipulator examples.

Chapter 3

Nonminimum Phase Systems and Limits of Feedback Performance

3.1 Linear Systems

3.1.1 Sensitivity Theory

In the following discussion, we shall limit ourselves to the well developed theory for continuous time, finite dimensional, linear, time-invariant systems.

The problems of control with which feedback theory is concerned can be described quite generally as follows [41]. There is a set of objectives which is assumed to be mathematically expressible by a finite set of variables. There is a specialized array of equipment needed to achieve (and capable of achieving) the objectives. This array is denoted as the *plant* and it has a discrete set of (controllable) inputs (see Fig. 3.1).

The solution to this

problem would be to insert between R and M a network G which translates
... the set of objectives into the language appropriate to the plant.*

This solution may not be practicable due to uncertainty (ignorance for Horowitz) both of the plant and of the environment (e.g., uncontrollable and uncertain inputs to the

*I.M. Horowitz, *Synthesis of Feedback Systems*, Academic Press, N.Y., p.1

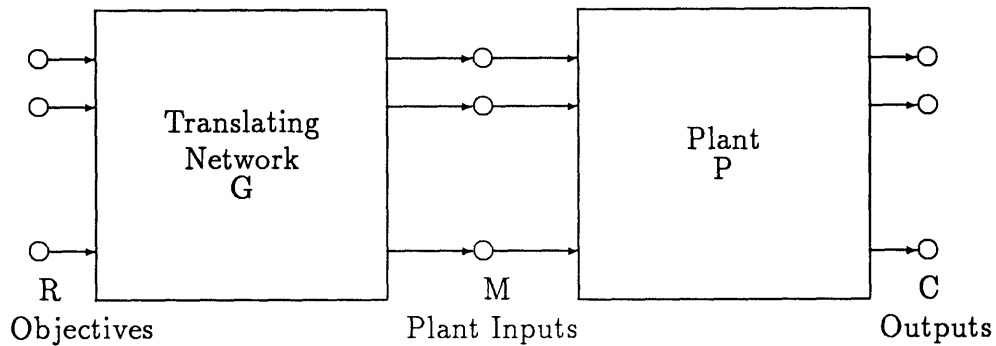


Figure 3.1: Definitions for Feedback Control Theory

plant). If the desired objectives are not achievable within the permitted tolerances due to this uncertainty, it may still be possible to achieve the desired accuracies by means of feedback.

Feedback theory is concerned with processing the information gained by sensing the outputs and comparing them with the objectives and using this difference to drive the plant until the differences become satisfactorily small. Horowitz [41] suggests that there are three general and all-encompassing reasons to use feedback:

- (i) to contend with plant uncertainty
- (ii) to contend with ignorance of exogenous inputs
- (iii) to change the static and dynamic characteristics of a given element through the use of feedback.

3.1.2 Structure of the Feedback System

If a plant has only two access points, and if access to the output is only via the plant (what Bode [14] calls a zero leakage transmission) then it is impossible to create more

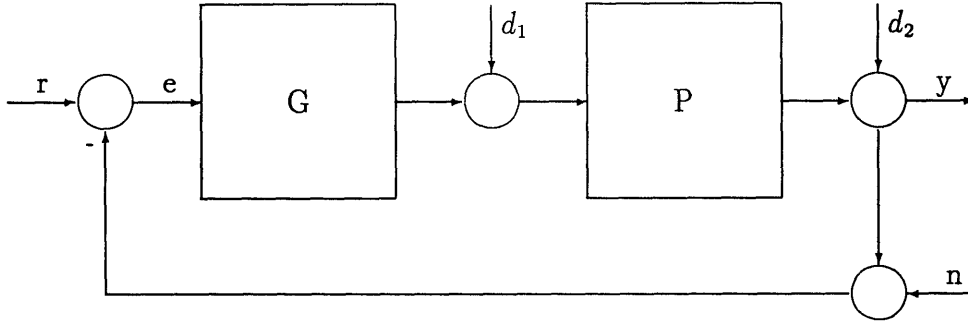


Figure 3.2: Single Degree of Freedom Feedback Configuration

than two design degrees of freedom, no matter how complicated a configuration is built around the plant.

The basic system capabilities (as far as plant sensitivity and plant disturbances are concerned) are completely determined by the number of access points of the plant.[†]

The structure of the feedback system of Fig. 3.2 exhibits a single degree of freedom, $L = GP$, where P is the a priori given plant with which the control designer must work.

For both G and P finite dimensional linear time-invariant (FDLTI), with $G(s)$ and $P(s)$ being the corresponding transfer functions, the system (closed-loop) input-output relation and the error between the reference input and the output are given by:

$$y = (1 + PG)^{-1}[PG(r - n) + Pd_1 + d_2] \quad (3.1)$$

$$\begin{aligned} e &= r - y \\ &= (1 + PG)^{-1}[r - d_2 + PGn - Pd_1] \end{aligned} \quad (3.2)$$

[†] *Ibid.*, p. 249.

It is apparent from the closed-loop transfer function, Eq. 3.1, that the effect of feedback around the plant is given by the quantity $(1 + PG)$. The physical interpretation of this quantity is obtained by breaking the loop anywhere and, setting all other inputs to zero, introducing a unit impulse where the loop was broken. The resulting output is $-PG$, and the difference between the input and the output is exactly $(1 + PG)$. For this reason $(1 + PG)$ is called the return difference for PG , and $L(s) = P(s)G(s)$ is called the loop transmission or loop gain.

Let $T(s)$ be the closed-loop transfer function from r to y . The sensitivity of $T(s)$ to plant parameter variations, i.e., to variations in $P(s)$, is given by [41]

$$S(s) = \frac{\frac{\Delta T}{T + \Delta T}}{\frac{\Delta P}{P + \Delta P}} = \frac{1}{1 + L(s)}. \quad (3.3)$$

Equation 3.3 indicates that the system sensitivity to plant uncertainty ($S(s)$), for the system depicted in Fig. 3.1, is equivalent to the inverse of the return difference for the system. From the above, and equations 3.1 and 3.2, it is clear that $S(s)$ is a measure of the benefits of feedback, as set forth in the Introduction section. For systems with only one structural degree of freedom (as in Fig. 3.2), it is impossible to independently specify the filter transfer function, given by $T(s)$, and the properties of feedback, characterized by $L(s)$ (via $S(s)$).

Because the older classical feedback control theory deals mostly with the single degree of freedom structure of Fig. 3.2, its synthesis techniques allow the designer to achieve compromises between the filter and feedback problems. Due to the single degree of freedom constraint, $T(s)$ is not formally specified and instead the various design requirements are expressed in terms of the loop transmission $L(s)$. This way the designer has control over the feedback properties and the system response over a large part of the significant frequency range, i.e., over the frequency range in which $|L(j\omega)| \gg 1$, where $T = L/(1 + L) \approx L/L = 1$. In the classical theory all design specifications are given in terms of $L(s)$. The loop transmission is shaped in the frequency domain (via Bode and Nyquist plots) to achieve the required specifications. More recent design procedures include the root locus method and the $T(s)$ pole-zero method.

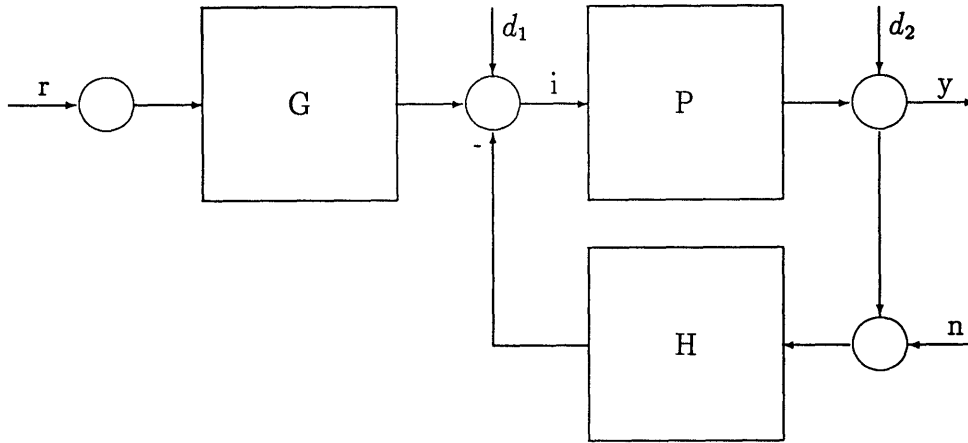


Figure 3.3: Two Degree of Freedom Feedback Configuration

The one degree of freedom feedback structure suffers from some shortcomings. This configuration is inherently very sensitive to parameter variations near crossover, where it turns out that $|S(s)| > 1$ and thus sensitivity to plant variation is worse than if no feedback were used. This situation is exacerbated in higher order systems. In addition, sensitivity of the time response is very poor: the system overshoot is very sensitive to variations in P , while the final steady state value is unaffected, given $S(0) = 0$. Furthermore, only special kinds of disturbances at the output can be handled by this configuration. Only when the bandwidth of $T(s)$ is much larger than the important frequency range of the disturbance can we make $y_{d_2} = (1 - T)d_2$ small (since then $T \approx 1$).

Disturbances at the plant input are also poorly rejected in the case when P has highly underdamped complex poles. Since these poles are nearly cancelled by G , and $y_{d_1} = P/(1 + L)d_1$, L does not have the poles to cancel those of P and these poles lead to relatively large disturbance output. Finally, it is not possible to guarantee stability margins in the presence of large uncertainty and to increase the system bandwidth (improve the transient response), since large gain and phase margins are associated with overdamped dominant poles which make the system response more sluggish.

The feedback system of Fig. 3.3 exhibits a configuration with two degrees of freedom. In this case, the input-output relation and the error between the reference input and the output are given by

$$\begin{aligned} y &= (1 + L)^{-1}[PGr - Ln + Pd_1 + d_2] \\ &= Tr - S_cn + SPd_1 + Sd_2 \end{aligned} \quad (3.4)$$

$$\begin{aligned} e &= r - y \\ &= (1 - T)r + S_cn - SPd_1 - Sd_2 \end{aligned} \quad (3.5)$$

$$S_c(s) = 1 - S(s) = \frac{L(s)}{1 + L(s)} \quad (3.6)$$

where now $L = PH$ is the loop transmission function and $T = GP/(1+L)$ is the filter transfer function. As before, the system sensitivity (to plant variations) function is given by $S = 1/(1 + L)$. S_c is the so-called complementary sensitivity function. We have assumed, as for the one-degree-of-freedom case, that all system blocks in Fig. 3.3 represent FDLTI elements. The significant feature of a two-degree-of-freedom configuration is that it allows for the independent realization of the system sensitivity function, S , and the system transmission function, T .[†] These two functions fix the values of G and H in Fig. 3.3. As mentioned earlier, if the plant has only two access points, and if it is a zero leakage transmission, then it is impossible to obtain more than two degrees of freedom.

Even with the two-degree-of-freedom structure there are several limitations on the achievable benefits of feedback [41]. One serious limitation is due to noise or to parameter variation in the return path of the feedback loop (n in Figs. 3.2 and 3.3). It is well known that since the transfer function from sensor noise (n) to plant output (y) is given by the complementary sensitivity function, S_c , and since not both S and S_c can be made small in the same frequency range, the significant frequency range for sensor noise better be higher than the range where the loop gain is greater than one (where S is small and the benefits of feedback are achieved). Another detrimental

[†]*Ibid.*, p. 246.

effect of noise in the feedback path is that the noise level at the plant input can exhibit a high level of the higher frequency components of the sensor noise. This can be seen as follows.

Setting all other inputs to zero, the transfer function from n to i (the plant input) in Fig. 3.3 is given by

$$\frac{i}{n} = \frac{-H(s)}{1 + L(s)} = \frac{-\frac{L}{P}}{1 + P}.$$

For $|L| < 1$, $i/n \approx -L/P$ and if $|L| > |P|$ in this mid-frequency region we see that the magnitude of the i/n transfer function is greater than one. This problem also exists when $|L| > 1$ and $|P| < 1$, because then $i/n \approx -1/P$. It is clear that this problem only occurs when the demand for the benefits of feedback is greater than what the plant by itself is capable of supplying, i.e., when H must make up the gain difference between that available in P and that desired in L .

To reduce this limitation on the achievable benefits of feedback, it is necessary to decrease $|L|$ as fast as possible (after the significant frequency range where the benefits of feedback are obtained). Unfortunately, the rate of decrease of $|L|$ is limited by stability considerations and the Bode gain-phase theorem. We will look at this later when we study in greater detail the limitations imposed on the achievable benefits of feedback by right half plane zeros. Suffice it to note now that if a plant has more than one right half plane zero then there is an absolute limit on the loop gain-bandwidth achievable. Finally, another limitation is the limit on the loop transmission crossover frequency imposed by practical considerations due to neglected higher order dynamics.

It is important to note that the factors determining the feedback capabilities and the cost of feedback for a given system are system constraints such as: whether it is zero leakage or not; the number of access points in the plant; and, the kind of stability permitted (i.e., conditional or unconditional). The way to reduce some of the above limitations, then, is by relaxing some to these constraints. This leads to multi-loop designs, designs with parallel plants, multi-input multi-output (MIMO) systems, and conditionally stable designs.

3.1.3 Nonminimum Phase Systems

A function $F(s)$ of the complex variable s is called a minimum phase function if it satisfies the Bode gain phase theorem; one of whose forms is

$$\pi B(\omega_x) = \int_{-\infty}^{\infty} \frac{dA}{du} \ln \coth \frac{|u|}{2} du \quad (3.7)$$

$$u = \ln \frac{\omega}{\omega_x}$$

and

$$F(j\omega) = A(\omega) + jB(\omega) = \overline{F(-j\omega)} \quad (3.8)$$

The last equality in Eq. 3.8 is a property of transforms of impulse responses of real systems (time functions) for which $A(j\omega)$ and $B(j\omega)$ are even and odd functions of ω , respectively. Equation 3.7 can be interpreted as follows: the argument of $L(s)$ at any frequency ω_x is determined by the rate of change (on a log frequency scale) of the log magnitude of $L(s)$ in the neighborhood of ω_x . The function $\ln(\coth(|u|/2))$ can be considered a weighting function which weighs the point ω_x the most and rapidly decays over a few octaves on either side.

For our purposes, we consider functions of the type $F(s) = \ln L(s)$ so that $A = \ln |L(j\omega)|$, $B = \arg L(j\omega)$. In this case, Eq. 3.7 holds for functions $L(s)$ which satisfy Eq. 3.8 and such that $L(s)$ can be zero or infinite at infinity, but must be analytic and have no zeros in the right half plane. Note that if $F(s)$ satisfies Eq. 3.8, then so does $\ln(F(j\omega))$. ($F(s)$ must also belong to the class \mathcal{R} (see Ref. [33]), but it may have poles and zeros of any multiplicity on the $j\omega$ -axis.) In particular, we see that unstable functions and functions with right half plane zeros and/or time delays are not minimum phase. Of functions that satisfy Eq. 3.7 Horowitz says that

[n]o other stable function ... with the same magnitude vs. frequency characteristic can have any less phase lag.[§]

Stable functions for which Eq. 3.7 does not hold are called nonminimum phase functions. Systems represented by nonminimum phase transfer functions are called

[§] *Ibid.*, p. 333.

nonminimum phase systems. Examples of nonminimum phase systems are systems with right half plane zeros, with unstable minor loops, and with time delays. Essentially, nonminimum phase systems have faulty behavior at start of response (due to large phase lag at high frequencies) which makes response slow [66, p. 391].

In order to begin to understand why nonminimum phase systems exhibit inherent performance limitation, let us first consider the following qualitative arguments. A loop transmission with right half plane zeros can be written as $L(s) = L_1(s)(s - a) \cdots (s - g)$ where $L_1(s)$ has only left half plane poles and zeros. Equivalently $L(s) = L_M(s)A(s)$ where

$$A(s) = \frac{(s - a) \cdots (s - g)}{(s + a) \cdots (s + g)}.$$

$A(s)$ is called an all-pass function (also a Blaschke product) since its modulus is equal to one for all frequencies when evaluated at $s = j\omega$. Consequently, $L(s)$ differs from $L_M(s)$ only in phase. An all-pass function has an increase of phase lag from zero to infinite frequency equal to $180^\circ n$, where n is the number of right half plane zeros. $L_M(s)$, which satisfies Bode's gain phase theorem (Eq. 3.7), is seen to have the minimum phase lag possible for its magnitude characteristic (as a function of frequency). Thus the term minimum phase function introduced above.

Using Eq. 3.7 and its physical interpretation given above, the detrimental effects of right half plane zeros can be understood as follows. The faster the loop transmission decreases, the larger is its phase lag. This implies that if the modulus of L decreases too fast the phase lag could be large enough to cause instability. The actual bandwidth before we can make the modulus of L less than 1 is much greater than the desired bandwidth for large loop gain. This is one of the important costs of feedback.[¶] Since $A(s)$ increases the phase lag of $L_M(s)$ by $180^\circ n$, the rate of decrease of the modulus of $L_M(j\omega)$ must be even less than before, especially in the critical crossover region. The same is true of systems with pure time delays. This is clear from the fact that e^{-sT} can be approximated to arbitrary accuracy by an all-pass network.

[¶] *Ibid.*, p. 324.

Freudenberg and Looze [33] formalize the above qualitative discussion with definitive quantitative bounds on the achievable benefits of feedback due to nonminimum phase systems and unstable systems. These bounds take the form of integral relations that must be satisfied by both the sensitivity and complementary sensitivity functions in the presence of right half plane poles and zeros. Effectively these constraints show that desirable properties of $S(j\omega)$ and $S_c(j\omega)$ in one frequency range must be traded off against undesirable properties at other frequencies.

These tradeoffs are a direct consequence of properties of linear time-invariant systems.^{||}

In the sequel we give a concise summary of these results of Freudenberg and Looze for the single-input, single-output (SISO) case. The generalization to multi-input, multi-output (MIMO) systems is credited to Boyd and Desoer [15] and is also presented below.

SISO Systems

The integral relations derived in this section, which represent bounds on the achievable sensitivity function for an FDLTI system, result from the following realizability property: the Laplace transform of the impulse response of a physical system is a locally analytic function of the complex frequency variable. In particular, Poisson integral formulas apply [22].

Referring to the single degree of freedom configuration of the system in Fig. 3.2, we have as before the loop transfer function given by $L(s) = P(s)G(s)$, the sensitivity function by

$$S(s) = \frac{1}{1 + L(s)},$$

and the complementary sensitivity function by $T(s) = 1 - S(s)$. Assuming that $L(s)$ is free of unstable hidden modes, i.e., the controller does not attempt to cancel any

^{||}J.S. Freudenberg, and D.P. Looze, Right Half Plane Poles and Zeros and Design Tradeoffs in Feedback Systems, *IEEE Transactions on Automatic Control*, Vol. AC-30, No. 6, June 1985, pp. 555–565.

unstable modes and no unstable modes are unobservable, then the feedback system is stable if $S(s)$ is bounded in the closed right half plane.

Assume that $L(s)$ can be factored as

$$L(s) = L_M(s)B_p^{-1}(s)B_z e^{-s\tau} \quad (3.9)$$

where

$$B_z(s) = \prod_{i=1}^{N_z} \frac{z_i - s}{\bar{z}_i + s} \quad (3.10)$$

is the Blaschke product of open right half plane zeros, z_i , including multiplicities,

$$B_p(s) = \prod_{i=1}^{N_p} \frac{p_i - s}{\bar{p}_i + s} \quad (3.11)$$

is the Blaschke product of open right half plane poles, p_i , also including multiplicities, and $e^{-s\tau}$ with $\tau \geq 0$ representing a time delay. A line over a complex-valued variable represents complex conjugation. $L_M(s)$ is assumed proper, stable and minimum phase.

If the feedback system is stable, then $S(s)$ can be factored as $S(s) = S_M(s)B_p(s)$, where following the convention established above, $S_M(s)$ is stable and minimum phase. Recall that a Blaschke product is all-pass with unit magnitude, so that $|S(j\omega)| = |S_M(j\omega)| \forall \omega$. For the results presented below to be valid we further require $S(s)$ to belong to the class of functions \mathcal{R} . Given a function $F(s)$, define

$$M(R) = \sup_{\theta} |F(Re^{j\theta})|, \quad \theta \in [-\pi/2, \pi/2].$$

Then if

$$\lim_{R \rightarrow \infty} \frac{1}{R} M(R) = 0$$

$F(s)$ is said to belong to the class \mathcal{R} .

If $L_0(s)$ is a proper rational function, then $\log L_0(s)$ and $d^i/ds^i \log L_0(s)$ are in \mathcal{R} . If $L(s) = L_0(s)e^{-s\tau}$, $\tau > 0$, then $\log L(s)$ is not in \mathcal{R} . However, if the feedback system is stable with sensitivity function $S(s)$, then $\log S(s)$ and $d^i/ds^i \log S(s)$ are in \mathcal{R} in spite of any time delays in $L(s)$.

After these preliminaries, the following two theorems, due to Freudenberg and Looze [33], state the constraints upon the sensitivity and complementary sensitivity

functions due to right half plane poles and zeros in terms of the values of the respective function on the $j\omega$ -axis.

Theorem 3.1 *Let $z = x + jy$ be an open right half plane zero, with multiplicity m , of the open loop transfer function $L(s)$. Assume that $d^i/ds^i \log S_M(s)$ is in the class \mathcal{R} , $i = 0, 1, \dots, m-1$. Then, if the corresponding feedback system is stable, the sensitivity function must satisfy the following integral constraints:*

$$\pi \log |B_p^{-1}(z)| = \int_{-\infty}^{\infty} \log |S(j\omega)| d\theta_z(\omega) \quad (3.12)$$

$$\pi \arg B_p^{-1}(z) = \int_{-\infty}^{\infty} \arg S_M(j\omega) d\theta_z(\omega) \quad (3.13)$$

$$\pi \frac{d^i}{ds^i} \log B_p^{-1}(s) \Big|_{s=z} = \int_{-\infty}^{\infty} \frac{d^i}{ds^i} \log S_M(s) \Big|_{s=j\omega} d\theta_z(\omega) \quad (3.14)$$

$(i = 1, \dots, m-1).$

The function $\theta_z(\omega)$ is given by

$$\theta_z(\omega) = \arctan \left[\frac{\omega - y}{x} \right]. \quad (3.15)$$

The complementary sensitivity function for a stable feedback system can be factored as

$$T(s) = T_M(s) B_z(s) e^{-s\tau}$$

where $T_M(s)$ has no poles or zeros in the right half plane.

Theorem 3.2 *Let $p = x + jy$ be an open right half plane pole, with multiplicity n , of the open loop transfer function $L(s)$. Assume that $d^i/ds^i \log T_M(s)$ is in the class (\mathcal{R}) , $i = 0, 1, \dots, n-1$. Then, if the corresponding feedback system is stable, the complementary sensitivity function must satisfy the following integral constraints:*

$$\pi \log |B_z^{-1}(p)| + \pi x\tau = \int_{-\infty}^{\infty} \log |T(j\omega)| d\theta_p(\omega) \quad (3.16)$$

$$\pi \arg B_z^{-1}(p) + \pi y\tau = \int_{-\infty}^{\infty} \arg T_M(j\omega) d\theta_p(\omega) \quad (3.17)$$

$$\pi \frac{d^i}{ds^i} \left(\log B_z^{-1}(s) e^{s\tau} \right) \Big|_{s=p} = \int_{-\infty}^{\infty} \frac{d^i}{ds^i} \log T_M(s) \Big|_{s=j\omega} d\theta_p(\omega) \quad (3.18)$$

$$(i = 1, \dots, n-1). \quad (3.19)$$

The function $\theta_p(\omega)$ is given by

$$\theta_p(\omega) = \arctan \left[\frac{\omega - y}{x} \right]. \quad (3.20)$$

Note in particular the constraints given by Eqs. 3.12 and 3.16. These represent constraints on the weighted area under the $\log |S(j\omega)|$ and the $\log |T(j\omega)|$ curves. The $j\omega$ -axis is weighted by the location of the right half plane zero or pole, respectively, using the function $\theta_s(\omega)$, $s = z, p$. It is easy to see that $\theta_s(\omega)$ is an increasing function of ω . Since the left hand sides of Eqs. 3.12 and 3.16 are nonnegative, we see that if $|S(j\omega)| < 1$ or $|T(j\omega)| < 1$ at some frequency ranges, then these quantities must necessarily be greater than one at other frequency ranges. This establishes a fundamental tradeoff between feedback properties at different frequencies.

Moreover, from the weighting function $\theta_s(\omega)$ it is clear that right half plane poles and zeros which are close to frequency ranges where desired feedback properties are to be attained present a greater obstacle through the above constraining relations than those right half plane poles and zeros that are far away. This weighting function clearly defines the notion of proximity of a right half plane pole or zero. Finally, note that the weighted length of the $j\omega$ -axis is finite and equal to π . This means in particular that we cannot assign an arbitrarily low value of $|S(j\omega)|$ over some frequency range and expect to satisfy the constraint relation by allowing $|S(j\omega)|$ to be only slightly less than one over an infinitely large frequency range.

We close this section by quantifying the comments in the last paragraph. The following theorem [33] gives a lower bound on the maximum sensitivity that must be present at some frequency range due to the achievement of some level of sensitivity reduction over another frequency range for a nonminimum phase systems.

Theorem 3.3 *Let the open loop transfer function $L(s)$ have open right half plane poles and zeros given by $p_i, i = 1, \dots, N_p$, and $z_i, i = 1, \dots, N_z$. Suppose that the closed-loop system is stable and that the level of sensitivity reduction α has been achieved over the frequency range Ω , i.e.,*

$$|S(j\omega)| \leq \alpha < 1 \quad \forall \omega \in \Omega,$$

where Ω is a conjugate symmetric range of frequencies (i.e., $\omega \in \Omega \Rightarrow -\omega \in \Omega$). Then for each zero right half plane zero z of $L(s)$ the following bound must be satisfied:

$$\|S\|_\infty \geq \left(\frac{1}{\alpha}\right)^{\frac{\Theta_z(\Omega)}{\pi - \Theta_z(\Omega)}} |B_p^{-1}(z)|^{\frac{\pi}{\pi - \Theta_z(\Omega)}} \quad (3.21)$$

where $\|S\|_\infty = \sup_\omega |S(j\omega)|$, and

$$\Theta_z(\Omega) = \int_\Omega d\theta_z(\omega).$$

Notice that this lower bound is greater than one, since $\alpha < 1$, $|B_p^{-1}(z)| > 1$, $\Theta_z(\Omega) < \pi$. This implies that the closed-loop system will exhibit a sensitivity increase over some frequency range. Further, in most classical design situations, this increase in sensitivity occurs around crossover and its net effect is to reduce stability margins. Recall that

$$GM = -20 \log \left(1 - \frac{1}{|S(j\omega_c)|} \right)$$

$$PM = 2 \arcsin \frac{1}{2|S(j\omega_c)|}$$

where GM is the gain margin, PM is the phase margin, and ω_c is the crossover frequency.

Finally, we remark that a sensitivity function that satisfies the bound given by Theorem 3.3 tightly is not achievable in practice, i.e., any practical closed-loop system will have a sensitivity with an even larger infinity norm. In particular, finite bandwidth constraints, which require the sensitivity function to be almost one after a certain cutoff frequency, result in a modified form of Eq. 3.21 which shows that $\|S\|_\infty$ increases as the cutoff frequency decreases.

In summary, given a stable feedback system with an open loop gain that contains nonminimum phase zeros, the magnitude of the sensitivity function will necessarily be greater than one over a significant frequency range if sensitivity reduction has been achieved over a desired frequency range. Bandwidth constraints aggravate this by pushing the lower bound on the maximum value of $S(j\omega)$ further up. Peaking in $|S(j\omega)|$ is bad for stability margins because it occurs near crossover.

MIMO Generalizations

First we recall the notion of transmission zeros of a MIMO system. Consider the FDLTI MIMO system denoted by (A, B, C, D)

$$\begin{aligned} \dot{x} &= Ax + Bu \\ y &= Cx + Du \end{aligned} \tag{3.22}$$

where $x \in R^n$ is the state, $u \in R^m$ is the input, $y \in R^r$ is the output and A, B, C, D are constant matrices of appropriate dimensions. We assume that $n \geq 1, m \geq 1, r \geq 1, \max(r, m) \leq n$. The following definition is due to Davison and Wang [25].

Definition 3.4 *Given the system 3.22, the transmission zeros of 3.22 are defined to be the set of complex numbers λ which satisfy the following inequality*

$$\text{rank} \begin{bmatrix} A - \lambda I & B \\ C & D \end{bmatrix} < n + \min(r, m).$$

If a system has transmission zeros in the open right half plane, then it is said to be a nonminimum phase system, in analogy with the SISO case.

This is the more familiar notion of transmission zeros defined for finite dimensional state space systems. The results we are about to present, however, were derived by Boyd and Desoer [15] in the more general context of an algebra of transfer functions [18,28] which includes infinite dimensional (distributed) linear systems.

As is true for SISO systems, right half plane transmission zeros of a MIMO plant impose fundamental limitations on the achievable closed-loop transfer functions of a feedback system. Cheng and Desoer [21] present the following result, valid for distributed systems, using a two degree of freedom configuration:

under reasonable assumptions, the closed right-half plane transmission zeros of the plant will remain as transmission zeros of the I/O map of any stable feedback system (here the plant output is the feedback-system output).

As in the SISO case, there also exist in this case fundamental tradeoffs between the feedback properties achievable at different frequency ranges for nonminimum phase systems. Recall that in the SISO case the integral constraints due to Freudenberg and Looze were obtained by using the analyticity of the Laplace transform of physical SISO systems. In particular, the property of the real part of an analytic function being harmonic is fundamental.

Boyd and Desoer [15] extend the Freudenberg and Looze constraints to the multivariable setting through the use of subharmonic functions. Without going into excessive detail, suffice it to say that if $H(s) \in H_\infty^{m \times n}$, where $H_\infty^{m \times n}$ is the set of $m \times n$ matrices whose entries are in H_∞ (and thus are analytic and bounded in the open right half plane), then any induced norm $\|\cdot\|$ (and $\log \|\cdot\|$) is subharmonic. Subharmonic functions satisfy the Poisson inequality [15] and this leads to results similar to those for the SISO case.

While Boyd and Desoer [15] give MIMO generalizations to many classical results such as the Paley-Wiener theorem, the Bode integral, Zames' inequality, etc., we limit ourselves to reproducing their generalization of Theorem 3.3 above, and we use the same notation as in that theorem.

Theorem 3.5 *Suppose that the plant P has a nonminimum phase zero at z and $\log \|H_{yd}(j\omega)\| \leq \log(\alpha)$ for $\omega \in \Omega$. Then*

$$\log \sup_{\omega \in \mathbb{R}} \|H_{yd}(j\omega)\| \geq -\log(\alpha) \frac{\Theta_z}{\pi - \Theta_z}. \quad (3.23)$$

where $H_{yd} = (I + PC)^{-1}$, the disturbance to output map, is also the sensitivity of the system as defined in the SISO case.

3.2 Nonlinear Systems

In this section we present some of the recent developments in the theory on nonlinear systems which extend some of the above presented concepts to the nonlinear realm. The concepts presented herein are necessary background for understanding some of the developments of Chapters 4 and 5.

In Chapter 4, the notions of nonlinear zero dynamics and of nonminimum phase nonlinear systems play an important role in the analysis of *inverse dynamics* solutions. In Chapter 5 the zero dynamics of a system is shown to play an intrinsic role in the solution of the nonlinear output regulation problem. In addition, the results of Chapter 5 show that, even for nonlinear systems, the results of section 3.1.3 for linear systems play a crucial role.

The following concepts are best presented within the context of single-input single-output (SISO) nonlinear systems. Generalization to certain kinds of multi-input multi-output (MIMO) systems is straight-forward, as will be pointed out towards the end of this chapter. The definitive reference for the material reviewed below is the book on nonlinear control systems by Isidori [43].

Consider the following SISO nonlinear system

$$\dot{x} = f(x) + g(x)u \tag{3.24}$$

$$y = h(x) \tag{3.25}$$

where $f(x)$ and $g(x)$ are smooth vector fields in R^n and $h(x)$ is a smooth mapping from R^n to R . Avoiding the differential geometric theory, we shall say that the system of Eqs. 3.24–3.25 has relative degree r at a point x° if it is necessary to differentiate the output $y(t)$ r times at time t° in order for the value $u(t^\circ)$ of the input to appear explicitly. This definition is completely compatible with the definition for linear systems.

It can be shown that if a system has relative degree r at x° then $r \leq n$. Further, there exists a local coordinate transformation, in terms of the first $r - 1$ total time derivatives of the output function $h(x)$ along the system trajectory, such that in terms of these new coordinates the state space description of the system enjoys a *normal form*:

$$\dot{z}_1 = z_2$$

$$\dot{z}_2 = z_3$$

$$\vdots$$

$$\begin{aligned}
\dot{z}_{r-1} &= z_r & (3.26) \\
\dot{z}_r &= b(\xi, \eta) + a(\xi, \eta)u \\
\dot{\eta} &= q(\xi, \eta)
\end{aligned}$$

where we have used the same notation as in [43] and

$$\eta = \begin{bmatrix} z_1 \\ \vdots \\ z_n \end{bmatrix}, \quad \xi = \begin{bmatrix} z_1 \\ \vdots \\ z_r \end{bmatrix}.$$

In the normal form, we have that the output $y(t)$ is given by $z_1(t)$, i.e., $y(t) = z_1(t)$. If x° is an equilibrium point of the original system such that $h(x^\circ) = 0$, then $(\xi, \eta) = (0, 0)$ can be made to be an equilibrium for the new system.

Feedback control laws for nonlinear systems of the form of Eqs. 3.24–3.25 can be used to solve a variety of problems [43, 81]: the state space exact linearization problem; partial linearization of systems with relative degree strictly less than the system order; the problem of zeroing the output; the problem of reproducing the reference output; the local asymptotic stabilization problem; the problem of tracking the output; asymptotic model matching (which requires dynamic state feedback); the problem of disturbance decoupling; local asymptotic stabilization by means of (high gain) output feedback; etc.

A system with relative degree equal to its order can be exactly linearized by means of static state feedback and coordinate transformations. If the relative degree of a nonlinear system is less than the order of the system, it is still possible to achieve partial linearization. In this case, we must be concerned with the stability properties of the internal dynamics. In some cases, the study of internal dynamics is simplified locally by considering the zero dynamics instead. The zero dynamics of a nonlinear system is an intrinsic property of the system.

We are now in a position to introduce the concept of zero dynamics in a natural way.

3.2.1 Zero Dynamics

Consider the problem of zeroing the output for the system of Eq. 3.26:**

Find, if any, pairs consisting of an initial state x° and of an input function $u^\circ(t)$, defined for all t in a neighborhood of $t = 0$, such that the corresponding output $y(t)$ of the system is identically zero for all t in a neighborhood of $t = 0$.

Because in the normal form $y(t) = z_1(t)$, we have that requiring $y(t) = 0$ for all t results in the condition

$$\dot{z}_1(t) = \dot{z}_2(t) = \cdots = \dot{z}_r(t) = 0$$

which is equivalent to $\xi(t) = 0$ for all times.

The required input is the (unique) solution of the equation

$$0 = b(0, \eta(t)) + a(0, \eta(t))u(t).$$

The behavior of the variable $\eta(t)$ when $\xi(t)$ is identically zero is determined by the equation

$$\dot{\eta}(t) = g(0, \eta(t)). \quad (3.27)$$

From this it is clear that in order to solve the output zeroing problem, the initial state of the system must be such that $\xi(0) = 0$ while $\eta(0) = \eta_0$ can be chosen arbitrarily. The input must be of the form

$$u(t) = -\frac{b(0, \eta(t))}{a(0, \eta(t))}$$

where $\eta(t)$ is given by Eq. 3.27 with initial condition η_0 .

The dynamical system described by Eq. 3.27 corresponds to the *internal* behavior of the system when the input and the initial conditions have been chosen so as to force the output to remain identically zero. For this reason, the dynamics described by Eq. 3.27 are called the *zero dynamics* of the system. See also Ref. [45].

**A. Isidori, *Nonlinear Control Systems*, 2^d ed., Springer-Verlag, Berlin, p. 173.

If we carry out the program described above for linear system, we obtain linear dynamics with eigenvalues coinciding with the zeros of the transfer function of the original linear system, thus the term zero dynamics. It can be shown that the linear approximation of the zero dynamics of a nonlinear system at $\eta = 0$ coincides with the zero dynamics of the linear approximation of the entire system at $x = 0$, i.e.,^{††}

that the operations of taking the linear approximation and calculating the zero dynamics essentially commute.

The zero dynamics have a prominent role in many developments of the nonlinear control systems theory. In the following chapters we shall have occasion to witness this.

Nonminimum Phase Systems

From the presentation in section 3.1.3, it is clear that the zero dynamics defined above, when applied to a linear minimum phase system, are stable. Conversely, the zero dynamics for a nonminimum phase system are unstable. It is then natural to extend the terminology to nonlinear systems in the following way.

Definition 3.6 *The nonlinear system given by Eqs. 3.24–3.25 is said to be (asymptotically, exponentially) minimum phase if its zero dynamics are (asymptotically, exponentially) stable.*

A nonlinear system of the form of Eqs. 3.24–3.25 is said to be nonminimum phase if it is not minimum phase.

As in the linear case, the minimum phase property is highly desirable in a nonlinear setting as well. Any minimum phase nonlinear system can always be locally stabilized by smooth state feedback [16]. Similar results hold for tracking control under more restrictive assumptions [81].

^{††}Ibid., p. 177.

MIMO Extensions

All of the above results have a straight-forward extension to MIMO systems that satisfy some *regularity* conditions. These include, in particular, the class of multivariable nonlinear systems that can be rendered noninteracting via static state feedback, i.e., that can be reduced from an input-output point of view to a collection of independent SISO channels.

Systems that can be rendered noninteracting are those for which a *vector* relative degree $\{r_1, \dots, r_m\}$ at a point x° is defined and for which the so-called decoupling matrix is nonsingular at x° . The vector relative degree has an analogous definition to the SISO relative degree: r_i is the number of times that the i -th output channel has to be differentiated before any input appears. The decoupling matrix, defined in terms of Lie derivatives, is presented here for completeness.

$$A(x) = \begin{bmatrix} L_{g_1} L_f^{r_1-1} h_1(x) & \cdots & L_{g_m} L_f^{r_1-1} h_1(x) \\ \vdots & \vdots & \vdots \\ L_{g_1} L_f^{r_m-1} h_m(x) & \cdots & L_{g_m} L_f^{r_m-1} h_m(x) \end{bmatrix}$$

where g_i , $i = 1, \dots, m$, are smooth vector fields in R^n that form the control distribution matrix $g(x)$ of the MIMO systems, and h_i , $i = 1, \dots, m$, are smooth real-valued mappings that form the output matrix $h(x)$. If $\lambda(x)$ is a real-valued function and $f(x)$ is a vector field both defined on a subset U of R^n , then

$$L_f \lambda(x) = \sum_{i=1}^n \frac{\partial \lambda}{\partial x_i} f_i(x)$$

is called the Lie derivative of λ along f .

Chapter 4

Inverse Dynamics and Feedforward Control

The problem of finding the inverse dynamics of a system is of great interest and goes back to Bode's remarks quoted at the beginning of Chapter 3. Given a plant, the best way to achieve a desired output is to invert or cancel the plant and replace it with one that exactly produces the desired objectives. This is the idea behind the *computed torques* approach used in robotics, for example.

It is conceivable to carry out this cancellation or inversion by placing the *inverse* plant in series with the given plant, i.e., this process could be carried out in open loop without the need for feedback. We remark here that this is often referred to as *feedforward* control to differentiate it from the case when the inverse dynamics problem is solved via feedback. This does not mean that there is a direct feedthrough term from the input to the output. It is to be interpreted rather as the opposite of feedback control, although it can complement feedback control with very good results, as we shall see in Chapter 5.

On the other hand, given the benefits that feedback carries with it, we might ask if we can somehow invert the plant while also closing a feedback loop. In sum, we want to know when, and if, we can invert the plant using either feedback or feedforward control.

The purpose of this chapter is to perform an in-depth investigation of the issues

involved in the inverse dynamics control of manipulators with flexible links. Much work has been presented in the literature, and the author feels it is time to catalog some of this material by clearly stating the important issues, limitations, and contributions.

In order to understand some of the fundamentals of inverse dynamics control, we begin by presenting some results for the relatively simple SISO nonlinear system introduced at the end of Chapter 3. Using these general results, we then confront the problem of solving the inverse dynamics problem for open chains of bodies. The bulk of this chapter is dedicated to a survey of results found in the literature and to a critical analysis of these results *vis à vis* the nonlinear feedback theory and other considerations.

4.1 Nonlinear Feedback Linearization

Consider again a nonlinear SISO system of the form

$$\dot{x} = f(x) + g(x)u \quad (4.1)$$

$$y = h(x) \quad (4.2)$$

where the reader is referred to section 3.2 for the technical assumptions. If this system has relative degree $r < n$ defined at a point x^o , then Eqs. 4.1–4.2 can be put in the normal form

$$\begin{aligned} \dot{z}_1 &= z_2 \\ \dot{z}_2 &= z_3 \\ &\vdots \\ \dot{z}_{r-1} &= z_r \\ \dot{z}_r &= b(\xi, \eta) + a(\xi, \eta)u \\ \dot{\eta} &= q(\xi, \eta) \\ y &= z_1. \end{aligned} \quad (4.3)$$

See also Eq. 3.26. By construction of the normal form (and by definition of relative degree), $a(\xi, \eta) = L_g L_f^{r-1} h(x) \neq 0$ at x° , and thus by the smoothness assumption on $h(x)$ it is nonzero in a neighborhood of x° in R^n .

It is now a trivial matter to solve the partial linearization (exact if $r = n$) problem for the system of Eqs. 4.1–4.2: just choose the control law as

$$u = \frac{1}{a(z)}(-b(z) + v). \quad (4.4)$$

The computed torques procedure of rigid robotics is indeed an exact feedback linearization of the equations of motion possible because the relative degree of the system from torque inputs to joint angular position outputs is the same as the number of states.

Notice that implementing the controller of Eq. 4.4 in Eqs. 4.3 results in a linearized subsystem plus an unobservable (from the chosen output) subsystem given by

$$\dot{\eta} = q(\xi, \eta). \quad (4.5)$$

This subsystem can be viewed as the internal dynamics corresponding to the linearizing control. If the new control input v is chosen so as to command the output to be zero for all time, Eq. 4.5 becomes the zero dynamics defined in Chapter 3. These considerations are summarized graphically in Figs. 4.1–4.2.

Consider now the problem of reproducing a reference output $y_R(t)$. To track this reference exactly, it is apparent from the normal form of the system that we must have initial conditions $\xi(0) = \xi_R(0)$, where

$$\xi_R(t) = \begin{bmatrix} y_R(t) \\ y_R'(t) \\ \vdots \\ y_R^{(r-1)}(t) \end{bmatrix},$$

and controller

$$u(t) = \frac{y_R^{(r)}(t) - b(\xi_R(t), \eta(t))}{a(\xi_R(t), \eta(t))}. \quad (4.6)$$

With this controller, the internal dynamics becomes the *forced* dynamics

$$\dot{\eta}(t) = q(\xi_R(t), \eta(t)). \quad (4.7)$$

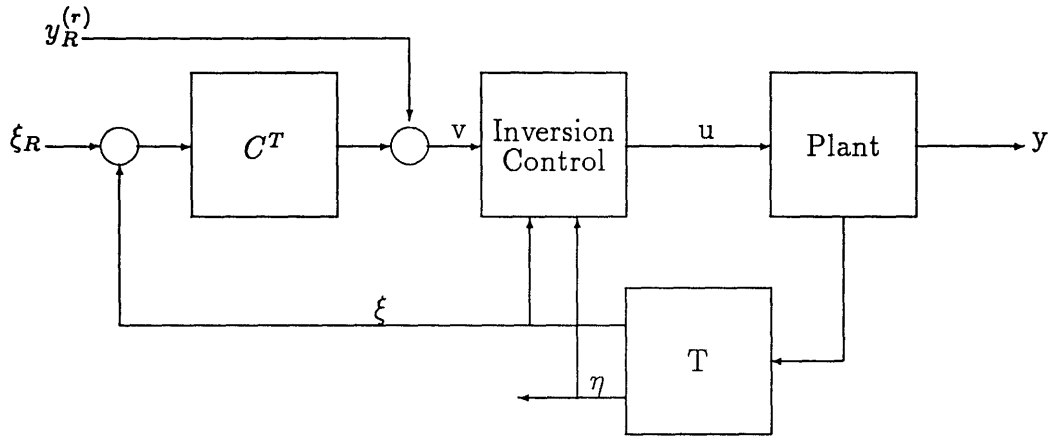


Figure 4.1: Feedback Linearization — Original System

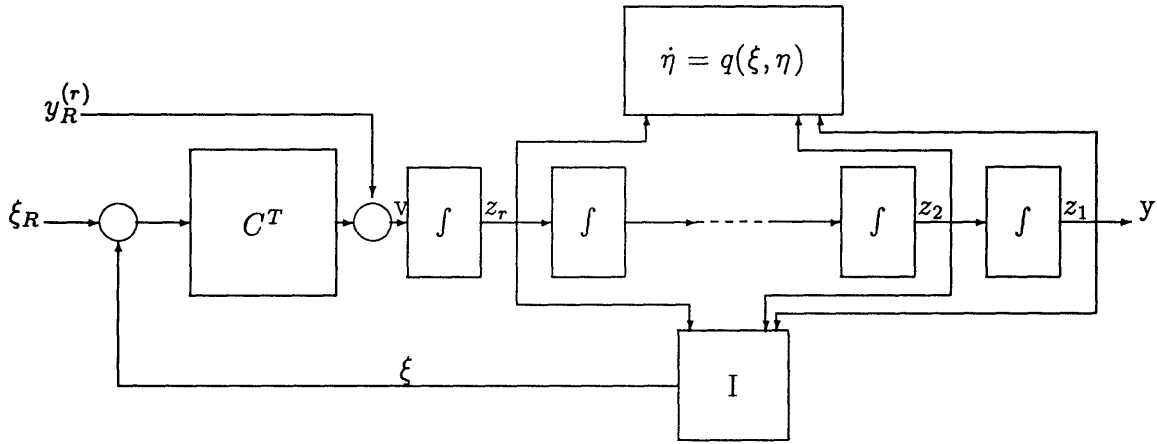


Figure 4.2: Feedback Linearization — Transformed System

The system of Eqs. 4.6–4.7 can be interpreted as a realization of the inverse of the original system, i.e., the inverse dynamics. Note that the above definition for $u(t)$, together with the appropriate initial conditions, guarantee the exact tracking of the reference output.

In practice, setting the initial conditions of a system exactly is not usually possible. For this reason it is of interest to study the asymptotic tracking problem. It is enough to modify Eq. 4.6 in the following way

$$u(t) = \frac{1}{a(\xi, \eta)} \left(-b(\xi, \eta) + y_R^{(r)}(t) - \sum_{i=1}^r c_{i-1} (z_i - y_R^{(i-1)}) \right). \quad (4.8)$$

By proper choice of the real constants c_{i-1} the output $y(t)$ can be made to exponentially converge to the desired output $y_R(t)$.

In all cases it becomes apparent that if the zero dynamics (represented by Eq. 4.5 with $\xi = 0$) are unstable, neither version of the inverse dynamics is implementable or causally feasible. Clearly then, this represents a fundamental limit for nonminimum phase nonlinear systems: the inverse dynamics system is unstable and therefore no causal inverse dynamics solution exists. In the next section we see how some researchers have tried to avoid this limitation. Among others, there are non-causal solutions in which *a priori* selection of the manipulator initial conditions is required so that the inverse dynamics proceed along its stable manifold. Not all of the following are practically feasible.

4.2 Inverse Dynamics Problem

Consider now the problem of open chains of elastic bodies connected by rotary joints with torque actuators at the joints, angular displacement and rate sensors also at the joints, and possibly tip position sensors. If the bodies are rigid, the forward dynamics problem consists of finding the angular displacements, velocities, and accelerations produced by a set of known external torques. Conversely, the inverse dynamics problem consists of finding the joint torques that will produce a desired joint trajectory. Since the bodies are rigid, and in the absence of joint compliance, tip position trajectories can be found by dead-reckoning via the forward kinematics. Alternatively, the tip position trajectories (Cartesian space) can be specified, then the joint trajectories (Joint space) can be determined via the inverse kinematics problem and the inverse dynamics problem proceeds as before.

4.2.1 Chains of Rigid Bodies

For rigid manipulators, the solution of the inverse dynamics problem can be implemented either as a feedforward or a feedback control scheme. In a feedforward scheme, the nominal torques for a predetermined trajectory are used in hopes of increasing the steady state accuracy of a tracking task over the accuracy obtained using a simple error-driven feedback regulator. As a feedback control scheme, the

model-based nonlinear static state-feedback transforms the closed-loop system into a linear and decoupled system made of input-output strings of double integrators ... [t]he tracking of desired trajectories is then easily achieved on the linear side of the problem.*

This feedback implementation is referred to in the literature as computed torques. This is equivalent to the exact feedback linearization presented above. A drawback of computed torques, and all other inversion techniques, is that the effectiveness of the control scheme depends on having the exact model for the nonlinear rigid manipulator. For reasons explained in the previous paragraph, the above two control schemes work equally well for joint-based and cartesian-based control of rigid manipulators.

4.2.2 Chains of Flexible Bodies

As expressed in Ref. [27],

[i]t is appealing to try to find the analogue for flexible arms of the so-called computed torque or inverse control method for rigid robots.

When the bodies in the chain are flexible, the forward and inverse kinematics are complicated by the flexible deflections that the bodies can undergo. For a clear exposition of the kinematics in the presence of flexibility see Ref. [88]. Furthermore, the inverse dynamics problem is nontrivial because certain choices of output result in a nonminimum phase system from joint torque inputs to the output. This is equivalent to saying that the inverse dynamics of the plant is unstable. In these cases, there is no causal solution to the inverse dynamics problem.

Output Definition for Flexible Manipulators

There have been several attempts at solving the inverse dynamics problem for flexible revolute manipulators where the tip position is the desired output. When the manipulator links are modelled as beams, the resulting system is nonminimum phase from

*A. De Luca, *et al.*, Inversion Techniques for Trajectory Control of Flexible Robot Arms, *Journal of Robotic Systems*, Vol. 6, No. 7, 1989

the joint torque inputs to the tip position output. From the discussion in section 4.1 above, it is clear that the solution to the inverse dynamics problem (or input-output linearization, or partial linearization) via state feedback depends entirely on the choice of outputs. For this reason it is convenient to determine from the outset the set of outputs that we shall consider for our system. It is also crucial for the relatively simple nonlinear results presented above that the selected output have a well-defined relative degree (see Chapter 3 for definitions).

In the case of manipulator systems, it is clear that of paramount interest is the position of the tip. As for rigid manipulators, this position can be determined either through cartesian coordinates of the end-effector or through angular coordinates of the hub and kinematic transformations to reconstruct the cartesian coordinates of the tip. When the manipulator links are allowed to bend, we can no longer rely on dead-reckoning to determine the tip position.

In the past, many researchers have chosen as output variable the so-called arc-length tip position. Referring now to the one-link case for simplicity, the arc-length output is defined as

$$y = \eta_y(x, t) + l\theta(t),$$

where l is the link length, θ is the hub angle, and as in Chapter 2 $\eta_y(x, t)$ is the transverse displacement of the link from the cantilvered frame. This choice of output generates a nonminimum phase system. This nonminimum phase nature for similar non-collocated but linear systems involving beams has been reported in the literature [30, 85, 84, 83].

This result, while not unexpected, is definitely not desirable for reasons explained in section 3.2 above. Mainly, we cannot partially linearize a nonminimum phase system. Many attempts have been made to avoid this difficulty by considering new choices of output. See for example Refs. [92, 7]. In Ref. [7] *five* new output definitions which involve some fractional version of the arc-length output are considered. Some even enjoy the property of making the system passive for certain choices of parameters (recall that a passive nonlinear system is one which is minimum phase and has a relative degree of one [17]).

Some of the output redefinitions have merit for the purpose of stabilizing control. The problem remains, however, that we are interested in the performance of the real tip position. Another disadvantage of the arc-length output is the fact that its relative degree is ill-defined as the number of modes in a discretized version of the equations of motion for the flexible beam is increased. This was pointed out by Wang and Vidyasagar [92].

De Luca *et al.* propose the use of the inertial tip angular position for the one-link example as the output of interest. While this output retains the nonminimum phase character of the system, as could be expected, it has a well-defined relative degree for any number of assumed modes in the discretized approximation to the equations of motion. The definition of this output is given in our context by

$$y = \theta + \eta'_y(l, t)$$

where $\eta'_y(x, t)$ was defined in Chapter 2 as the slope of the beam deflection at the x location along the neutral axis in the cantilevered frame.

By defining successive tip angles relative to the previous tip angle, we extend this output definition to the multi-link case. See Chapter 7 for the application to a manipulator with two flexible links.

Review of the State of the Art

In this section we investigate various schemes found in the literature for the inverse dynamics and feedforward control of flexible manipulators. We analyze the different methods in the light of the developments of previous sections and thus determine the validity and wisdom (or lack thereof) of pursuing said methods. We conclude with some definite ideas and insights that carry us into the next chapter and an investigation of yet another method of feedforward control: the nonlinear output regulation theory.

Gebler in Ref. [34] proposed a feedforward control strategy where the inverse dynamics problem is solved approximately. This is done by choosing appropriate nominal values for the joint angles used to determine the feedforward torques under

the assumption of rigid joints and links. These nominal angles consist of the actual desired angles if the manipulator were indeed rigid plus a correction term that takes into account *nominal deflections*. This correction term is determined quasi-statically, assuming that the dynamic forces resulting from deviations from the nominal position are small and can be neglected to determine the feedforward control. Simulation results indicate that oscillations of the endpoint are reduced significantly. Since this method depends on linearization about the nominal trajectory, it is not only highly sensitive to model uncertainty as is the computed torques method, but also relies on a priori knowledge of the trajectories; the *nominal deflections* and corresponding feedforward torques must be computed for each trajectory.

In a similar vein, Asada and Ma [2] solved the inverse dynamics problem for flexible robots in an approximate manner. As is the case with Gebler's scheme, the solution is obtained off-line; a recursive algorithm determines the feedforward torques given a pre-determined desired trajectory. Unlike Ref. [34], however, this solution scheme utilizes a dynamic generator to determine the flexible motion. Further, instead of an approximate *nominal deflection* correction term to the nominal angle, Asada and Ma make use of the *exact* nominal angle to determine the feedforward torques as if the links were rigid. This is accomplished by the use of a *virtual rigid link coordinate system* in the description of the system kinematics. This is nothing other than the floating reference frame (or shadow-beam) obtained when the beam is assumed to be pinned-pinned to its reference frame. The use of these frames to describe the links allows for the exact description (to within first order in the elastic deformations) of the tip trajectory in terms of the virtual rigid link joint angles.

Once these angles are determined, the impressed motion causes elastic deformations which are determined using a dynamic generator. A closed form expression for the relationship between the impressed rigid angular motion and the elastic coordinates is obtained after simplifying the equations of motion assuming that angular rates are small enough. This closed form expression constitutes the dynamic generator and has a special form which is exploited by Asada and Ma to generate a more efficient recursive algorithm than the direct integration of the closed form equation

would yield. In Ref. [3], the authors formulated the inverse dynamics problem of a planar, multi-link, flexible arm by using virtual rigid link coordinate systems. The model there “is still complex and cannot be solved directly.”

In Ref. [27], De Luca et al. analyze the feasibility of both open-loop and closed-loop control for trajectory tracking of flexible robot arms using nonlinear inversion techniques (see Refs. [39,38]). It turns out that in all cases a given control approach is possible if a certain dynamic system associated with the plant, the so-called reduced order inverse system [45] of the flexible arm dynamics, is stable. As was the case in Ref. [2], a dynamic inverse system is seen to be needed for the open-loop torque generator (feedforward scheme). The inverse dynamic system, which may be of full or reduced order, determines the

natural behavior of those system variables which are not directly constrained by the outputs specification ... obtained under the action of the inversion-based input.[†]

This suggests that in Ref. [2] this inverse dynamic system must have been unstable. This inconsistency has not been resolved.

The closed-loop approach is obtained by using the inversion-based algorithm to provide nonlinear static state-feedback, in analogy to the rigid manipulator computed torques scheme. In this case, however, implementation of the closed-loop control scheme results in linear decoupled equations for the output variables together with a second set of equations. This second set of equations are the unobservable part of the system, called the sink (see [27]) or the internal dynamics (see ref. [81]). As suggested above, the open-loop and closed-loop control schemes are feasible only if the associated inverse dynamics or internal dynamics, respectively, are stable.

Under some conditions, it has been shown that the stability properties of these associated dynamic systems are the same, i.e., the closed-loop and open-loop control

[†]A. DeLuca et al., Inversion Techniques for Trajectory Control of Flexible Robot Manipulators, *Journal of Robotic Systems*, pp.325-344.

approaches either both work or both fail. In addition, it has been proven (see ref. [45]) that

in order to conclude on the local stability of the overall system, it is enough to show asymptotic stability of [the zero] dynamics.[†]

De Luca et al. derived the above results assuming a finite dimensional system (same as Refs. [34] and [2]). Using an overly simple finite order model, they found that “there exists a continuous set of points along the flexible arm” that if chosen as outputs yield minimum phase systems. This clearly is only true when one assumes a finite order model. Since a system with distributed flexibility is an infinite order system, their statement would have to be qualified to state that certain points along the flexible body will yield minimum phase systems up to a certain frequency, beyond which higher order modes become evident which unstably interact with the torque inputs (i.e., cause the system with the given output to be nonminimum phase). Note finally that in their paper, De Luca *et al.* do not specify the nature of the spatial discretization used to obtain a finite order model.

Bayo *et al.* in Refs. [8–11, 62] use a frequency domain approach to iteratively solve the inverse dynamics and kinematics of multi-link elastic robots. This iterative solution scheme relies on local linearization of the problem: the solution of each linearization is carried out in the frequency domain. A finite element description of the individual links is obtained with respect to nominal frames associated with each link. The nominal motion of each nominal frame is specified, which permits the linearization of the problem from the outset. In a manner reminiscent of the virtual rigid link coordinate system of Ref. [2], Bayo *et al.* require that the elastic normal deflection at the tip of each link be zero. This is equivalent to saying that the tip will follow the nominal trajectory of the *shadow* rigid beam defined by the nominal hub motion.

For a single link, the linear time-varying equations in the finite element coordi-

[†]A. DeLuca et al., Inversion Techniques for Trajectory Control of Robots, *Journal of Robotic Systems*, pp.325-344

nates are obtained and then Fourier transformed. The torque is then found for each frequency under the condition that the elastic normal deflection at the tip be zero. The solution algorithm also provides the values of the finite element elastic coordinates. When the torque is found for all frequencies of interest, it is inverse Fourier transformed to obtain a non-causal torque in the time domain. The solution process in the frequency domain is iterative in order to handle the time-varying inertial forces due to the impressed motion of the frames. For multiple links, the solution process starts with the last link which has no tip reaction forces. Once the inverse dynamics problem is solved for this link, the reaction forces at the tip of the previous link are determined from equilibrium considerations and included in the linear equations for that link. The solution then proceeds as before. An outer loop iteration is needed in the case of three-dimensional manipulators to correct for elastic tip deflections in the plane formed by the joint axis and the tip of the link; the tip motion of the previous link affects the nominal trajectory of the next link. These deflections are uncontrollable from the joint actuators and thus cannot be forced to zero.

For this solution of the inverse dynamics problem for the tip control of flexible arms to work, the velocity and acceleration profiles, together with the forcing terms, must be Fourier transformable. Further, as mentioned in the previous paragraph, the resulting control law is non-causal:

in order to track the desired trajectory the flexible torques need to be applied before the tip actually moves.[§]

Besides needing a very accurate model for success, as is the case in the computed torques of rigid arms, this solution scheme must be performed off-line for each trajectory of interest. The process has been tested through the use of simulation (see refs. [9–11]) and experiments, see refs. [11, 62] where the computed torques were implemented in open loop except that joint feedback position control was used to ensure zero initial conditions in the presence of offsets due to gravity. This joint

[§]E. Bayo et al., Inverse Dynamics Kinematics of Multi-Link Elastic Robots: An Iterative Frequency Domain, *The International Journal of Robotics and Research*, pp.49-62

feedback control probably does a lot more for the success of the feedforward scheme than is attributed to it. Due to the non-causal and highly model dependent nature of the solution process, I would expect that errors in initial conditions could affect the accuracy of the tracking immensely.

De Luca *et al.* [27] explain the success of the non-causal scheme of Bayo *et al.*, in view of their own results, as follows:

in spite of dynamic instability, a particular choice of initial conditions for the elastic variables ... describing the zero-dynamics may possibly lead to a bounded evolution of these in time.

The output trajectory may be reproduced in a stable way if the system is properly initialized. Because the choice of initial conditions depends on the entire trajectory, the initialization is an off-line, non-causal procedure. In Ref. [62], Moulin *et al.* treat the existence and uniqueness of solutions for the recursive, frequency domain solution to the inverse dynamics problem for flexible multi-link manipulators presented by Bayo *et al.* In short, it is concluded that for a given manipulator, there exists a range of desired motions for which there is a unique solution to the inverse dynamics problem for planar, open-chain, multi-link manipulators. It was established previously that this solution can only be obtained non-causally due to the instability of the zero dynamics. The numerical recursive algorithm proposed by Bayo *et al.* is shown to converge, also for an *appropriate* range of motion.

Note: Geometric stiffening terms are addressed and included in the equations of motion for the first time in Ref. [62]. Previous references ignored their existence (i.e., suffered from premature linearization). In Refs. [2] and [3], erroneous results resulting from inconsistent equations are actually examined and worked into their theory. In Ref. [2], fortunately, the erroneous results lead to the correct conclusion that in order to linearize the equations of motion the angular rates must be below a certain limit.

In Ref. [67] Paden *et al.* present a (δ, T) solution to the inverse dynamics problem: an approximate torque command with the property that the true initial condition is close to the initial condition required to cause the end-effector to follow a delayed version of the desired trajectory. Accordingly, the Bayo *et al.* solution is a $(0, 0)$.

The solution is used for feedforward and together with passive joint controllers is shown to yield exponentially stable tracking under some restrictive assumptions (like sufficiently stiff and damped links).

De Luca [56] solves the inverse dynamics problem for a two-link, planar, revolute manipulator with joint elasticity. He shows that in this case the system is fully linearized and I/O decoupled using dynamic state feedback (i.e., through the introduction of integrators). The resulting length of the I/O chains of integrators equals 6 in this case, but varies if different arm topologies are used. Note that for the case of joint compliance, these chains will never have less than 4 integrators, as opposed to the rigid manipulator case in which the length of the chains is 2 and does not vary. The variability of the integration structure depends on the kind of interactions that arise between elastic and rigid degrees of freedom. The dynamic compensation (in the form of additional integrators) delays the contributions of the inertial interacting effects (parasitic effects); this allows the high authority control paths (those due to the elastic forces directly) to come into play and thus cancellation of nonlinearities is possible.

Madhavan and Singh [58] consider the inverse dynamics problem for a one flexible link arm. They redefine the output by choosing

$$y = \theta_H(t) + \alpha \frac{\eta_y(x, t)}{l}$$

where $\alpha \in [-1, 1]$, and perform input-output linearization. They show that the stability of the resulting zero dynamics depends on α , with stability guaranteed (in the case of a finite number of modes) for $-1 \leq \alpha \leq \alpha^* < 1$. The value of α^* depends on the value of the terminal equilibrium point. They round off their control strategy by designing a linear stabilizer for the final capture of the terminal state and for the stabilization of the elastic modes.

4.2.3 Summary

In summary, because the system whose output is tip position and whose inputs are joint torques is nonminimum phase, an inverse dynamic solution cannot be imple-

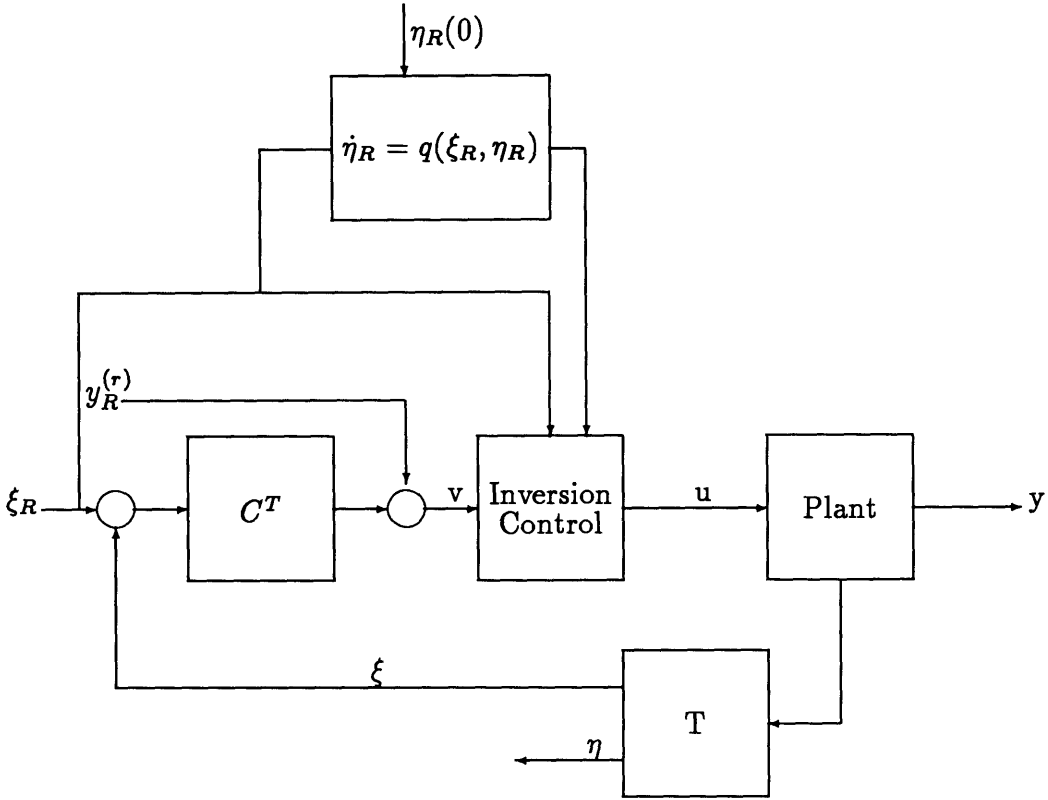


Figure 4.3: Feedforward Inversion Control

mented in feedback form via input/output linearization. It is still possible for off-line, non-causal schemes to be used in order to obtain a feedforward signal [53] through proper initialization of the unstable inverse dynamics. The noncausal schemes are feasible because they are implemented as feedforward control on the non-inverted system. The problem that remains is to ensure that the off-line generator remain stable through proper initialization. Such a procedure is detailed in Ref. [53] for a linear one flexible link system. Figure 4.3 depicts such a noncausal feedforward control. Comparing this figure with Fig. 4.1 we note that the inversion control block is now driven by the desired trajectory and the properly initialized internal dynamics generator.

A much more satisfying, if perhaps equivalent way of looking at the problem is the following. In reality, we want the system outputs (e.g., tip angular positions) to follow some desired trajectories that in a large sense are independent of what the system dynamics are. The only restrictive requirement is that the trajectory be within the manipulator workspace (we ignore for the sake of argument actuator and material

limitations).

Given such a trajectory, and the output as a function of the states, we might ask if there is some manifold within which the states remain bounded yet satisfy the output relation. This is a geometric problem in nature, and it is not surprising to find that the solution exists within the differential geometric control theory. To put it another way, given the trajectories in the state space governed by the nonlinear system equations, find if possible a subspace where the combination of the states through the output function yields the desired trajectories.

The solution to this problem is given by the nonlinear output regulation theory. As we shall see in Chapter 5, in this theory the desired output is assumed to be generated by a dynamical system external to the plant. Lanari and Wen [53] point out that the regulator solution is a particular solution to the plant inversion. We interpret it as the projection of the inverse dynamics solution into the (stable) manifold defined by the exosystem. In this way problems of unstable zero dynamics are circumvented. It is also noteworthy that the nonlinear output regulation scheme is implemented in feedforward.

It is a given that in order to obtain an *inverse* type of controller for the tip (angular) position of flexible manipulators we will have to resort to off-line, non-causal procedures. In this context, we have determined that the nonlinear output regulation theory, to be described in the sequel, holds several advantages over the other non-causal schemes described above. First of all, it generates the desired tip trajectory, and not a delayed, initial condition-dependent version. Its solution does not involve an improper integral over all time in order to obtain the initial conditions that will start the motion along the stable manifold. This in particular does not seem to be a very robust procedure. As we shall see in Chapter 5, there are well defined conditions for the existence of solutions and these define in particular the motions that are possible. Thus this scheme is intuitively appealing as it results in natural trajectories that the manipulator dynamics can follow. Further, approximate solutions of any order can be obtained. This important practical result is a consequence of center manifold theory (see Appendix A) on which the nonlinear output regulation theory is based.

Chapter 5

Output Regulation Theory and Limits of Performance

As seen in Chapter 4, if we take the end-effector (angular) position as the output of the multi-flexible-link manipulator system, the resulting zero dynamics are unstable. This means that inversion-based controllers, such as the computed torques of rigid manipulators, cannot be used to track the end-effector trajectory. For a one-link flexible robot arm, De Luca *et al.* [27] have shown that a nonlinear regulator approach solves this problem by allowing asymptotic trajectory tracking with internal stability. Their approach is based on the nonlinear output regulation theory developed in recent years by Isidori and Byrnes [44].

It is the aim of this chapter to exploit the nonlinear output regulation theory to elucidate the performance limitations inherent in the joint-based control of flexible manipulator end-effectors. In the process we shall make use of both the linear and nonlinear feedback results presented in Chapter 3. First, we shall detail the main results of the theory and highlight those aspects which lead to the development of a performance measure. With this at hand, we shall investigate the existence of inherent performance limits due to the particular nature of our system. Finally, alternative actuator configurations are considered and several control strategies found in the literature are compared *vis à vis* our performance measure.

5.1 Output Regulation Theory

The linear multivariable regulator problem concerns itself with the task of regulating the output of a linear time-invariant (LTI) system, which is subjected to disturbance and reference signals, in the presence of parameter uncertainty. The reference and disturbance signals are assumed produced by some external generator, called the *exosystem*. While this problem has been dealt with by several authors (see for example Refs. [31, 32, 96, 97, 13] and the references in [31]), the work of Francis [31] is of particular interest and utility. In this paper, Francis provides a simpler algebraic solution to the regulator problem than was previously available: he shows that the solvability of a multivariable linear regulator problem corresponds to the solvability of a system of two linear matrix equations. In a related work, Hautus [37] shows that this is in turn equivalent to the transmission polynomials of a composite system, which incorporates the plant and the exosystem, having a certain property.

In recent years, some authors have considered the multivariable regulator problem in a nonlinear setting. A short list of references for their results can be found in Ref. [44]. The definitive work on the subject seems to be the paper by Isidori and Byrnes [44], who extend the results of Francis to autonomous, affine, nonlinear systems with exosystems capable of generating time-varying reference signals and/or disturbances. They further extend Hautus' interpretation to the nonlinear setting through the notion of *zero dynamics* (see Chapter 3). In our presentation, we will closely adhere to the developments in Ref. [44], and, where it is convenient, we will adopt their notation as well.

Let us begin by stating the problem. Consider a nonlinear system of the form

$$\dot{x} = f(x) + g(x)u + p(x)w \quad (5.1)$$

$$\dot{w} = s(w) \quad (5.2)$$

$$e = h(x) + q(w). \quad (5.3)$$

The first of these equations describes the plant with state x defined in a neighborhood X of the origin of R^n and input $u \in R^m$. The term $p(x)w$ represents a disturbance to the plant. The second equation describes the exosystem with state w defined in

a neighborhood W of the origin of R^s . As suggested above, the exosystem describes the class of disturbances and of reference signals that we want to consider. The third equation defines the error $e \in R^p$ between the actual plant output $h(x)$ and the reference signal $q(w)$ that is to be tracked.

The vector $f(x)$, the m columns of the matrix $g(x)$, and the s columns of the matrix $p(x)$ are C^∞ vector fields on X ; $s(w)$ is a smooth vector field on W ; $h(x)$ and $q(w)$ are C^∞ mappings defined on X and on W , respectively, with values in R^p . Further, assume that $f(0) = 0, s(0) = 0, h(0) = 0, q(0) = 0$. This implies that, in the absence of inputs ($u = 0$), the composite system of Eqs. 5.1–5.3 has an equilibrium at the origin of the state space $(x, w) = (0, 0)$, with zero output error.

Definition 5.1 *A state feedback controller for the system of Eqs. 5.1–5.3 will have the form*

$$u = \alpha(x, w) \tag{5.4}$$

where $\alpha(x, w)$ is a C^k mapping defined on $X \times W$, for some integer $k \geq 2$. The closed-loop system obtained by composing Eq. 5.4 with Eq. 5.1 is given by

$$\dot{x} = f(x) + g(x)\alpha(x, w) + p(x)w \tag{5.5}$$

$$\dot{w} = s(w) \tag{5.6}$$

For convenience, we assume $\alpha(0, 0) = 0$. This results in the closed-loop system having an equilibrium at the origin of the state-space. The following definition is included for completeness and for future reference.

Definition 5.2 *An error feedback controller will have the form*

$$u = \theta(z) \tag{5.7}$$

$$\dot{z} = \eta(z, e). \tag{5.8}$$

This is a dynamical system with state z , defined on a neighborhood Z of the origin of R^v . For each $e \in R^p$, $\eta(z, e)$ is a C^k vector field on Z , and $\theta(z)$ is a C^k mapping

defined on Z , for some $k \geq 2$. Composing Eqs. 5.7–5.8 with Eq. 5.1 yields the closed-loop system

$$\dot{x} = f(x) + g(x)\theta(z) + p(x)w \quad (5.9)$$

$$\dot{z} = \eta(z, h(x) + q(w)) \quad (5.10)$$

$$\dot{w} = s(w) \quad (5.11)$$

Again we assume for convenience that $\eta(0, 0) = 0$ and $\theta(0) = 0$.

As stated by Isidori and Byrnes [44], the purpose of control action in this context is to achieve local asymptotic stability and output regulation. By *local asymptotic stability* of the system of Eqs. 5.1–5.3 we mean that when the exosystem is disconnected (w is set to zero), the closed-loop system given by Eqs. 5.5–5.6 (respectively, Eqs. 5.9–5.11) has an asymptotically stable equilibrium at $x = 0$ (respectively, $(x, z) = (0, 0)$). By *output regulation* we mean that in the respective closed-loop systems, for all initial states sufficiently close to the origin, $e(t) \rightarrow 0$ as $t \rightarrow \infty$.

We now state the two relevant synthesis problems.

Problem 5.1 (State Feedback Regulator Problem) *Find, if possible, $\alpha(x, w)$ such that:*

(i) *the equilibrium $x = 0$ of*

$$\dot{x} = f(x) + g(x)\alpha(x, 0)$$

is exponentially stable;

(ii) *there exists a neighborhood $U \subset X \times W$ of $(0, 0)$ such that, for each initial condition $(x(0), w(0)) \in U$, the solution of Eqs. 5.5–5.6 satisfies*

$$\lim_{t \rightarrow \infty} (h(x(t)) + q(w(t))) = 0.$$

Problem 5.2 (Error Feedback Regulator Problem) *Find, if possible, $\theta(z)$ and $\eta(z, e)$, such that:*

(i) *the equilibrium $(x, z) = (0, 0)$ of*

$$\dot{x} = f(x) + g(x)\theta(z)$$

$$\dot{z} = \eta(z, h(x))$$

is exponentially stable;

(ii) *there exists a neighborhood $U \subset X \times Z \times W$ of $(0, 0, 0)$ such that, for each initial condition $(x(0), z(0), w(0)) \in U$, the solution of Eqs. 5.9–5.11 satisfies*

$$\lim_{t \rightarrow \infty} (h(x(t)) + q(w(t))) = 0.$$

In the following we shall present in some detail the results of the nonlinear output regulation theory as developed by Isidori and Byrnes. The reader is also directed to Ref. [43, Chapter 7] for a more leisurely exposition. We start with the linear theory to facilitate an understanding of the more cumbersome nonlinear version.

5.1.1 Linear Regulator Theory

In what follows, we proceed as in Ref. [44] and regard the linear system in question as an approximation of the nonlinear system given by Eqs. 5.1–5.3 at the equilibrium $(x, w) = (0, 0)$:

$$\dot{x} = Ax + Bu + Pw \tag{5.12}$$

$$\dot{w} = Sw \tag{5.13}$$

$$e = Cx + Qw \tag{5.14}$$

where

$$A = \left[\frac{\partial f}{\partial x} \right]_{x=0} \quad B = g(0) \quad P = p(0)$$

$$S = \left[\frac{\partial s}{\partial w} \right]_{w=0} \quad C = \left[\frac{\partial h}{\partial x} \right]_{x=0} \quad Q = \left[\frac{\partial q}{\partial w} \right]_{w=0}.$$

In a similar fashion, the state feedback and error feedback controllers are approximated respectively as

$$u = Kx + Lw \tag{5.15}$$

and as

$$u = Hz \tag{5.16}$$

$$\dot{z} = Fz + Ge \tag{5.17}$$

where

$$K = \left[\frac{\partial \alpha}{\partial x} \right]_{x=0, w=0} \quad L = \left[\frac{\partial \alpha}{\partial w} \right]_{z=0, e=0}$$

$$H = \left[\frac{\partial \theta}{\partial z} \right]_{z=0} \quad F = \left[\frac{\partial \eta}{\partial z} \right]_{z=0, e=0} \quad G = \left[\frac{\partial \eta}{\partial e} \right]_{z=0, e=0}$$

We now express the results of the linear regulator theory, due to Francis [31], in a very succinct manner. Given the following assumptions:

A1: $\sigma(S) \subset \overline{C^+} \triangleq \{\lambda \in C : \text{Re}[\lambda] \geq 0\}$;

A2: the pair (A, B) is stabilizable;

A3: the pair

$$[C \quad Q], \begin{bmatrix} A & P \\ 0 & S \end{bmatrix}$$

is detectable,

the following results describe necessary and sufficient conditions for the existence of solutions to Problems 5.1 and 5.2.

Proposition 5.3 *Suppose A1 and A2 hold. Then, the linear state feedback regulator problem is solvable if and only if there exist matrices Π and Γ which solve the linear matrix equations*

$$\Pi S = A\Pi + B\Gamma + P \tag{5.18}$$

$$C\Pi + Q = 0. \tag{5.19}$$

Proposition 5.4 *Suppose A1, A2, and A3 hold. Then, the linear error feedback regulator problem is solvable if and only if there exist matrices Π and Γ which solve the linear matrix equations 5.18–5.19.*

For completeness, we state the result due to Hautus [37] to which reference was made at the beginning of this section.

Proposition 5.5 *The linear matrix equations 5.18–5.19 are solvable if and only if the system given by Eqs. 5.12–5.14 has the same transmission polynomials as the following system*

$$\dot{x} = Ax + Bu \tag{5.20}$$

$$\dot{w} = Sw \tag{5.21}$$

$$e = Cx. \tag{5.22}$$

5.1.2 Nonlinear Output Regulation Theory

The solution of the nonlinear regulator problem is based upon the following three hypotheses:

H1: $w = 0$ is a stable equilibrium of the exosystem, and there exists a neighborhood $\hat{W} \subset W$ of the origin with the property that each initial condition $w(0) \in \hat{W}$ is Poisson stable [43, p. 352];

H2: the pair $f(x), g(x)$ has a stabilizable linear approximation at $x = 0$;

H3: the pair

$$\begin{bmatrix} f(x) + p(x)w \\ s(w) \end{bmatrix}, \quad h(x) + q(w)$$

has a detectable linear approximation at $(x, w) = (0, 0)$.

We now present the solution to Problems 5.1 and 5.2 in the form of two theorems and supporting lemmas due to Isidori and Byrnes [44]. We include the proofs of Lemma 5.6 and Theorem 5.7 as this will naturally lead into a discussion of some results of center manifold theory (see Appendix A) that form the basis for the development of a performance measure in section 5.2 below.

Lemma 5.6 *Suppose H1 holds and assume that, for some $\alpha(x, w)$, condition 1 of Problem 5.1 is fulfilled. Then, condition 2 is also fulfilled if and only if there exists a*

$C^k, k \geq 2$, mapping $x = \pi(w)$, with $\pi(0) = 0$, defined in a neighborhood $W^\circ \subset W$ of 0, satisfying the conditions

$$\frac{\partial \pi}{\partial w} s(w) = f(\pi(w)) + g(\pi(w))\alpha(\pi(w), w) + p(\pi(w))w \quad (5.23)$$

$$h(\pi(w)) + q(w) = 0. \quad (5.24)$$

Proof: The closed-loop system of Eqs. 5.5–5.6 can be written in the form

$$\dot{x} = (A + BK)x + (P + BL)w + \phi(x, w)$$

$$\dot{w} = Sw + \psi(w)$$

where $\phi(x, w)$ and $\psi(w)$ vanish at the origin with their first-order derivatives. By condition 2 the eigenvalues of the matrix $(A + BK)$ are all in the open left-half complex plane, and by H1 those of the matrix S are on the imaginary axis. This implies that the system in question has a center manifold at $(0, 0)$, the graph of a C^k mapping

$$x = \pi(w)$$

where $\pi(w)$ satisfies Eq. 5.23. From the results of center manifold theory (see Appendix A), this manifold is locally invariant under the flow of Eqs. 5.5–5.6. Using this and H1, we have that for any sufficiently small w° and for every $\epsilon > 0$ and every $T > 0$, the trajectory $(x(t), w(t))$ of Eqs. 5.5–5.6 with $(x(0), w(0)) = (\pi(w^\circ), w^\circ)$, is such that

$$\|x(t) - \pi(w^\circ)\| < \epsilon, \quad \|w(t) - w^\circ\| < \epsilon$$

at some $t > T$. This implies that condition 2 can only hold if this center manifold is annihilated by the error map $e = h(x) + q(w)$, that is, if Eq. 5.24 holds. This shows necessity.

To prove sufficiency, note that if Eq. 5.23 holds, the graph of the mapping $x = \pi(w)$ is a center manifold for the closed-loop system described by Eqs. 5.5–5.6. The equilibrium $(x, w) = (0, 0)$ of the closed-loop system is stable and the center manifold is locally attractive and thus satisfies (see Appendix A and section 5.2 below)

$$\|x(t) - \pi(w(t))\| \leq M e^{-at} \|x(0) - \pi(w(0))\| \quad (M > 0, a > 0)$$

for all $x(0), w(0)$ sufficiently close to zero and all $t \geq 0$. Now by Eq. 5.24

$$e(t) = h(x(t)) - h(\pi(w(t))),$$

and thus by continuity of $h(x)$, $e(t) \rightarrow 0$ as $t \rightarrow \infty$. \square

The following theorem gives the solution to the state feedback regulator problem.

Theorem 5.7 *Under hypotheses H1 and H2, the state feedback regulator problem is solvable if and only if there exist $C^k, k \geq 2$, mappings $x = \pi(w)$, with $\pi(0) = 0$, and $u = c(w)$, with $c(0) = 0$, both defined in a neighborhood $W^\circ \subset W$ of 0, satisfying the conditions*

$$\frac{\partial \pi}{\partial w} s(w) = f(\pi(w)) + g(\pi(w))c(w) + p(\pi(w))w \quad (5.25)$$

$$h(\pi(w)) + q(w) = 0. \quad (5.26)$$

Proof: The necessity follows immediately from Lemma 5.6. To prove sufficiency, note that, by hypothesis H2, there exists a matrix K such that $(A + BK)$ has all its eigenvalues in the open left-half of the complex plane. Suppose conditions 5.25–5.26 are satisfied for some $\pi(w)$ and $c(w)$, and set

$$\alpha(x, w) = c(w) + K(x - \pi(w)). \quad (5.27)$$

This satisfies condition 1 of Problem 5.1. Now note that by construction

$$\alpha(\pi(w), w) = c(w)$$

and thus Eq. 5.25 reduces to Eq. 5.23. But Eqs. 5.26 and 5.24 are identical, so by Lemma 5.6 condition 2 of Problem 5.1 is also satisfied. \square

Equation 5.27 yields a controller that solves the state feedback regulator problem. This controller has the form of a state feedback and the additional input $c(w) - K\pi(w)$. The state feedback portion exponentially stabilizes the closed-loop nonlinear system (locally) since $A + BK$ has all of its eigenvalues in the left-half complex plane. The input $c(w) - K\pi(w)$ induces a forced response which exponentially converges to the desired steady state response $y_{ss}(t) = -q(w(t))$. We shall refer below to $\pi(w)$ as the steady state manifold. Figure 5.1 shows a block diagram of the composite

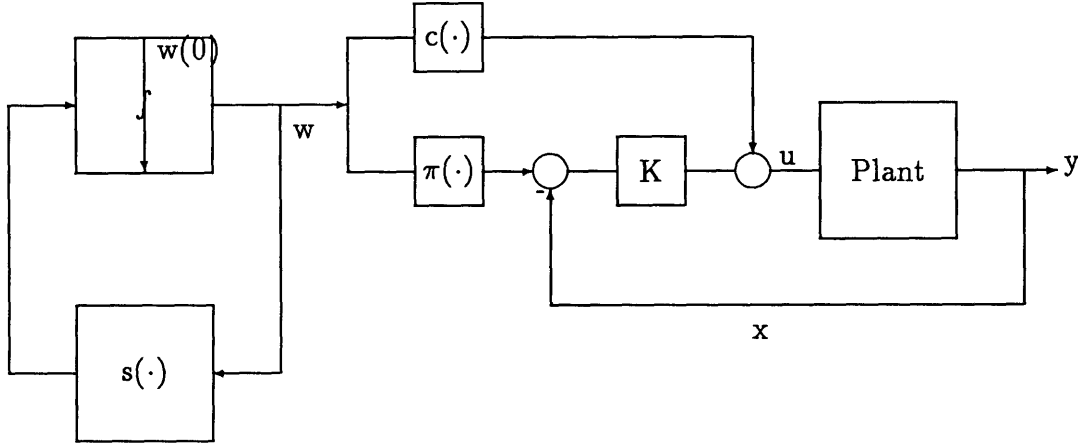


Figure 5.1: Output Regulation Control

feedforward-feedback output regulation controller. This figure should be compared to those presented in Chapter 4.

For the sake of completeness, we now include without proof the solution to the error feedback regulator problem. These results are significant in that they extend the above theory to the class of general dynamic feedback controllers.

Lemma 5.8 *Suppose H1 holds and assume that, for some $\theta(z)$ and $\eta(z, e)$, condition 1 of Problem 5.2 is fulfilled. Then, condition 2 of Problem 5.2 is also fulfilled if and only if there exist C^k , $k \geq 2$, mappings $x = \pi(w)$, with $\pi(0) = 0$, and $z = \sigma(w)$, with $\sigma(0) = 0$, both defined in a neighborhood $W^\circ \subset W$ of 0, satisfying the conditions*

$$\frac{\partial \pi}{\partial w} s(w) = f(\pi(w)) + g(\pi(w))\theta(\sigma(w)) + p(\pi(w))w \quad (5.28)$$

$$\frac{\partial \sigma}{\partial w} s(w) = \eta(\sigma(w), 0) \quad (5.29)$$

$$h(\pi(w)) + q(w) = 0. \quad (5.30)$$

Theorem 5.9 *Under hypotheses H1, H2, and H3, the error feedback regulator problem is solvable if and only if there exists C^k , $k \geq 2$, mappings $x = \pi(w)$, with $\pi(0) = 0$, and $u = c(w)$, with $c(0) = 0$, both defined in a neighborhood $W^\circ \subset W$ of 0, satisfying the conditions*

$$\frac{\partial \pi}{\partial w} s(w) = f(\pi(w)) + g(\pi(w))c(w) + p(\pi(w))w \quad (5.31)$$

$$h(\pi(w)) + q(w) = 0. \quad (5.32)$$

Solvability of the Output Regulator Equations

In Ref. [44], sufficient conditions for the solvability of the nonlinear regulator equations are given in terms of the spectrum of the linearized exosystem equations. In particular, it is proven that if the equilibrium of the exosystem is not hyperbolic, i.e., the eigenvalues of the linearized system have zero real parts, then the regulator equations are solvable. This is consistent with the results from the center manifold theory on which the nonlinear output regulation is founded.

As mentioned in Chapter 7 in the context of a two link manipulator example, these exosystems are capable of generating p -times differentiable trajectories, as well as sinusoidal trajectories.

5.2 Performance Measure

To paraphrase De Luca [26], the output regulation approach enables us to separate clearly the computation of nominal control action, which serves to impose steady-state performance, from the derivation of a feedback law which takes care of system stabilization. This suggests, in analogy to the linear case, two *types* of performance measures that are of relevance. On the one hand there is the steady state performance (steady state error in linear systems) and on the other there is *transient* performance (reaching time or settling time of linear systems).

If the nonlinear output regulation problem is solvable, we are guaranteed that the system will exponentially reach a steady state such that there is no steady state error, in the absence of parameter uncertainty. This is the measure of steady state performance. A contribution of this thesis is the realization that the exponential rate of convergence to this so-called steady state manifold defines the *transient* performance as would be expressed by the settling time in a linear system.

We define our transient performance measure in terms of the error between the actual system trajectory and the desired trajectory on the steady state manifold

$$e(t) = x(t) - \pi(w(t))$$

where we use the same notation as in section 5.1. Recall from the proof of Lemma 5.6 above that, under the proper assumptions, the *center manifold is locally attractive*:

$$\|x(t) - \pi(w(t))\| = \|e(t)\| \leq M e^{-at} \|e(0)\| \quad (5.33)$$

where $M > 0, a > 0$. Of particular note is the exponential nature of the above relation. This implies that under the hypothesis of the nonlinear regulator theory, if a solution exists, $e(t) \rightarrow 0$ exponentially as $t \rightarrow \infty$. Our measure of transient performance consists in determining the rate of this exponential decay, or, more explicitly, in determining the values that the positive constant a can have.

5.2.1 Stability of the Center Manifold

In order to determine the qualitative (as well as quantitative) nature of the constant a in Eq. 5.33, it is necessary to take a closer look at the results from center manifold theory. In Ref. [20], the local asymptotic stability of the center manifold is summarized in the lemma that follows. It is instructive to study the proof of this lemma not only to understand the nature of the exponential constant a , but also to understand the *local* nature of the results of the entire nonlinear regulation theory.

The reader is referred to Appendix A for more details and some preliminary considerations.

Consider the following set of equations

$$\dot{x} = Ax + F(x, y) \quad (5.34)$$

$$\dot{y} = By + G(x, y). \quad (5.35)$$

where the A and B are constant matrices such that the all the eigenvalues of A have zero real parts, and those of B have negative real parts. F and G are defined in Appendix A. By Theorem A.3, the system of Eqs. 5.34–5.35 has a center manifold which we denote by $\pi(x)$.

Lemma 5.10 *Let $(x(t), y(t))$ be a solution of Eqs. 5.34–5.35 with $\|(x(0), y(0))\|$ sufficiently small. Then there exist positive constants C_1 and μ such that*

$$\|y(t) - \pi(x(t))\| \leq C_1 e^{-\mu t} \|y(0) - \pi(x(0))\|$$

for all $t \geq 0$.

Proof: Let $(x(t), y(t))$ be a solution of Eqs. 5.34–5.35 with $(x(0), y(0))$ sufficiently small. Let $z(t) = y(t) - \pi(x(t))$. Then we have that

$$\dot{z} = Bz + N(x, z) \quad (5.36)$$

where

$$N(x, z) = \pi'(x)[F(x, \pi(x)) - F(x, z + \pi(x))] + G(x, z + \pi(x)) - G(x, \pi(x)).$$

Now using the definitions of F and G , there exists a continuous function $\delta(\epsilon)$ with $\delta(0) = 0$ such that

$$\|F(x_1, y_1) - F(x_2, y_2)\| \leq \delta(\epsilon)(\|x_1 - x_2\| + \|y_1 - y_2\|) \quad (5.37)$$

$$\|G(x_1, y_1) - G(x_2, y_2)\| \leq \delta(\epsilon)(\|x_1 - x_2\| + \|y_1 - y_2\|) \quad (5.38)$$

for all $x_1, x_2 \in R^n$ and all $y_1, y_2 \in R^m$ with $\|y_1\|, \|y_2\| < \epsilon$. Further, note that since $\pi(x)$ is C^k , $k \geq 2$, $\pi'(x)$ is bounded over any bounded neighborhood in R^n . Thus, there exists a continuous function $k(\epsilon)$ with $k(0) = 0$ such that $\|N(x, z)\| < k(\epsilon)\|z\|$ if $\|z\|, \|x\| < \epsilon$. Note that this is equivalent to saying that the nonlinearity is Lipschitz in some sufficiently small neighborhood about the origin.

Since all the eigenvalues of B have negative real parts, there exist $\beta > 0$ and $C > 0$ such that for $s \leq 0$ and $y \in R^m$,

$$\|e^{-Bs}y\| \leq Ce^{\beta s}\|y\| \quad (5.39)$$

where β and C depend on the particular vector norm chosen. Using Eqs. 5.36 and 5.39 we get

$$\|z(t)\| \leq Ce^{-\beta t}\|z(0)\| + Ck(\epsilon) \int_0^t e^{-\beta(t-\tau)}\|z(\tau)\|d\tau$$

and the result follows from Gronwall's inequality (see Appendix B):

$$\|z(t)\| \leq C\|z(0)\|e^{-\beta_1 t} \quad (5.40)$$

where

$$\beta_1 = \beta - Ck(\epsilon) \quad (5.41)$$

□

We highlight here for later reference that the local nature of the above results derives from two sources. On the one hand, the existence of a center manifold is a local result (witness the definition of F and G). On the other hand, the nonlinear term $N(x, z)$ above is required to be Lipschitz in some neighborhood of the equilibrium point. In the light of Eq. 5.41, we see that the neighborhood about the origin wherein the above results hold true is bounded by the value that $k(\epsilon)$ takes. By definition, $k(\epsilon)$ is a monotonically increasing function of ϵ . We are thus limited to values of ϵ such that $\beta_1 > 0$. We return to this point in section 5.2.3 below.

By its nature, the exponential decay of Eq. 5.33 is a lower bound on the actual system rate of decay, i.e., the system will decay no slower than this. If the system were linear the rate of decay would be given by the largest (negative) real part of the eigenvalues of the closed-loop system matrix. Indeed this lower bound is *tight* in the sense that, except for very special combinations of initial conditions and forcing, it is also the upper bound for the rate of decay of the system as the linear terms dominate, i.e., if the system is nearly linear, the response cannot decay faster than the eigenvalue with the largest (negative) real part will allow.

The offshoot of all this is that the transient performance of a nonlinear system of the form of Eqs. 5.5–5.6 is determined, at least locally to the steady state manifold, by the closed-loop eigenvalues of the linear approximation to the system at equilibrium. This intuitively appealing result is nonetheless important because it clearly establishes the significant performance measures for nonlinear systems. In some important cases, as we shall see below, the local nature of the results is not as restrictive and in effect nearly global results can be inferred. Finally, the linear aspects of the performance measure facilitate the use of the well-developed linear theory to determine bounds on performance.

5.2.2 Frequency Domain Heuristics

Given an asymptotically stable system, the linear approximation of the system dominates when the state gets close enough to the equilibrium point, assuming of course

the existence of a nontrivial linear approximation. Therefore, locally, the linear performance limits ultimately determine the system performance.

In this context, we note that the *transient* performance measure defined above is determined by the feedback portion of the regulator. In the presence of parameter uncertainty, the feedback controller plays a similar role (at least locally) as in the linear case, namely that of reducing sensitivity to parameter uncertainty and unknown disturbances. In this sense, the frequency domain performance limits discussed in Chapter 3 apply locally to nonlinear systems.

In the light of the already defined transient performance measure in the time domain, it is clear that limits in the gain of the feedback controller directly affect the rate of convergence to the steady state manifold. If these limits are imposed by linear frequency domain considerations such as sensitivity reduction for nonminimum phase systems, the effect will again be observable in the rate of convergence of the trajectory of the nonlinear system to its steady state manifold. Thus, for nonlinear closed-loop systems with a non-trivial linear approximation about the equilibrium, the performance measure defined above clearly establishes the performance bounds derived from the linear approximation to the system as the ultimate performance bounds for the nonlinear system.

We note that these results are not limited to nonlinear systems under static state feedback control. In fact, Theorem 5.9, which is concerned with error feedback, can be extended to any nonlinear dynamic feedback controller that satisfies the nonlinear output regulation assumptions. In particular, the theory is valid for any (linear or nonlinear) controller which locally exponentially stabilizes the nonlinear closed-loop system. In this case, it is again the linear approximation of the closed-loop system that determines the ultimate performance bounds.

5.2.3 On the Local Nature of Results

Recall from the proof of Lemma 5.10 that the local character of the results is due to two facts: first, the proof of existence of the center manifold $\pi(x)$ is local in nature; and second, the nonlinear terms are required to be Lipschitz in some neighborhood

of the equilibrium point. It is the second condition that is most limiting in terms of our performance measure. We note in passing that the first effect is not as restrictive because a global center manifold could exist even if the contraction mapping-based proof of existence failed. The second condition, on the other hand, is equivalent to a measure of nonlinearity that directly limits the rate of exponential decay to the steady state manifold.

In the proof of Lemma 5.10 it was also pointed out that the actual rate of decay to the center manifold is given by the exponential constant β_1 which was defined in Eq. 5.41 as

$$\beta_1 = \beta - Ck(\epsilon)$$

where β and C depend only on B , and $k(\epsilon)$ is a continuous, monotonically increasing function of ϵ that was identified as a local Lipschitz constant for the nonlinear term $N(x, z)$. In effect, $k(\epsilon)$ is the largest first derivative that the norm of N can attain inside a neighborhood $\|x\|, \|z\| < \epsilon$. If $k(\epsilon)$ were bounded with respect to ϵ , then global results could be inferred. A perfunctory examination of the dynamic equations for chains of bodies (e.g., see Chapter 2) shows, however, that these nonlinear terms depend on square velocity terms which are not bounded *a priori*. Nevertheless, this suggests that for sets of bounded trajectories the Lipschitz condition can be met for $k(\epsilon)$ sufficiently large.

The problem now arises that $k(\epsilon)$ cannot be arbitrarily large, since β_1 must remain positive. Since β is determined by the eigenvalues of the linear approximation to the closed-loop system, we have clearly defined quantitatively as well as qualitatively the local nature of the results.

This investigation leads naturally to bounds on the acceptable trajectories. For example, for the local results to remain valid, we might have to limit the magnitude of the angular rates in a manipulator. Given a nonlinear term of the form

$$\|\dot{\theta}^2\| < k(\epsilon)\|x\|, \quad \|x\| < \epsilon, \quad x = \begin{bmatrix} \theta \\ \dot{\theta} \end{bmatrix},$$

we see that $k(\epsilon) \approx \epsilon$ and thus if we require $\beta > Ck(\epsilon)$ then

$$\epsilon < \frac{\beta}{C} \Rightarrow \|\dot{\theta}^2\| < \left(\frac{\beta}{C}\right)^2.$$

5.3 Application to Flexible Robotics

In this section we apply the results from the nonlinear regulator theory to open chains of flexible bodies (e.g., manipulators). The purpose of this program is to expound on and clarify the notion of a performance measure introduced in the previous section. To this end, we present a series of exosystems which will generate desired output trajectories for manipulators with flexible links. We will analyze in particular the one link planar manipulator with revolute joint. In Chapter 7 we will examine in detail the planar two-link manipulator with flexible links and revolute joints.

Once the system, exosystem, and control configuration (number and locations of acutators and sensors) are chosen, the regulator equations (Eqs. 5.25–5.26) are solved for the feedforward control as well as for the steady state manifold. A simple constant gain state feedback is chosen in all cases for the feedback stabilization to the steady state manifold. The constant gain matrix is chosen using linear quadratic regulator (LQR) theory [52] and the linear approximation at equilibrium of the open loop system as the design model. Simulation results show the compliance of the final nonlinear closed-loop system with the performance limits predicted by the linear theory.

Let us begin by noting that the limitations inherent on our system due to its nonminimum phase nature are already apparent in the fact that we cannot use input-output decoupling to implement an inverse dynamics solution. Further limitations in the context of the output regulation theory are expressed by unachievable steady state solutions, e.g., if the regulator problem is not solvable for certain exosystems (see solvability conditions in terms of zero dynamics in Ref. [44]).

The limitations due to an unachievable steady state express limits on the steady state performance. Further, we encounter limits on the *transient* performance. These are due to the limits of performance inherent in linear nonminimum phase systems.

Recall from section 5.2 that the error dynamics has an exponential bound as it converges to the steady state manifold. This bound can be approximated by the linear approximation to the closed-loop dynamics at equilibrium. Because the linear approximation to the open loop dynamics is nonminimum phase, the linear closed-loop dynamics exhibits those performance limits expressed in Chapter 3. Thus, the closed-loop nonlinear system will tend to the steady state manifold at a rate limited by the largest (negative) eigenvalue of the linearized closed-loop system matrix, which in turn is limited by linear nonminimum phase considerations.

5.3.1 Joint Actuation

Manipulator with One Flexible Link

In this section we use the one flexible link manipulator presented in Chapter 2 as our system. We refer in the following to the discretized equations of motion 2.13 which we reproduce here for convenience.

$$M \begin{bmatrix} \ddot{\theta}_H(t) \\ \ddot{\mathbf{q}}(t) \end{bmatrix} + D_t \begin{bmatrix} \dot{\theta}_H(t) \\ \dot{\mathbf{q}}(t) \end{bmatrix} + K \begin{bmatrix} \theta_H(t) \\ \mathbf{q}(t) \end{bmatrix} = -\dot{\theta}_H^2(t) K_t^g \begin{bmatrix} \theta_H(t) \\ \mathbf{q}(t) \end{bmatrix} + B\tau \quad (5.42)$$

The input to this system is the joint torque τ . The output of interest, for reasons described in Chapter 4, is the angular position of the tip. According to De Luca *et al.* [27], this yields a nonminimum phase system with well defined relative degree of two for any number of assumed modes n . In our case the output is given by

$$\begin{aligned} y &= \theta_H(t) + \sum_{i=1}^n \phi'_i(l) q_i(t) \\ &= \begin{bmatrix} 1 & \mathbf{c}_1^T \end{bmatrix} \begin{bmatrix} \theta_H(t) \\ \mathbf{q}(t) \end{bmatrix} \\ \mathbf{c}_1^T &= \begin{bmatrix} \phi'_1(l) & \cdots & \phi'_n(l) \end{bmatrix}. \end{aligned} \quad (5.43)$$

The arm parameters chosen are given in Table 5.1. The space-dependent mode shapes are taken to be the natural mode shapes for a cantilevered-loaded beam with the same parameters (see Appendix C). In this simple example we ignore material damping.

Kg	Kg m ²	m	N m ²
$\rho l = 1.0$	$J_H = 0.0333$	$l = 1.0$	$EI = 15.0$
$m_T = 0$	$J_T = 0$	$b_H = 0.01$	

Table 5.1: Parameters for the One-flexible-link Manipulator

Poles	Zeros
$p_{1,2} = 0$	
$p_{3,4} = \pm 38.8422i$	$z_{1,2} = \pm 18.8251$
$p_{5,6} = \pm 97.8966i$	$z_{3,4} = \pm 108.8176$

Table 5.2: Open Loop Poles and Zeros for the One-flexible-link Manipulator

Choosing the state vector as

$$\mathbf{x} = \begin{bmatrix} \theta_H(t) \\ \mathbf{q} \\ \dot{\theta}_H(t) \\ \dot{\mathbf{q}} \end{bmatrix},$$

and linearizing about the equilibrium point at $\mathbf{x} = 0$, we obtain using MATLAB [59] the poles and zeros given in Table 5.2. Note that we have taken the number of assumed modes to be $n = 2$.

The system of Eqs. 5.42–5.43, with the parameters of Table 5.1 satisfies hypotheses H2 and H3 of the nonlinear regulator problem. In fact, its linear approximation about the equilibrium is both controllable and observable.

Set-point Regulation The exosystem for the set-point regulator problem is trivial:

$$\dot{w} = 0, \quad w(0) = \theta_d, \quad q(w) = w(t) \quad (5.44)$$

where θ_d is the desired final angular position of the tip in inertial space. We follow the notation of section 5.1 above. This exosystem clearly satisfies hypothesis H1 of

Poles		
$p_{1,2} = -18.8251$	$p_{3,4} = -39.7635 \pm 39.7635i$	$p_{5,6} = -108.8176$

Table 5.3: Closed-Loop Poles for the One-flexible-link Manipulator; $\mu = 1 \times 10^{-7}$.

the nonlinear regulator theory. Solving the output regulation equations 5.25–5.26 for $\pi(w)$ and $c(w)$ we obtain

$$c(w) = 0, \quad \pi(w) = \left. \begin{array}{c} w \\ 0 \\ \vdots \\ 0 \end{array} \right\} 2n + 2 \quad (5.45)$$

where we note in particular that the above solution is valid for any number n of assumed modes.

In accordance with the results of the nonlinear regulator theory, we now implement the following control law

$$\tau = K_{reg}(\pi(w(t)) - x(t)) \quad (5.46)$$

where the gains K_{reg} are obtained from the solution of the linear quadratic regulator problem with weighting μ on the control effort and weighting

$$Q = [1 \quad c_1^T \quad 0 \quad 0 \cdots 0]^T [1 \quad c_1^T \quad 0 \quad 0 \cdots 0]$$

on the states.

Starting from zero initial conditions, a desired final tip angular position of $\theta_d = 90^\circ$ is commanded. This is a very large angle maneuver. We reduced the weighting μ on the control effort to achieve the fastest possible response. The linearized closed-loop poles for the lowest weighting ($\mu = 1 \times 10^{-7}$) are presented in Table 5.3. As expected from the results of Chapter 3, a pair of poles gets “stuck” at the mirror image on the left half plane of the first nonminimum phase zero. Simulation results are presented in Fig. 5.2.

From the figure it is first apparent that for this very nonlinear maneuver (with large angle and angular rate) the nonlinear closed-loop system remains stable even for very large controller gains. This stems from the fact that in this case the local results of the nonlinear output regulation theory can be shown to be in fact global (see Chapter 6). Next we see that, in accordance with the theory presented in section 5.2, the nonlinear performance is in fact limited by the linear performance bounds: the settling time for the output error (and the state error) is approximately $4/\text{Real}(z_1) \approx 0.27$ sec, even if the control effort is allowed to increase without limit.

Recall from the linear theory that an even more restrictive limit caused by nonminimum phase zeros is the increase in sensitivity around crossover when the crossover frequency approaches the nonminimum phase zero location from below. This implies that the limit shown in Fig. 5.2 is only ideal and the practical limit will be a decay about ten times slower to account for parameter and disturbance uncertainties.

Sinusoidal Exosystem The following exosystem produces a sinusoidal signal that we want the inertial tip angular position to track. This exosystem is given by

$$\dot{\mathbf{x}} = \begin{bmatrix} 0 & \omega \\ -\omega & 0 \end{bmatrix} \mathbf{w}, \quad \mathbf{w}(0) = \begin{bmatrix} \theta_d(0) \\ \dot{\theta}_d(0) \end{bmatrix}, \quad q(\mathbf{w}) = w_1.$$

This exosystem also satisfies hypothesis H1 of the nonlinear output regulation theory.

In order to solve the regulator equations for this more complicated exosystem, we follow De Luca *et al.* [27] and first invert the system using only one assumed mode. This results in the output tracking the input exactly, while the internal dynamics are unstable. However, since the linear approximation to the system at equilibrium is controllable, we can stabilize the closed-loop system using the results of the output regulation theory.

Because our new system has an unstable minor loop as shown in Chapter 3, with unstable poles of the linear approximation at the locations of the old system's nonminimum phase zeros, this results in performance limitations analogous to those in the case of nonminimum phase zeros, since of course the overall system with the unstable minor loop remains nonminimum phase.

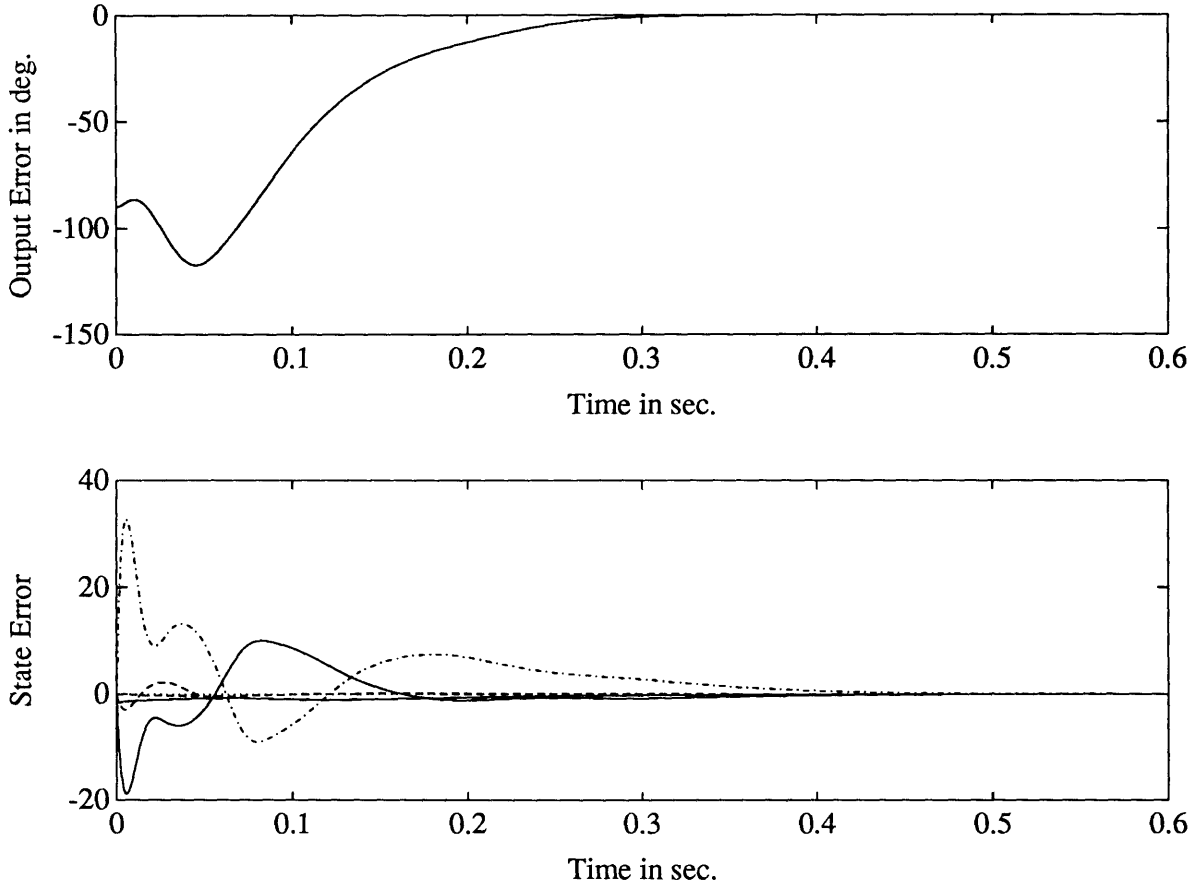


Figure 5.2: Output of One-flexible-link Arm: Set Point Regulation; $\mu = 1 \times 10^{-7}$.

The inversion-based controller given by

$$\tau = \frac{v}{\alpha + \mathbf{c}_1^T \beta} + \frac{\beta^T + \mathbf{c}_1^T \Gamma}{\alpha + \mathbf{c}_1^T \beta} [H\mathbf{q} + D\dot{\mathbf{q}} + \dot{\theta}_H^2(t)K^g\mathbf{q}] \quad (5.47)$$

yields the inverted system

$$\ddot{\mathbf{y}}(t) = v \quad (5.48)$$

$$\ddot{\mathbf{q}}(t) = -(G - \mathbf{m}\mathbf{c}_1^T)^{-1}H\mathbf{q} - (G - \mathbf{m}\mathbf{c}_1^T)^{-1}\mathbf{m}v \quad (5.49)$$

where we have set

$$M^{-1} = \begin{bmatrix} \alpha & \beta^T \\ \beta & \Gamma \end{bmatrix}.$$

We now design for the control input v .

This transformation from our original system of Eq. 5.42–5.43 to the inverted system of Eqs. 5.48–5.49 results in a simpler form of the regulator equations. These are solved, as in Ref. [27], by assuming a solution of $\pi(\mathbf{w})$ in terms of a complete polynomial of the third degree. The results of the Center Manifold Theory presented in Appendix A ensure that we can thus approximate the center manifold to any degree of accuracy desired.

The above decision to use the inverted system points to the fundamental question of the tradeoff between feedback control and feedforward control. The inversion-based control of Eq. 5.47 requires full state feedback. If the nonlinear regulator equations were solved for the original non-inverted system, any (output) error feedback controller that satisfied the conditions of the theory could be used and thus feedback would be minimized.

Solving the regulator equations 5.25–5.26 for the system of Eqs. 5.48–5.49 produces

$$c(\mathbf{w}) = -\omega^2 w_1, \quad \pi(\mathbf{w}) = \begin{bmatrix} w_1 \\ a_1 w_1 + a_{111} w_1^3 + a_{122} w_1 w_2^2 \\ \omega w_2 \\ (3a_{111} - 2a_{122})\omega w_1^2 w_2 + a_1 \omega w_2 + a_{122} \omega w_2^3 \end{bmatrix}$$

where the nontrivial coefficients of the polynomial expansion of $\pi_2(\mathbf{w})$ are defined as

$$a_1 = \frac{m_1 \omega^2}{H_{11} - \omega^2 \text{den}} \quad a_{122} = \left(3\omega^2 - \frac{H_{11}}{\text{den}}\right) \frac{a_{111}}{2\omega^2}$$

$$a_{111} = \frac{-2\omega^2 K^g \text{den}(\omega^2 a_1 - 2\phi_1'(l)\omega^2 a_1^2 + (\phi_1'(l))^2 \omega^2 a_1^3)}{12\omega^4 \text{den}^2 - (H_{11} - 7\omega^2)(H_{11} - 3\omega^2)} \quad \text{den} = G_{11} - m_1 \phi_1'(l).$$

Recall that in solving for the steady state manifold $\pi(\mathbf{w})$ and for the feedforward control $c(\mathbf{w})$ above we have used only one assumed mode so that $n = 1$. It is important to emphasize that this approximate solution is local in nature. If a chosen sinusoidal trajectory has either large frequency or large amplitude the actual steady state manifold will differ from the one given above and this will be reflected in steady state errors.

We now implement the following control law

$$\tau = c(\mathbf{w}(t)) + K_{reg}(\pi(\mathbf{w}(t)) - \mathbf{x}(t)) \quad (5.50)$$

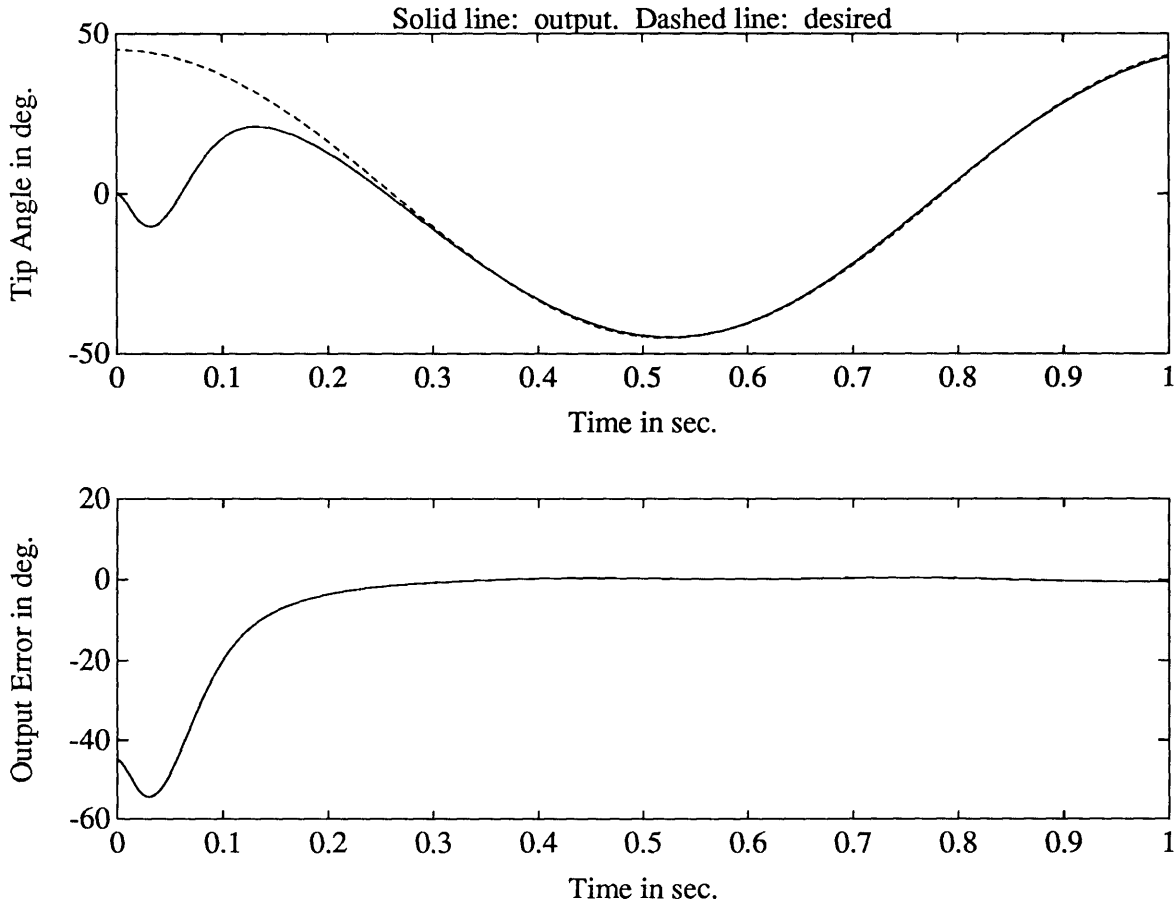


Figure 5.3: Output of One-flexible-link Arm: Sinusoidal Regulation; $\mu = 1 \times 10^{-7}$, $A = 45^\circ$, $\omega = 6$ r/s.

where as in the set-point regulation case the gains K_{reg} are obtained from the solution of the linear quadratic regulator problem with weighting μ on the control effort and weighting Q as before on the states.

Starting from zero initial conditions, two desired sinusoidal trajectories are specified for the motion of the tip angular position. In the first one, a sinusoid with amplitude of 45° and frequency $\omega = 6$ rad/sec is specified. The resulting output and state errors are shown in Fig. 5.3.

In order to show the usefulness of the nonlinear output regulation theory, and to further demonstrate the validity of our performance measure, a second sinusoid is commanded with a frequency of $\omega = 60$ rad/sec. Notice that this frequency is quite a bit higher than the first natural frequency of the linearized system. To stay within the

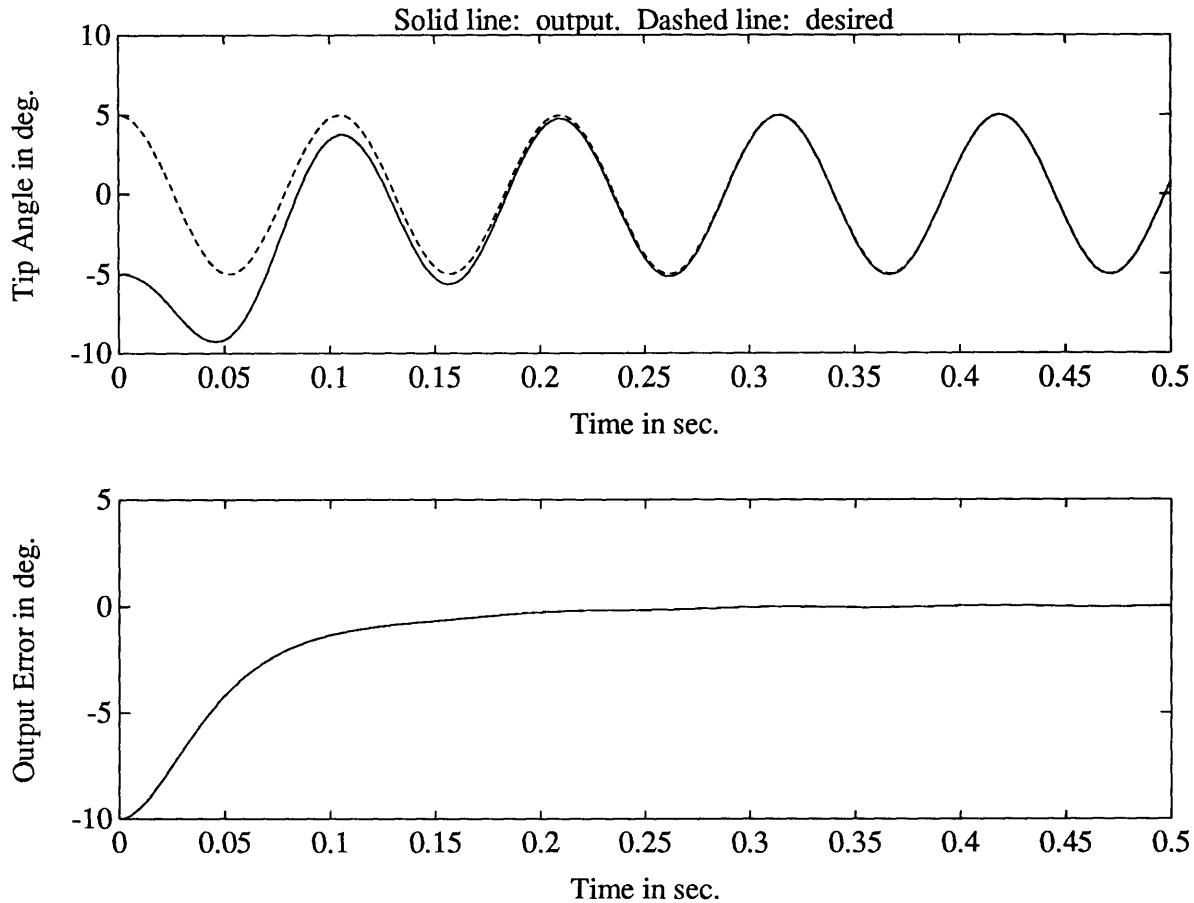


Figure 5.4: Output of One-flexible-link Arm: Sinusoidal Regulation; $\mu = 1 \times 10^{-7}$, $A = 5^\circ$, $\omega = 60$ r/s.

realm of validity of the theory, however, we are forced to use a much smaller amplitude so that our local approximate solution to the steady state manifold remains accurate. For this reason we select an amplitude of 5° . Figure 5.4 shows the actual versus the desired tip angular positions, and the corresponding output error.

In Fig. 5.4 we see first that tracking of a very fast sinusoid is achieved in steady state. It is also clear that the rate of convergence to the steady state, the *performance measure* defined above, is again limited by the pole that gets stuck at the first nonminimum phase zero location. Notice in particular that in the simulation of the faster sinusoid we have used a new initial condition: -5° . We did this because if we start at the origin of the state space, as before, the feedforward element of the control law exceeds the feedback element, which depends on initial errors. In this particu-

lar instance, and since we are applying our control design to the nominal plant, it happens that the feedforward control helps the state reach its steady state. For this reason, the feedforward control is given by $c(\mathbf{w}) + K\pi(\mathbf{w})$, as we decrease the control weighting μ the feedforward control helps the state reach the steady state even faster and we do not see the limit of performance due to the feedback portion of the control. Of course, this is deceiving since all the limits to sensitivity, i.e., to the benefits of feedback, are still in effect even if they are not apparent in the time domain simulation.

As can be seen from Fig. 5.4, however, when the feedback portion of the control dominates due to a large enough initial error, the limits of the feedback control again become apparent.

5.3.2 Other Actuators

In this section we briefly examine the effect that the addition of more actuators has in the performance limits for manipulators with flexible links. For this purpose we select again the one-link arm analyzed in section 5.3.1 and implement a set-point regulator. The difference is in the control topology: we now include an ideal torque actuator at the tip as well as at the joint of the arm.

The equations of motion are identical to those shown in section 5.3.1, Eqs. 5.42–5.43 except for the control weighting matrix B which now becomes

$$B = \begin{bmatrix} 1 \\ \mathbf{c}_1 \end{bmatrix}$$

where \mathbf{c}_1 is the same as in Eq. 5.43. This reflects the fact that there is a torque actuator at the tip of this new system. The output under consideration is still the same: the tip angular position in inertial space. The arm parameters are chosen as before to be those shown in Table 5.1, and the open loop poles are the same as those shown in Table 5.2. However, in this case there are no open loop zeros. Note that as before we have chosen the number of assumed modes to be $n = 2$.

Using the exosystem given by Eq. 5.44, and solving the regulator equations 5.25–5.26 for $\pi(\mathbf{w})$ and $c(\mathbf{w})$, we obtain similar results as those of Eq. 5.45, except

Poles	
$p_{1,2} = -6.71505 \pm 10.3232i$	$p_{3,4} = -13.6243 \pm 56.9732i$
$p_{5,6} = -111.819 \pm 143.088i$	

Table 5.4: Closed-Loop Poles for the One-flexible-link Manipulator; $\mu = 1 \times 10^{-5}$.

that now $\mathbf{c}(\mathbf{w}) = 0$ and \mathbf{w} are 2×1 vectors, with $w_1 = \theta_d$, $w_2 = 0$, and $\pi_1(\mathbf{w}) = w_1$, $\pi_i(\mathbf{w}) = 0$ for $i = 2, \dots, 2 + 2n$.

The controller is given by

$$\tau = K_{reg}(\pi(\mathbf{w}(t)) - \mathbf{x}(t)) \quad (5.51)$$

where τ is a 2×1 vector and K_{reg} is a $2 \times (2 + 2n)$ matrix of gains obtained from the solution of the linear quadratic regulator problem with control weighting $\mu = 1 \times 10^{-5}$ and state weighting matrix Q defined above. The closed-loop poles are given in Table 5.4.

The response to a desired step of 45° is shown in Fig. 5.5. Zero error steady state is achieved and the state remains bounded, as expected from the output regulation theory. Notice that the steady state manifold is reached much faster than what was possible when only the joint torquer was available (~ 0.075 sec settling time as opposed to ~ 0.27 sec in the joint actuator case). In theory, since there are no transmission zeros in the present case, there are no fundamental limitations to the benefits of feedback of the kind presented in Chapter 3 (other than of course practical ones due to disturbances, parameter uncertainties, unmodelled dynamics and actuator bandwidth).

Notice from Table 5.4 that the bottom two complex pole pairs would seem to indicate a much slower response than what we observe in Fig. 5.5. However, these poles are nearly cancelled by zeros of the transfer function from tip torque to tip angle obtained after closing the joint torque state feedback as an inner loop. Thus in the state response we see a decay commensurate with the lowest closed-loop poles, while

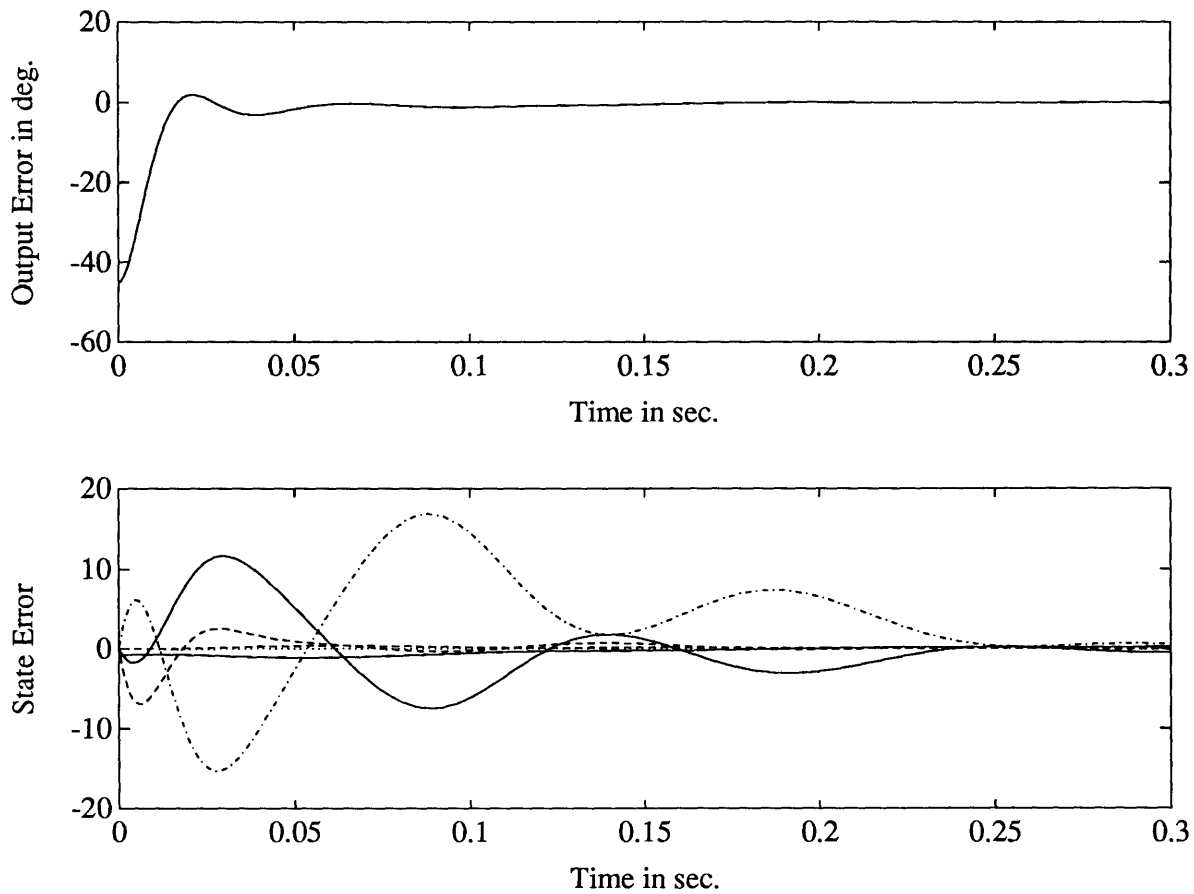


Figure 5.5: Output of One-flexible-link Arm: Set Point Regulation; $\mu = 1 \times 10^{-5}$.

in the tip response we see a much faster response corresponding to the complex pole pair with the largest modulus.

Chapter 6

Robustness vs. Performance in Feedback Control

In Chapter 5 we saw that in the context of the nonlinear output regulation theory the complementary roles of feedback control and feedforward control are made explicit. In this chapter we examine in more detail the stabilizing role of feedback and analyze the tradeoffs between robust, globally stabilizing feedback control, and high performance, locally defined feedback control.

We start this chapter with some mathematical preliminaries needed in order to prove the global asymptotic stability of the joint proportional plus derivative (PD) control of a single flexible link manipulator. We proceed to present this very basic result, which is shown here for the first time in the literature. We then examine full state feedback control options and the possibilities for higher performance stabilizing control.

6.1 Mathematical Preliminaries

In the following we assume the reader is familiar with the basic concepts from functional analysis. In particular, the concepts of linear vector spaces, norms, Banach spaces, and L^p spaces. A basic introduction to these topics is given in Ref. [57]. Reference [76] provides a more rigorous treatment. The following definitions, which

pertain in particular to the study of partial differential equations, are less common and are thus provided here for convenience. The reference for this material is Adams [1].

Let $\alpha = (\alpha_1, \dots, \alpha_n)$ be an n -tuple of nonnegative integers α_i . Then α is called a *multi-index* and

$$x^\alpha = x_1^{\alpha_1} \cdots x_n^{\alpha_n},$$

where x is in R^n .

Definition 6.1 *If $D_i = \partial/\partial x_i$, for $1 \leq i \leq n$, then*

$$D^\alpha = D_1^{\alpha_1} \cdots D_n^{\alpha_n}$$

denotes a differential operator of order $|\alpha|$.

Consider the arbitrary domain $\Omega \subset R^n$. Define a functional $\|\cdot\|_{m,p}$, where m is a nonnegative integer and $1 \leq p \leq \infty$, as

$$\|u\|_{m,p} = \left(\sum_{0 \leq |\alpha| \leq m} \|D^\alpha u\|_p^p \right)^{1/p} \quad \text{if } 1 \leq p < \infty, \quad (6.1)$$

$$\|u\|_{m,\infty} = \max_{0 \leq |\alpha| \leq m} \|D^\alpha u\|_\infty \quad (6.2)$$

for any function u for which the right sides are well defined. $\|\cdot\|_p$ is the $L^p(\Omega)$ norm.

Define now the following three spaces:

1. $H^{m,p} \equiv$ the completion of $u \in C^m(\Omega) : \|u\|_{m,p} < \infty$ with respect to the norm $\|\cdot\|_{m,p}$,
2. $W^{m,p}(\Omega) \equiv u \in L^p(\Omega) : D^\alpha u \in L^p(\Omega)$ for $0 \leq |\alpha| \leq m$, and
3. $W_0^{m,p} \equiv$ the closure of $C_0^\infty(\Omega)$ in the space $W^{m,p}(\Omega)$.

$C^\infty(\Omega) = \bigcap_{m=0}^\infty C^m(\Omega)$, where $C^m(\Omega)$ is the vector space of all functions ϕ which, together with all their partial derivatives $D^\alpha \phi$ of orders $|\alpha| \leq m$, are continuous on Ω . $C_0^\infty(\Omega)$ consists of all those functions in $C^\infty(\Omega)$ which have compact support in Ω .

These spaces, equipped with the appropriate norm given by Eqs. 6.1 or 6.2, are the so-called *Sobolev spaces* over Ω . Note that $W^{0,p}(\Omega) = L^p(\Omega)$, and if $1 \leq p < \infty$,

$W_0^{0,p}(\Omega) = L^p(\Omega)$. Further, $H^{m,p}(\Omega) = W^{m,p}(\Omega)$ for every domain Ω . The Sobolev imbedding theorem asserts the existence of imbeddings of $W^{m,p}(\Omega)$ into spaces of the type $W^{j,q}(\Omega)$, $j \leq m$. For an exhaustive treatment of the imbedding theorem and its properties, the reader is referred to Ref. [1].

6.1.1 Dynamical Systems in Banach Spaces

Further background on the material presented in this section can be found in Refs. [35, 98, 36].

Definition 6.2 *A dynamical system on a Banach space \mathcal{B} is a function $u : \mathbb{R}^+ \times \mathcal{B} \rightarrow \mathcal{B}$ such that u is continuous, $u(0, \phi) = \phi$, $u(t + \tau, \phi) = u(t, u(\tau, \phi))$ for all $t, \tau \geq 0$ and ϕ in \mathcal{B} .*

Definition 6.3 *A positive orbit (half-trajectory) $\gamma^+ = \gamma^+(\phi)$ through ϕ in \mathcal{B} is defined to be $\gamma^+(\phi) = \cup_{t \geq 0} u(t, \phi)$.*

In Refs. [98, 35], conditions are given for the stability of invariant sets of general dynamical systems in terms of Lyapunov functionals. The general philosophy is the same as for dynamical systems defined by ordinary differential equations in finite dimensional spaces. That is to say, stability being a property essentially determined by the distance or metric function in a given space, the existence of a Lyapunov function (or functional) guarantees that the system trajectories remain in the neighborhood of the invariant set. In this sense the results of Lyapunov stability theory extend in a straightforward manner to general dynamical systems in metric spaces.

For a discussion of the Lyapunov stability results in finite dimensional spaces, the reader is referred to [90].

6.1.2 An Invariance Principle

As expressed pithily by Hale*:

*J.K.Hale, "Dynamical Systems and Stability," *J. of Math Anal. and Appl.*, 26, 1969, p. 39.

Of basic importance in the theory of a dynamical system on a Banach space \mathcal{B} is the concept of a limit set $\omega(\gamma)$ of an orbit γ through a point ϕ in \mathcal{B} . One can be assured that $\omega(\gamma)$ is nonempty and invariant if γ belongs to a compact subset of \mathcal{B} . In applications it is much easier to show that an orbit belongs to a bounded set than it is to show it belongs to a compact set.

In the case that a dynamical system is given by ordinary differential equations, and thus \mathcal{B} is finite dimensional (e.g., R^n), the local compactness of \mathcal{B} guarantees that a bounded orbit belongs to a compact set of \mathcal{B} . Dynamical systems defined on infinite dimensional Banach spaces do not possess this nice property, since these spaces are not locally compact. Some dynamical systems, such as those generated by retarded functional differential equations, possess the property that trajectories become smoother as the system evolves in time. In this case, even though \mathcal{B} is infinite dimensional, it can be shown that bounded orbits belong to compact subsets.

Unfortunately, partial differential equations, as well as functional differential equations of neutral type, do not in general possess this smoothing property. However[†]

[t]he basic space \mathcal{B} in such situations is usually a Sobolev space and the well-known Sobolev imbedding theorems imply in general the existence of a Banach space \mathcal{C} such that the unit ball in \mathcal{B} belongs to a compact set in \mathcal{C} . Therefore, any bounded orbit of the dynamical systems on \mathcal{B} would have a nonempty limit set in \mathcal{C} . The limit set in \mathcal{C} should then enjoy an invariance property.

In this section, we will follow closely the development presented by Hale in Ref. [36]. We start with some definitions concerning limit sets and Lyapunov functions.

Definition 6.4 *Let u be a dynamical system on \mathcal{B} . For any ϕ in \mathcal{B} , the ω -limit set $\omega(\phi)$ of the orbit through ϕ is the set of ψ in \mathcal{B} such that there is a nondecreasing sequence $\{t_n\}$, $t_n > 0$, $t_n \rightarrow \infty$ as $n \rightarrow \infty$ such that $\|u(t_n, \phi) - \psi\|_{\mathcal{B}} \rightarrow 0$ as $n \rightarrow \infty$.*

[†]*Ibid.*

Definition 6.5 Let u be a dynamical system on \mathcal{B} . A set M in \mathcal{B} is an invariant set of the dynamical system if for each ϕ in M there is a function $U(t, \phi)$ defined and in M for t in $(-\infty, \infty)$ such that $U(0, \phi) = \phi$ and for any σ in $(-\infty, \infty)$,

$$u(t, U(\sigma, \phi)) = U(t + \sigma, \phi)$$

for all t in \mathbb{R}^+ .

Lemma 6.6 Let u be a dynamical system on \mathcal{B} and suppose the orbit $\gamma^+(\phi)$ through ϕ belongs to a compact subset of \mathcal{B} . Then the ω -limit set $\omega(\phi)$ of $\gamma^+(\phi)$ is a nonempty, compact, connected invariant set.

Let u be a dynamical system on \mathcal{B} and V be a continuous scalar function defined on \mathcal{B} . Define $\dot{V}(\phi) = \dot{V}_{\mathcal{B}}(\phi)$ as

$$\dot{V}(\phi) = \limsup_{t \rightarrow 0^+} \frac{1}{t} [V(u(t, \phi)) - V(\phi)]. \quad (6.3)$$

Then we can define, following LaSalle [54],

Definition 6.7 A function $V : \mathcal{B} \rightarrow \mathbb{R}$ is a Lyapunov function on a set G in \mathcal{B} if V is continuous on \overline{G} , the closure of G , and $\dot{V}(\phi) \leq 0$ for ϕ in G .

Let S be the set defined by

$$S = \{\phi \text{ in } \overline{G} : \dot{V}(\phi) = 0\}$$

and let M be the largest invariant set in S of the dynamical system. Then the following theorem is a straightforward extension of a similar theorem for ordinary differential equations (see Ref. [54]).

Theorem 6.8 Suppose u is a dynamical system on \mathcal{B} . If V is a Lyapunov function on G and an orbit $\gamma^+(\phi)$ belongs to G and is in a compact set of \mathcal{B} , then $u(t, \phi) \rightarrow M$ as $t \rightarrow \infty$.

Note that, as remarked by Hale [36], a sufficient condition for an orbit $\gamma^+(\phi)$ to remain in G if ϕ belongs to G is that the conditions of Thm. 6.8 be satisfied for G a component of the set $U_\rho = \{\phi \text{ in } \mathcal{B} : V(\phi) < \rho\}$. In other words, if in addition to the conditions stated in the theorem, G is such that $V(\phi) < \rho$, for some constant ρ , for all ϕ in G .

Limit Dynamical Systems

Theorem 6.8 describes the limiting behavior of an orbit of a dynamical system when this orbit remains in a compact subset of the space. We now present a formal procedure for determining when this is indeed the case in view of our comments (at the beginning of this sub-section) on dynamical systems generated by partial differential equations. The basic idea is to show that the given dynamical system on \mathcal{B} is also a dynamical system on a larger space \mathcal{C} ; and that when \mathcal{B} is considered as imbedded in \mathcal{C} , the unit ball in \mathcal{B} belongs to a compact subset of \mathcal{C} . In this manner, we can assert that a bounded orbit has a nonempty limit set if the convergence is taken in the appropriate space.

Again we follow the development in Ref. [36].

If \mathcal{B} and \mathcal{C} are Banach spaces, we shall say that $\mathcal{B} \subset \mathcal{C}$ if there exists a continuous linear injection $i : \mathcal{B} \rightarrow \mathcal{C}$. If $\mathcal{B} \subset \mathcal{C}$, there is a constant $K > 0$ such that $\|i(\phi)\|_{\mathcal{C}} \leq K\|\phi\|_{\mathcal{B}}$ for all ϕ in \mathcal{B} .

Definition 6.9 *Suppose $\mathcal{B} \subset \mathcal{C}$ and u is a dynamical system on \mathcal{B} and \mathcal{C} . Let $\mathcal{B}^* \subset \mathcal{C}$ be the set consisting of the union of \mathcal{B} and any ϕ in \mathcal{C} for which there is a ψ in \mathcal{B} such that ϕ belongs to $\omega_{\mathcal{C}}(\psi)$, the ω -limit set in \mathcal{C} of the orbit $\gamma^+(\psi)$ in \mathcal{C} . Then $u : \mathbb{R}^+ \times \mathcal{B}^* \rightarrow \mathcal{B}^*$ is a dynamical system and we refer to this dynamical system as the limit dynamical system of \mathcal{B} in \mathcal{C} .*

If \mathcal{B} is a Hilbert space, then $\mathcal{B}^* = \mathcal{B}$ in accordance with the Banach-Saks theorem [12].

The following lemma is a trivial extension of Lemma 6.6, where effectively \mathcal{B} is replaced by \mathcal{B}^* .

Lemma 6.10 *Suppose $\mathcal{B} \subset \mathcal{C}$ and u is a dynamical system on \mathcal{B} and \mathcal{C} . If ϕ in \mathcal{C} is such that $\gamma^+(\phi)$ belongs to a bounded set of \mathcal{B} and a compact set of \mathcal{C} , then the ω -limit set $\omega(\phi)$ of the orbit through ϕ is a nonempty, compact, connected set in \mathcal{B}^* , an invariant set of the limit dynamical system and $\text{dist}_{\mathcal{C}}(u(t, \phi), \omega(\phi)) \rightarrow 0$ as $t \rightarrow \infty$.*

Theorem 6.11 *Suppose $\mathcal{B} \subset \mathcal{C}$, u is a dynamical system on \mathcal{B} and \mathcal{C} and each bounded orbit of \mathcal{B} belongs to a compact set of \mathcal{C} . Also suppose the function $V_{\mathcal{B}}$ is*

a Lyapunov function on $G_{\mathcal{B}} = \{\phi \text{ in } \mathcal{B} : V_{\mathcal{B}} < \eta\}$, $V_{\mathcal{C}}$ is a Lyapunov function on $G_{\mathcal{C}} = \{\phi \text{ in } \mathcal{C} : V_{\mathcal{C}} < \eta\}$, $G_{\mathcal{B}} \subset G_{\mathcal{C}}$,

$$R = \{\phi \text{ in } \overline{G_{\mathcal{C}}} : \dot{V}_{\mathcal{C}}(\phi) = 0\}$$

and N is the largest invariant set in R of the limit dynamical system. If $G_{\mathcal{B}}$ is bounded and ϕ is in $G_{\mathcal{B}}$, then $u(t, \phi) \rightarrow N$ in \mathcal{C} as $t \rightarrow \infty$.

6.2 Joint PD Control

6.2.1 One Flexible Link Arm

In this section we are concerned with showing the stability of a flexible arm, consisting of a single flexible link, under the action of a simple joint proportional-plus-derivative (PD) controller. As described in greater detail in Chapter 2, the arm consists of a rigid hub free to rotate in the plane to which a flexible Bernoulli-Euler beam is attached in a cantilevered way (See Fig. 2.1). In what follows, we will refer to the nondimensionalized Eqs. 2.7–2.10. Notice that these equations assume that there is no tip body.

Dynamical System

In order to use the theory developed in the previous section, we must show that Eqs. 2.7–2.8 do indeed generate a dynamical system over an appropriate Banach space. As mentioned earlier, the natural spaces for partial differential equations are Sobolev spaces. Demonstrating that the equations under consideration form a dynamical system is equivalent to showing the existence, and uniqueness, and continuous dependence on the initial data of solutions to the said equations.

Showing existence and uniqueness of solutions to nonlinear partial differential equations is a nontrivial matter that is the current subject of much research in theoretical mathematics. Given the particular nature of the equations under consideration in this thesis, it is perhaps possible to extend results showing existence and uniqueness of the linear version of the equations. These results are based on the theory of

semigroups of operators [5]. Using the linear results, and proceeding in a manner similar to that of Dafermos [24], it might be possible to use contraction arguments to prove the existence and uniqueness of our ‘quasilinear’ equations.

Following the above procedure, one is likely to obtain local (in t) results. To obtain global existence, one constructs a Lyapunov function and invokes the continuation theorem to obtain a dynamical system of a subset of the space.

Dafermos uses the method of Faedo-Galerkin to show existence and uniqueness of quasilinear equations of nonlinear elasticity. This coincides with finite dimensional approximations to the solutions not unlike the assumed modes or finite element methods used in standard engineering practice to approximate solutions of equations of the type under consideration in this thesis. If numerical approximate solutions exist and are unique for increasing dimensions, as computer simulations suggest, and as could be surmised by the fact that the discretized equations of motion are not particularly ill-behaved, then the limiting infinite dimensional solution is likely to exist and be unique.

Carr [20] presents results from semigroup theory that show that for an infinite dimensional nonlinear system, such as the one we consider in this work, if the nonlinear terms are locally Lipschitzian then there exists a unique, maximally defined weak solution that is given by the variation of constants formula and that is local in time. However, here again it is possible to extend this solution for all time if for some initial conditions the trajectories remain bounded. Thus, if we can construct a Lyapunov functional for our system, we can show existence and uniqueness of a weak solution for all time.

Since for the system under consideration we can indeed construct a Lyapunov functional, and since our system exhibits nonlinearities which are locally Lipschitzian, in the following, existence and uniqueness of solutions to equations of the type of Eqs. 2.7–2.8 will be assumed. Furthermore, following results from the theory of linear partial differential equations [82], we will assume that if the initial conditions are infinitely differentiable on the whole of the (appropriate) space of the independent space variables (x in our case), and in the absence of inhomogeneous inputs, then the

solution itself has all derivatives of all orders. This means in particular that solutions will be defined on any Sobolev space W_2^k for arbitrary k .

Under these assumptions, and letting

$$\mathbf{x} = \begin{bmatrix} \eta_{\mathbf{y}}(x, t) \\ \theta_H(t) \end{bmatrix}, \text{ and } u = \begin{bmatrix} \mathbf{x} \\ \dot{\mathbf{x}} \end{bmatrix} \quad (6.4)$$

we have that u is a dynamical system on $\mathcal{B} = W_2^3 \times R \times W_2^1 \times R$ and also on $\mathcal{C} = W_2^2 \times R \times L_2[0, 1] \times R$.

Lyapunov Functions and Stability

In the following developments, we are concerned with showing the stability of the equilibrium at the origin of the dynamical system generated by the nonlinear partial differential equations 2.7–2.8. It is clear from these equations that $u(t, u_0) = 0 \forall t$ if $u_0 = 0$, where $u(t, u_0) = u(t)$ is the solution to Eqs. 2.7–2.8 with initial conditions $u(0) = u_0$. In other words, the origin is indeed an equilibrium of the system under consideration.

Let \mathcal{D} denote the class of functions $\mathbf{x}(s) = [\eta_{\mathbf{y}}(s), \theta_H]^T$ for $s \in [0, 1]$, such that $\eta_{\mathbf{y}} \in W_2^4$ and $\theta_H \in R$ and

$$\eta_{\mathbf{y}}(0) = \eta_{\mathbf{y}}'(0) = \eta_{\mathbf{y}}''(1) = \eta_{\mathbf{y}}'''(1) = 0. \quad (6.5)$$

Introduce in \mathcal{D} the inner product

$$\langle \mathbf{x}, \mathbf{y} \rangle = \int_0^1 \mathbf{x}(s)^T \mathbf{y}(s) ds$$

According to Balakrishnan [6], (must check this) the completion of \mathcal{D} in this inner product yields the Hilbert space

$$\mathcal{H} = L_2[0, 1] \times R.$$

On $\mathcal{D} \subset \mathcal{H}$, define the operator A by

$$\mathbf{x} = \begin{bmatrix} \eta_{\mathbf{y}}(\cdot) \\ \theta_H \end{bmatrix}; \quad A\mathbf{x} = \begin{bmatrix} \eta_{\mathbf{y}}''''(\cdot) \\ K\theta_H \end{bmatrix}. \quad (6.6)$$

Then for $\mathbf{x} \in \mathcal{D}$

$$\langle A\mathbf{x}, \mathbf{x} \rangle = \int_0^1 (\eta_y''(s))^2 ds + K\theta_H^2 \quad (6.7)$$

Note that A is self-adjoint and positive definite, for $K > 0$. In particular, $A\mathbf{x} = 0$ implies that $\mathbf{x} = 0$, since

$$\eta_y''''(s) = 0 \Rightarrow \eta_y(s) = a_3s^3 + a_2s^2 + a_1s + a_0$$

$$\mathbf{x} \in \mathcal{D} \Rightarrow a_i = 0 \quad \forall i$$

$$K\theta_H = 0 \Rightarrow \theta_H = 0.$$

Now define the mass operator $M(\mathbf{x})$ as

$$M(\mathbf{x})\mathbf{x} = \begin{bmatrix} 1 & s + b \\ s + b & I + (s + b + \eta_x(s))^2 + \eta_y^2(s) \end{bmatrix} \begin{bmatrix} \eta_y(s) \\ \theta_H \end{bmatrix} \quad (6.8)$$

Clearly, $M = M^T$. Furthermore, M can be shown to be uniformly positive definite as follows. Consider

$$\mathbf{x}^T M(s, \mathbf{x})\mathbf{x} \geq \lambda_{\min}(s, \mathbf{x})|\mathbf{x}|_2^2 \geq \left(\inf_{s \in [0,1]} \lambda_{\min}(s, \mathbf{x}) \right) |\mathbf{x}|_2^2$$

where the minimum eigenvalue λ_{\min} of M is given by

$$\begin{aligned} \lambda_{\min} &= \frac{1}{2}(I + (s + b + \eta_x(s))^2 + \eta_y^2(s) + 1) \\ &\quad - \frac{1}{2}\sqrt{(I + (s + b + \eta_x(s))^2 + \eta_y^2(s) + 1)^2 - 4(I + \eta_y^2(s))}. \end{aligned}$$

Notice that $\lambda_{\min} > 0 \quad \forall s, \eta_y(s)$. In fact

$$\inf_{s \in [0,1]} \lambda_{\min} = \min_{s \in [0,1]} \lambda_{\min} = \lambda_{\min}(0, 0) \triangleq \lambda_0 > 0.$$

Letting $K = 0$ for the moment, we obtain the following expressions for the Kinetic and Potential energies of our system when $\mathbf{x} \in \mathcal{D}$ (compare to Eqs. 2.9 and 2.10):

$$V = \frac{1}{2}\langle A\mathbf{x}, \mathbf{x} \rangle \quad (6.9)$$

$$T = \frac{1}{2}\langle M(\mathbf{x})\dot{\mathbf{x}}, \dot{\mathbf{x}} \rangle \quad (6.10)$$

We would like to use the above defined inner product, together with the operators A and $M(\mathbf{x})$, to define an energy norm in an appropriate space. However, we need \mathbf{x}

to be in \mathcal{D} since Eq. 6.9 is true only if \mathbf{x} is in the domain of A . To get around this problem, consider

$$u = \begin{bmatrix} \mathbf{x} \\ \dot{\mathbf{x}} \end{bmatrix}$$

in the cross product space $\mathcal{H}_E = \mathcal{D}(\sqrt{A}) \times \mathcal{H}$ with inner product

$$\langle u, v \rangle_E = \langle \sqrt{A}u_1, \sqrt{A}v_1 \rangle + \langle M(u_1)u_2, v_2 \rangle. \quad (6.11)$$

Define the candidate Lyapunov function V_E as

$$V_E(u) = \frac{1}{2} \langle u, u \rangle_E \quad (6.12)$$

for u defined as in Eq. 6.4. Recalling from section 6.1 the standard norm in Sobolev spaces, and using the fact that $\mathbf{x} \in \mathcal{D}$ implies that $\eta_y(x, t)$ satisfies the boundary conditions 6.5, it is possible to write the following equivalent norm in \mathcal{C} :

$$\|\cdot\|_{\mathcal{C}}^2 = \int_0^1 (\eta_y''(s))^2 ds + \theta_H^2 + \int_0^1 \dot{\eta}_y^2(s) ds + \dot{\theta}_H^2.$$

If we now let

$$\begin{aligned} \gamma_1 &= \min \left[\frac{\lambda_0}{2}, \frac{1}{2} \right] \\ \gamma_2 &= \min \left[\frac{K_p}{2}, \frac{1}{2} \right] \end{aligned}$$

then $0 < \gamma_1, \gamma_2 \leq \frac{1}{2}$, and it is clear that

$$V_{\mathcal{C}}(\cdot) \triangleq V_E(\cdot) \geq \gamma_1 \gamma_2 \|\cdot\|_{\mathcal{C}}^2. \quad (6.13)$$

This shows that $V_{\mathcal{C}}$ is indeed positive definite with respect to the norm in \mathcal{C} .

The total time derivative of $V_{\mathcal{C}}$, also called the *derivative of $V_{\mathcal{C}}$ along the motion* $u(t, u_0)$, is given by Eq. 6.3:

$$\begin{aligned} \dot{V}_{\mathcal{C}}(u) &= \frac{d}{dt}(T + V) + K_p \dot{\theta}_H \theta_H \\ &= \dot{\theta}_H (\hat{\tau} + K_p \theta_H) \\ &= -\dot{\theta}_H K_d \theta_H \leq 0 \quad \forall t \end{aligned} \quad (6.14)$$

In the last step above we have finally used the fact that we want to implement a joint PD controller. The controller is given by

$$\hat{\tau}(t) = -K_p \theta_H - K_d \dot{\theta}_H \quad (6.15)$$

where K_p and K_d are both positive constants. Notice also that we put $K = K_p$ in the definition of the operator A , which in the interest of clarity could be written as $A(K)$.

Equation 6.14 shows first of all that $V_{\mathcal{C}}$ is a Lyapunov function according to Def. 6.7 on every set G in \mathcal{C} . More importantly, Eqs. 6.13 and 6.14 together show that the equilibrium is stable in the sense of Lyapunov (i.s.L.) relative to the norm in \mathcal{C} . (Reference here to appropriate stability theorem taken from yellow Hahn p. 198 and written in section on stability at beginning of chapter.)

Invariance Principle and Asymptotic Stability

It is possible to extend the above results to show indeed asymptotic stability of the equilibrium. For this purpose we need to use the theory presented in section 6.1.2 concerning invariance properties of general dynamical systems on Banach spaces.

To use the developments of section 6.1.2, consider the smaller space $\mathcal{B} = W_2^4 \times R \times W_2^2 \times R$. As pointed out earlier, u is also a dynamical system on \mathcal{B} . Taking into account that motions $u(t, u_0)$ must satisfy the boundary conditions 6.5, we can write down the following equivalent norm on \mathcal{B} :

$$\|\cdot\|_{\mathcal{B}}^2 = \int_0^1 \left[(\eta_y''''(s))^2 + (\eta_y''(s))^2 \right] ds + \theta_H^2 + \int_0^1 \left[\dot{\eta}_y^2(s) + (\dot{\eta}_y'(s))^2 \right] ds + \dot{\theta}_H^2. \quad (6.16)$$

Define now the candidate Lyapunov function

$$V_{\mathcal{B}}(u) = V_E(\tilde{u}) + V_{\mathcal{C}}(u) \quad (6.17)$$

where

$$\tilde{u} = \begin{bmatrix} \eta_y''(s, t) \\ \theta_H(t) \end{bmatrix}.$$

It is then clear that

$$V_{\mathcal{B}}(\cdot) \geq \gamma_1 \gamma_2 \|\cdot\|_{\mathcal{B}}^2 \quad (6.18)$$

and thus $V_{\mathcal{B}}$ is positive definite with respect to the norm in \mathcal{B} .

Taking the total derivative of $V_{\mathcal{B}}$ with respect to time we obtain

$$\dot{V}_{\mathcal{B}}(u) = \dot{V}_{\mathcal{E}}(\tilde{u}) + \dot{V}_{\mathcal{C}}(u). \quad (6.19)$$

$\dot{V}_{\mathcal{E}}(\tilde{u})$ depends on the square of the angular acceleration $\ddot{\theta}_H(t)$. Examining the partial differential equation of motion, for consistency $\ddot{\theta}_H(t)$ must be of the same order as the small elastic deformations. This is equivalent to a smoothness condition on acceptable trajectories so that the elastic deformations do remain small and thus Bernoulli-Euler beam theory does apply. For this reason, $\dot{V}_{\mathcal{E}}(\tilde{u})$ is a second order term and neglecting it we obtain:

$$\dot{V}_{\mathcal{B}}(u) = -\dot{\theta}_H K_d \dot{\theta}_H \leq 0 \quad \forall t. \quad (6.20)$$

Equation 6.20 shows that $V_{\mathcal{B}}$ is a Lyapunov function in every set G in \mathcal{B} . Further, Eqs. 6.18 and 6.20 together show that the equilibrium is stable i.s.L. relative to the norm in \mathcal{B} .

Consider in particular a set $G_{\mathcal{B}} = \{\phi \text{ in } \mathcal{B} : V_{\mathcal{B}}(\phi) < \eta\}$. $V_{\mathcal{B}}$ is a Lyapunov function of $G_{\mathcal{B}}$ for any $\eta > 0$. Let $\eta = V_{\mathcal{B}}(u_0) + \epsilon$, $\epsilon > 0$. In this case it is clear that $V_{\mathcal{B}}(t) < \eta \quad \forall t$. From Eq. 6.17, this implies that $\eta_{\nu}(x, t)$, together with its spatial partial derivatives up to order 3, and $\theta_H(t)$ are bounded for all time, which in turn implies that $G_{\mathcal{B}}$ is bounded and further $u_0 \in G_{\mathcal{B}}$.

Now let $G_{\mathcal{C}} = \{\phi \text{ in } \mathcal{C} : V_{\mathcal{C}}(\phi) < \eta\}$, where $\eta = V_{\mathcal{B}}(u_0) + \epsilon$ as above. Then it is clear from the results of the previous section that $V_{\mathcal{C}}$ is a Lyapunov function on $G_{\mathcal{C}}$. In addition, $G_{\mathcal{B}} \subset G_{\mathcal{C}}$. Define

$$Q = \{\phi \text{ in } \overline{G_{\mathcal{C}}} : \dot{V}_{\mathcal{C}}(\phi) = 0\}$$

and let M be the largest invariant set in Q of the limit dynamical system.

In order to invoke the results of Thm. 6.11, we only need to show that $\mathcal{B} \subset \mathcal{C}$, and that every bounded orbit of \mathcal{B} belongs to a compact set of \mathcal{C} . Recall that we have already established that u is a dynamical system on both \mathcal{B} and \mathcal{C} . Furthermore, the famous Sobolev imbedding theorems [1] establish that the natural mapping which

imbeds \mathcal{B} into \mathcal{C} is a compact map, and consequently $\mathcal{B} \subset \mathcal{C}$, and every bounded orbit in \mathcal{B} is in a compact set in \mathcal{C} .

Theorem 6.11 then states that $u(t, u_0) \rightarrow M$ in \mathcal{C} as $t \rightarrow \infty$. It remains to show that the equilibrium at the origin is the only element of M .

Asymptotic Stability of the Equilibrium If u is in Q , then $\dot{\theta}_H(t) = 0 \forall t$. This implies that $\ddot{\theta}_H(t) = 0 \forall t$. Taking into account the control law given by Eq. 6.15, and the fact that $u(t)$ must be a solution of Eqs. 2.7–2.8, we obtain that u in Q must be generated by the following linear partial differential equation:

$$\ddot{\eta}_y(x, t) + \eta_y''''(x, t) = 0 \quad (6.21)$$

with boundary conditions given by Eq. 6.5, and an *additional* natural boundary condition at $x = 0$ given by

$$\eta_y''(0, t) - b\eta_y''''(0, t) = K_p\theta. \quad (6.22)$$

Notice that for u in Q , $\theta_H(t) = \theta$, where θ is a constant.

The boundary condition given by Eq. 6.22 can be given the following physical interpretation. It expresses the moment balance that must exist between the spring torque that the controller effectively generates, and the root moments the beam generates due to its internal elastic forces. In the absence of joint motion, as must be the case in Q , these moments must balance.

The partial differential equation 6.21, being linear, can be easily solved using a separation of variables arguments. This leads to the solution of an eigenvalue problem which generates a family of natural modes of vibration which form a complete set of orthonormal modes. Using these modes, and invoking the Expansion Theorem (see [60]), it is possible to write the solution of Eq. 6.21 as

$$\eta_y(x, t) = \sum_{i=1}^{\infty} \bar{\eta}_{y_i}(x) q_i(t) \quad (6.23)$$

where the $\bar{\eta}_{y_i}(x)$ satisfy the homogeneous boundary conditions 6.5 and the $q_i(t)$ satisfy

$$\ddot{q}_i(t) + \omega_i^2 q_i(t) = 0, \quad i = 1, 2, \dots \quad (6.24)$$

and $\omega_i^2 = \lambda_i^4$ and the λ_i are the eigenvalues associated with the orthonormal modes $\bar{\eta}_{y_i}(x)$. The reader is referred to Ref. [60] for further details.

Equation 6.24 can be solved directly, yielding

$$q_i(t) = q_i(0) \cos \omega_i t + \dot{q}_i(0) \frac{\sin \omega_i t}{\omega_i} \quad (6.25)$$

$$q_i(0) = \int_0^1 \bar{\eta}_{y_i}(x) \eta_y(x, 0) dx \quad (6.26)$$

$$\dot{q}_i(0) = \int_0^1 \bar{\eta}_{y_i}(x) \dot{\eta}_y(x, 0) dx. \quad (6.27)$$

Requiring the solution 6.23 to satisfy condition 6.22 we obtain

$$\sum_{i=1}^{\infty} \tau_i(0) q_i(t) = K_p \theta \quad (6.28)$$

$$\tau_i(0) = \bar{\eta}_{y_i}''(0) - b \bar{\eta}_{y_i}'''(0). \quad (6.29)$$

(Note that the series in Eq. 6.23 is absolutely and uniformly convergent—see Ref. [60]).

Since this must hold for all time, we have in particular that

$$\sum_{i=1}^{\infty} \tau_i(0) q_i(0) = K_p \theta \quad (6.30)$$

It is straightforward to show that $\tau_i(0) > 0 \forall i$. This condition has a nice physical interpretation: all system modes are observable at the joint.

Substituting Eq. 6.25 into Eq. 6.28, and given that $\omega_i \neq 0$ for any i , we get that

$$q_i(0) = \dot{q}_i(0) = 0 \forall i.$$

This in turn implies, from Eqs. 6.25 and 6.30 that

$$q_i(t) = \theta = 0 \forall i, t.$$

This leads us to the conclusion that if u is in Q , then

$$\eta_y(x, t) = \dot{\eta}_y(x, t) = \theta_H(t) = \dot{\theta}_H(t) = 0 \forall t, x \in [0, 1],$$

and thus the equilibrium at the origin is the only point in Q , and thus in M .

This concludes the proof of asymptotic stability of the origin for the one-flexible-link arm free to rotate in the plane under the action of a joint PD controller. More specifically, we have shown that every solution of our system that starts out with bounded initial conditions in \mathcal{B} approaches the origin in \mathcal{C} as time evolves:

$$\eta_y''(x, t), \eta_y'(x, t), \eta_y(x, t), \theta_H(t), \dot{\eta}_y(x, t), \dot{\theta}_H(t) \rightarrow 0 \text{ as } t \rightarrow \infty.$$

6.2.2 Manipulators with Multiple Flexible Links

It seems possible to extend the above results to manipulator systems with multiple flexible links when independent joint PD controllers are used. The general partial differential equations in this case, while being more complex, have the same fundamental properties of positive definiteness of the mass and stiffness operators and of possessing a natural Lyapunov function in the energy of the system. For this reason, the extension of the above stability results should proceed in a straightforward manner. This is left as a suggestion for future work.

In addition, we remark that by considering motions in Hilbert spaces, it seems likely that global asymptotic stability results can also be shown for passive joint controllers. This has been done for finite dimensional nonlinear systems (see for example Ref. [17]) and for infinite dimensional linear systems [93].

6.3 Full State Feedback

In this section we investigate how we can extend the results of the previous sections if we assume that full state feedback is available. In practice, this is possible through distributed strain measurements or through the use of modal sensors [23, 70]. We still assume only actuation at the joint in the form of a torquer is available.

We are interested in particular in obtaining higher performance stabilizing controllers and in investigating the feasibility of globally stable tracking control.

6.3.1 Trajectory Tracking

By using the feedback linearization schemes presented in Chapter 4, it is possible to partially linearize the system of Eqs. 2.7–2.8. As mentioned in that chapter, the feasibility of a feedback linearizing control scheme will depend on the choice of outputs and in the stability properties of the internal dynamics in the case only partial linearization is achieved.

The feedback linearizing controller for our system of Eqs. 2.7–2.8 is given by

$$\tau = Iv - \int_0^1 (x + b)\eta_y''''(x, t)dx + \int_0^1 (x + b)\dot{\theta}_H^2(t)\eta_y(x, t) \quad (6.31)$$

when the chosen output is the hub angle. This control law is everywhere defined and so is the trivial change of coordinates that yields the partially linearized system. For this reason, the joint trajectory control could be made globally exponentially stable if we could show that the internal dynamics are globally stable. In other words, the global or local property of the stability is determined by the global or local stability of the internal dynamics, while the linearized input output behavior can always be made exponentially stable by proper choice of the new input v . Of course, the internal dynamics could be unstable, in which case the controller is not implementable.

The internal dynamics for our system are given by Eq. 2.8 itself, where now $\theta_H(t)$ is to be considered as exponentially converging to the desired joint trajectory. Because the stability of the internal dynamics depend on the trajectories that $\theta_H(t)$ follows, we are forced to investigate these on a per case basis or to limit ourselves to local results by examining the linearized zero dynamics. Following the latter course, we obtain from Eq. 2.8 the equation for a Bernoulli-Euler clamped-loaded beam. This means that the zero dynamics are stable.

In conclusion, we can guarantee only local stability of the system with the linearizing feedback control law given by Eq. 6.31 and at this level of generality. For a given trajectory more could be said.

6.3.2 Higher Performance Feedback Control

In this section we resort to the spatially discretized equations of motion for the one-link case. This is particularly useful for comparison with the results of later chapters where design and implementation models are taken to be finite dimensional per force. At the end of this section we outline how the results would proceed in the more general infinite dimensional case.

The well-known and much used Lyapunov linearization [81] method establishes connections between local stability of a nonlinear system and the stability of its lin-

earization about equilibrium. In particular, if the system linearization is strictly exponentially stable, then the system itself is asymptotically stable about the equilibrium. If the linearized system is unstable, so is the nonlinear system. Finally, if the linear system is marginally stable, then nothing can be concluded from the linearization of the system at that equilibrium.

In cases when the linearized system is exponentially stable, we might be interested in determining if the stability of the nonlinear system itself is exponential to some degree, rather than just asymptotic. This of course is a question of performance and we are interested here in the possible tradeoffs between locality and higher performance. The quantification of such a tradeoff is of high practical interest.

Using as in Chapter 5 results inspired by the center manifold theory (see Appendix A), we are able to effect such a quantification by examining a system in the form

$$\dot{y} = By + g(y) \quad (6.32)$$

where B is a constant matrix with all of its eigenvalues having negative real parts; and the function g is assumed to be C^r , $r \geq 2$, with $g(0) = 0$, $g'(0) = 0$. Note that B can be looked at as the linearization of a closed-loop nonlinear system. Using the variations of constant formula, and if g is locally Lipschitzian with Lipschitz constant $k(\epsilon)$, then we get

$$\|y(t)\| \leq Ce^{-\beta t} \|y(0)\| + Ck(\epsilon) \int_0^t e^{-\beta(t-\tau)} \|y(\tau)\| d\tau \quad (6.33)$$

where, since all of the eigenvalues of B have negative real parts we can find $\beta > 0$ and $C > 0$ such that for $s \leq 0$ and $y \in \mathcal{R}^n$

$$\|e^{-Bs}y\| \leq Ce^{\beta s} \|y\|.$$

Using Gronwall's inequality (see Appendix B) we obtain that

$$\|y(t)\| \leq C \|y(0)\| e^{-\beta_1 t} \quad (6.34)$$

where

$$\beta_1 = \beta - Ck(\epsilon) \quad (6.35)$$

Equation 6.35 provides the desired tradeoff between the local nature of our control and the achievable performance. The actual performance is estimated by β_1 . The exponential constant β is determined by our controller designed using the linearized equations about equilibrium as a local design model. The Lipschitz constant $k(\epsilon)$ is a measure of the nonlinearity of the equations. In general $k(\epsilon)$ is a nondecreasing function of ϵ , which defines the neighborhood about the equilibrium.

Given a desired trajectory, we have no control over the resulting magnitude of the nonlinear terms, but it can be determined. Given β and C , which are determined by the linearization of our closed-loop system, and given a desired performance, we can calculate the maximum “allowable” value of $k(\epsilon)$. From the form of our nonlinear terms we are then able to bound possible trajectories and so determine the achievable performance for the given controller. See also .

It is clear from Eq. 6.35 that the larger our linearized controller gains are, or more generally, the larger we can make the magnitude of the linearized closed-loop system’s eigenvalues, the more nonlinear the desired trajectories we can afford. Notice of course that practical limits will arise. For manipulator systems, for example, the nonlinear terms have the form of squared velocity terms. Therefore in general $k(\epsilon)$ will be very large even for small neighborhoods.

We remark that extensions of these results to multi-link systems are fairly straightforward. In order to extend these results to infinite dimensional system, it is necessary to resort to semigroup theory [5] and to consider the resolvent of generators of semigroups. For the class of systems under study, however, the spectrum of the generator consists of eigenvalues, and the corresponding eigenfunctions form a complete orthonormal set. This means in particular that we can compute the asymptotic behavior of the systems in exactly the same manner that we have done above for the finite dimensional systems.

Chapter 7

Control of a Two Link Manipulator with Flexible Links

In this chapter we bring the results and insights of previous chapters into focus by considering the problem of control of a two link manipulator with flexible links. In Chapter 5 we introduced the nonlinear output regulation theory as a framework within which to elucidate the concept of a *transient performance measure*. We then proceeded to apply this theory to the one-flexible-link manipulator and we evidenced the limits on the transient performance due to the nonminimum phase nature of the system we considered.

In Chapter 6 we looked at various controllers in the light of their *robustness* properties. A clear tradeoff suggested itself between global properties of stability and degradation of local performance. In the first part of this chapter, we consider the output regulation control of a two link manipulator. For the feedback stabilization control we compare the results of using both a globally stable *robust* controller and a locally defined *higher performance* controller.

Due to the difficulty in solving the nonlinear regulator equations for more complex systems than the one-link manipulator, we investigate solutions using simplified forms of the equations of motion. In particular, we use both linearized equations (about equilibrium) and equations that are nonlinear in rigid body coordinates but linear in flexible coordinates. The results, not surprisingly, are locally quite good but depend

among other things on the level of excitation, expressed by the frequency content of the desired trajectory.

In the last part of this chapter we investigate the limits of performance from the point of view of linear sensitivity theory. In Chapter 5 it was suggested that, just as the linear approximation of the system locally set the limit on time-domain response, we could expect sensitivity considerations of the type discussed in Chapter 3 to also become significant locally. This is indeed the case and this albeit heuristic analysis concludes our in-depth study of the performance limits of flexible manipulators.

7.1 Output Regulation Control of the Two-Flexible-Link Arm

As pointed out in Chapter 2, the discretized (in space) equations of motion for a two link manipulator can be represented quite generally in the form of Eq. 2.15, which we reproduce here for convenience.

$$M(\boldsymbol{\theta}, \mathbf{q}) \begin{bmatrix} \ddot{\boldsymbol{\theta}} \\ \ddot{\mathbf{q}} \end{bmatrix} + D \begin{bmatrix} \dot{\boldsymbol{\theta}} \\ \dot{\mathbf{q}} \end{bmatrix} + K \begin{bmatrix} \boldsymbol{\theta} \\ \mathbf{q} \end{bmatrix} + G(\boldsymbol{\theta}, \mathbf{q}) = -C(\boldsymbol{\theta}, \mathbf{q}, \dot{\boldsymbol{\theta}}, \dot{\mathbf{q}}) + B\boldsymbol{\tau} \quad (7.1)$$

As in the one-link case, we consider only actuation at the joints provided by torquers, one at each joint. The outputs of interest are the relative angular positions at the tips of each link:

$$\begin{aligned} \mathbf{y} &= \begin{bmatrix} \theta(t) + \sum_{i=1}^n \phi'_i(l_1) q_i(t) \\ \beta(t) + \sum_{i=1}^m \psi'_i(l_2) p_i(t) \end{bmatrix} \\ &= \boldsymbol{\theta} + C_1 \mathbf{q} \end{aligned} \quad (7.2)$$

where

$$C_1 = \begin{bmatrix} \phi'_1(l_1) & \cdots & \phi'_n(l_1) & 0 & \cdots & 0 \\ 0 & \cdots & 0 & \psi'_1(l_2) & \cdots & \psi'_m(l_2) \end{bmatrix}. \quad (7.3)$$

The parameters chosen for the two link arm are given in Tables 7.1 and 7.2. See section 2.2.2 and Fig. 2.2 for the definitions. The space-dependent mode shapes are taken to be the natural mode shapes for cantilevered-loaded beams with the

Kg	Kg m ²	m	
$\rho_1 l_1 = 0.9$	$J_A = 0.103$	$l_1 = 0.686$	$EI_1 = 116.5 \text{ N m}^2$
$m_A = 2.3$	$J_{B_1} = 0.039$	$b_1 = 0.133$	$\beta_{12} = \pi \text{ rad}$
$m_{B_1} = 5.72$		$b_{21} = 0.121$	
		$b = 0.011$	

Table 7.1: Parameters for the Two-flexible-link Manipulator: Link 1

Kg	Kg m ²	m	
$\rho_2 l_2 = 0.5$	$J_{B_2} = 0.025$	$l_2 = 0.736$	$EI_2 = 14.16 \text{ N m}^2$
$m_{B_2} = 5.4$	$J_{C_1} = 0.32$	$b_{22} = 0.153$	$\beta'_{12} = 0 \text{ rad}$
$m_{C_1} = 4.42$		$b_t = 0.03$	
		$b' = 0.011$	

Table 7.2: Parameters for the Two-flexible-link Manipulator: Link 2

appropriate parameters (see Appendix C). Contrary to the one-link case, we include one percent modal damping for each link.

Proceeding as for the one-link case, we define a state vector \mathbf{x} as

$$\mathbf{x} = \begin{bmatrix} \theta \\ \mathbf{q} \\ \dot{\theta} \\ \dot{\mathbf{q}} \end{bmatrix},$$

and linearize about the equilibrium $\beta(t) = 45^\circ$ with all other states zero. Using MATLAB [59] we obtain the poles and transmission zeros presented in Tables 7.3–7.4. We have assumed two modes per link to obtain the values in Tables 7.3–7.4.

The system of Eqs. 7.1–7.2, with the parameters of Tables 7.1 and 7.2 and two assumed modes per link, satisfies hypotheses H2 and H3 of the nonlinear regulator problem. In fact, its linear approximation about the equilibrium is both controllable and observable.

Poles					
$p_{1,2}$	=	0	$p_{3,4}$	=	0
$p_{5,6}$	=	$-0.269007 \pm 12.7267i$	$p_{7,8}$	=	$-7.50916 \pm 58.42i$
$p_{9,10}$	=	$-5.27705 \pm 61.9152i$	$p_{11,12}$	=	$-12.8041 \pm 167.526i$

Table 7.3: Open Loop Poles for the Two-flexible-link Manipulator

Zeros					
z_1	=	-4.26386	z_2	=	4.35839
z_3	=	-9.58006	z_4	=	10.0961
z_5	=	-123.052	z_6	=	132.254
z_7	=	-273.694	z_8	=	298.340

Table 7.4: Open Loop Zeros for the Two-flexible-link Manipulator

7.1.1 Set-point Regulation

The exosystem for set-point regulation is given by:

$$\dot{\mathbf{w}} = \begin{bmatrix} 0 \\ 0 \end{bmatrix}, \quad \mathbf{w}(0) = \begin{bmatrix} \theta_d \\ \beta_d \end{bmatrix}, \quad \mathbf{q}(\mathbf{w}) = \mathbf{w}(t) \quad (7.4)$$

where θ_d is the desired final angular position of the tip of the inboard link in inertial space and β_d is the desired final angular position of the tip of the outboard link relative to the angular position of the tip of the inboard link. We note that this exosystem satisfies hypothesis H1 of the nonlinear regulator theory. The solution of the regulator equations 5.25–5.26 results in

$$\mathbf{c}(\mathbf{w}) = 0, \quad \boldsymbol{\pi}(\mathbf{w}) = \begin{bmatrix} \mathbf{w} \\ 0 \\ 0 \\ 0 \end{bmatrix}.$$

PD Feedback Control

From the results of Chapter 6, it was inferred that independent joint proportional plus derivative (PD) feedback for flexible multi-link systems would provide the same global robustness properties as for rigid manipulators. Because of this, it is of interest to examine the performance that a composite controller (such as the nonlinear output regulator of Chapter 5) can achieve when the feedback control is effected with independent joint PD.

Recall that in order to apply the results of the output regulation theory, the feedback stabilizing control must render the linear approximation of the closed-loop system exponentially stable. If we use only independent joint PD control, the results of chapter 6 suggest that in the absence of material damping we cannot exponentially stabilize the infinite dimensional system. While this problem is not apparent when we use a finite dimensional approximation, as we must in our simulations, it is evidenced in slower and slower settling times as the number of modes is increased. If we include material damping, however, then independent joint PD control does satisfy the exponential stability requirement.

The control law takes the simple form

$$\tau = K_P(\mathbf{w} - \theta) - K_D\dot{\theta} \quad (7.5)$$

where K_P and K_D are positive definite diagonal matrices. In practice, the gains for the PD control are obtained by solving an LQR problem and then zeroing out all the cross-coupling terms and all the terms associated with the flexible coordinates \mathbf{q} . The LQR is solved using the original, non-inverted system, so that the control law consists of pure PD control.

Starting from the open loop equilibrium (with $\beta(0) = 45^\circ$), desired final relative tip angular positions of $\theta_d = 0.01^\circ$ and $\beta_d = 44.99^\circ$ are commanded. The reason we limit the maneuver to such small steps is that, in order to reach the performance bound on the transient response due to the nonminimum phase zeros of our system, we had to increase the regulator gains considerably. This translates into very large start-up torques due to initial errors. This in turn results in very large angles and

displacements and these lead to mass matrix ill-conditioning since we note that the configuration-dependent mass matrix has been linearized in small elastic deflections. For this reason we have to be careful not to exceed acceptable *small* elastic deformations.

The results are shown in Fig. 7.1. We have assumed two modes per link, so that $n = 2$ and $m = 2$. We have increased the PD gains to try to obtain as fast a response as possible. However, as mentioned in Chapter 6, due to the collocated nature of the transfer function from joint angle to joint torque, the alternating structure of poles and zeros for the linearized system causes lightly damped poles to remain in the closed-loop transfer function, thus limiting performance. It is ironic that it is this same quality, that is, the alternating pole zero pattern, that results in the PD control's innate robustness.

In order to obtain a less oscillatory response, we must reduce the PD gains, and this in turn results in a slower reaching time. As could be expected, limiting ourselves to such a simple controller results in some severe performance limitations. This was shown experimentally for the first time by Schmitz [78]. Figure 7.2 shows the results of decreasing the PD gains. In the following section we compare these results to the performance obtained using an LQR-based feedback controller.

LQR Feedback Control

To obtain better feedback performance, at the cost of globality and robustness, we implement the control law

$$\boldsymbol{\tau} = K_{reg}(\boldsymbol{\pi}(\mathbf{w}(t)) - \mathbf{x}(t)). \quad (7.6)$$

The gain matrix K_{reg} is obtained from the solution of the linear quadratic regulator problem with control weighting μ and state weighting matrix

$$Q = [I_{2 \times 2} \quad C_1 \quad 0 \quad 0]^T [I_{2 \times 2} \quad C_1 \quad 0 \quad 0].$$

Starting from the open loop equilibrium (with $\beta(0) = 45^\circ$), desired final relative tip angular positions of $\theta_d = 0.5^\circ$ and $\beta_d = 44.5^\circ$ are commanded. The control

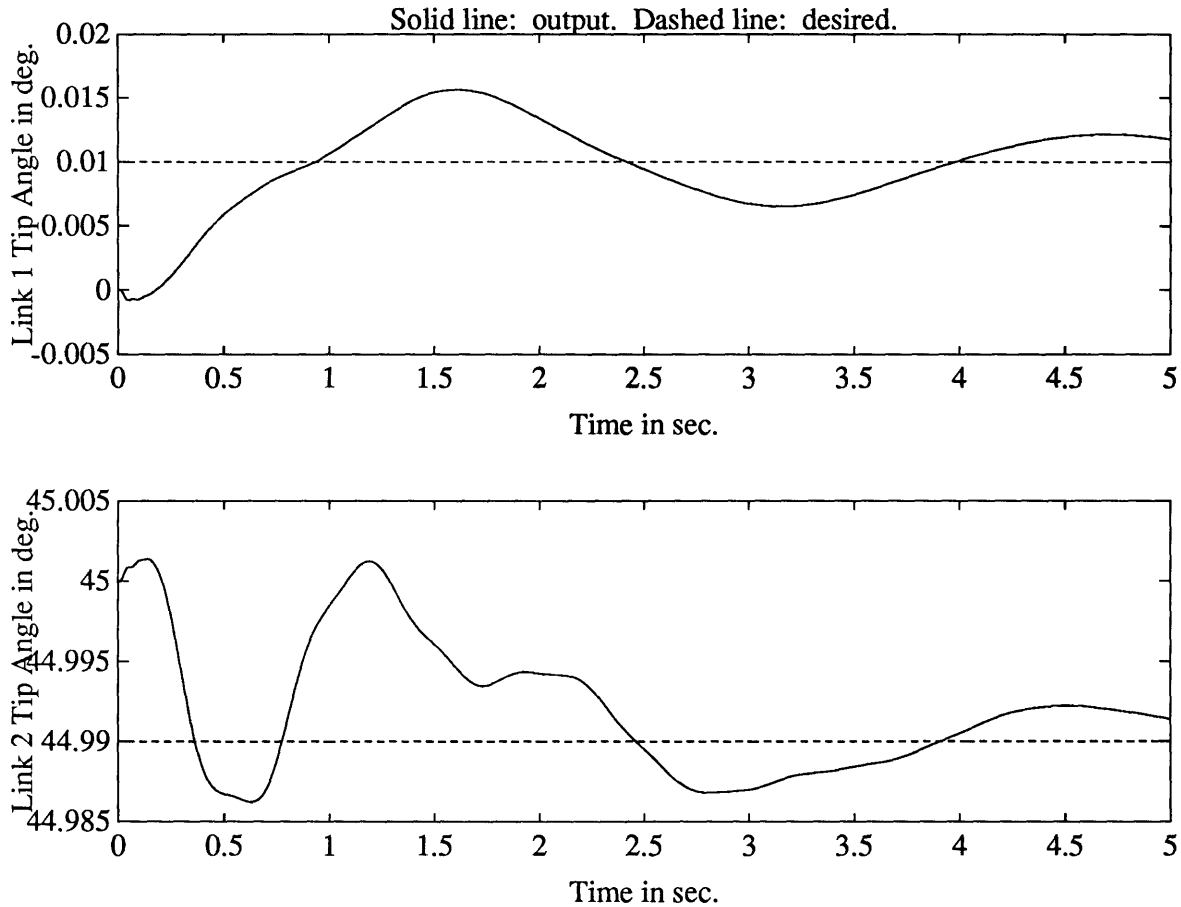


Figure 7.1: Output of Two-flexible-link Arm: Set-point Regulation; Independent Joint PD; $\mu = 1 \times 10^{-6}$.

weighting μ was reduced until the poles of the linearized system stuck at the left-half plane mirror images of the nonminimum phase zeros became the dominant poles. Simulation results are presented in Fig. 7.3 for the value $\mu = 1 \times 10^{-4}$. The closed-loop poles of the linearized system for this value of μ are given in Table 7.5.

From the figure we see that as expected there is zero steady state error and the state tends to the steady state manifold at a rate limited by the first nonminimum phase zero of the system. The settling time for the output errors is seen to be approximately $4/\text{Real}(z_1) \approx 1$ sec. Comparing to Fig. 7.2, we see that better transient performance is achievable, even though, in the light of the results of Chapter 6, the LQR-based feedback is local in nature and not as robust.

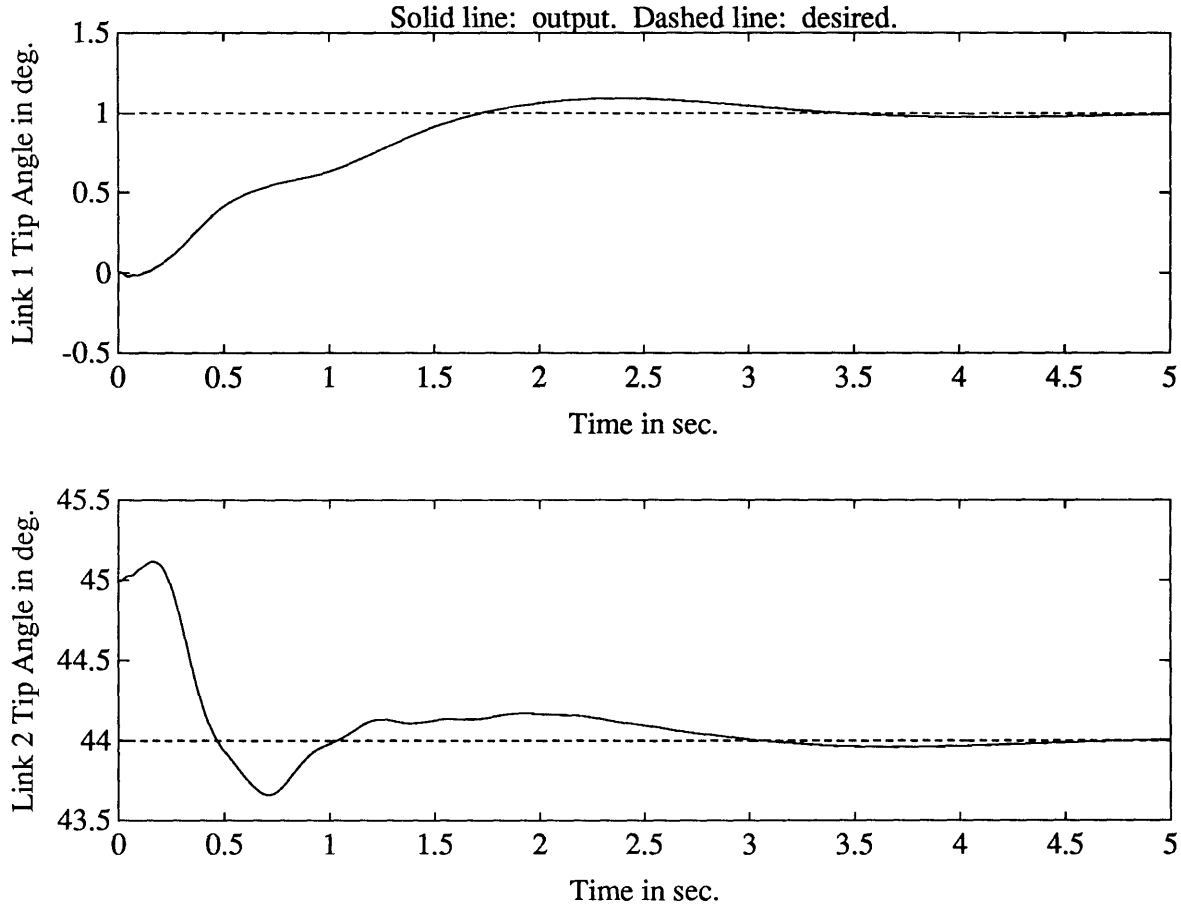


Figure 7.2: Output of Two-flexible-link Arm: Set-point Regulation; Independent Joint PD; $\mu = 1 \times 10^{-4}$.

7.1.2 Sinusoidal Exosystem

In order to have the output of our system (Eq. 7.2) track a sinusoidal signal we consider the following exosystem:

$$\dot{\mathbf{w}} = \begin{bmatrix} 0 & \omega_1 & 0 & 0 \\ -\omega_1 & 0 & 0 & 0 \\ 0 & 0 & 0 & \omega_2 \\ 0 & 0 & -\omega_2 & 0 \end{bmatrix} \mathbf{w}, \quad \mathbf{w}(0) = \begin{bmatrix} \theta_d \\ \dot{\theta}_d \\ \beta_d \\ \dot{\beta}_d \end{bmatrix}, \quad \mathbf{q}(\mathbf{w}) = \begin{bmatrix} w_1 \\ w_3 \end{bmatrix}.$$

This exosystem satisfies hypothesis H1 of the nonlinear output regulation theory.

As in the one-link case, we first invert the system in order to obtain a more tractable form of the equations of motion with which to solve the nonlinear regulator

Poles	
$p_{1,2} = -1.48281 \pm 1.20839i$	$p_{7,8} = -5.66036 \pm 61.6744i$
$p_{3,4} = -5.18571 \pm 3.10971i$	$p_{9,10} = -11.3181 \pm 59.8202i$
$p_{5,6} = -5.66295 \pm 13.5723i$	$p_{11,12} = -14.3093 \pm 167.552i$

Table 7.5: Closed-Loop Poles for the Two-flexible-link Manipulator; $\mu = 1 \times 10^{-4}$.

equations. The inversion-based controller is given by

$$\tau = C_R(\mathbf{z}, \dot{\mathbf{z}}) + (A_1 + C_1 A_2)^{-1} [\mathbf{v} + (A_2^T + C_1 A_3)(K_{EE} \mathbf{q} + D_{EE} \dot{\mathbf{q}} + C_E(\mathbf{z}, \dot{\mathbf{z}}))] \quad (7.7)$$

where we have defined

$$\mathbf{z} = \begin{bmatrix} \boldsymbol{\theta} \\ \mathbf{q} \end{bmatrix}, \quad M^{-1} = \begin{bmatrix} A_1 & A_2^T \\ A_2 & A_3 \end{bmatrix}.$$

The control law of Eq. 7.7 yields the inverted system:

$$\ddot{\mathbf{y}}(t) = \mathbf{v} \quad (7.8)$$

$$\ddot{\mathbf{q}}(t) = -\Delta^{-1} [K_{EE} \mathbf{q} + D_{EE} \dot{\mathbf{q}} + C_E(\mathbf{z}, \dot{\mathbf{z}}) + M_{ER}(\mathbf{z}) \mathbf{v}] \quad (7.9)$$

where we have set

$$\Delta = M_{EE}(\mathbf{z}) - M_{ER}(\mathbf{z}) C_1.$$

The solution of the regulator equations 5.25–5.26 is now carried out using Eqs. 7.8–7.9 with the new input \mathbf{v} .

The solution of the regulator equations is again carried out by expanding unknown terms of the steady state manifold $\boldsymbol{\pi}(\mathbf{w})$ as complete polynomials of the third degree in the w_i , $i = 1, \dots, 4$. The complex form of the equations in this case requires the use of a symbolic manipulator such as MATHEMATICA [95] (see Appendix D). Even using a symbolic manipulator, we were forced to limit the number of modes to one per link and to simplify the nonlinear terms until a solution was obtained.

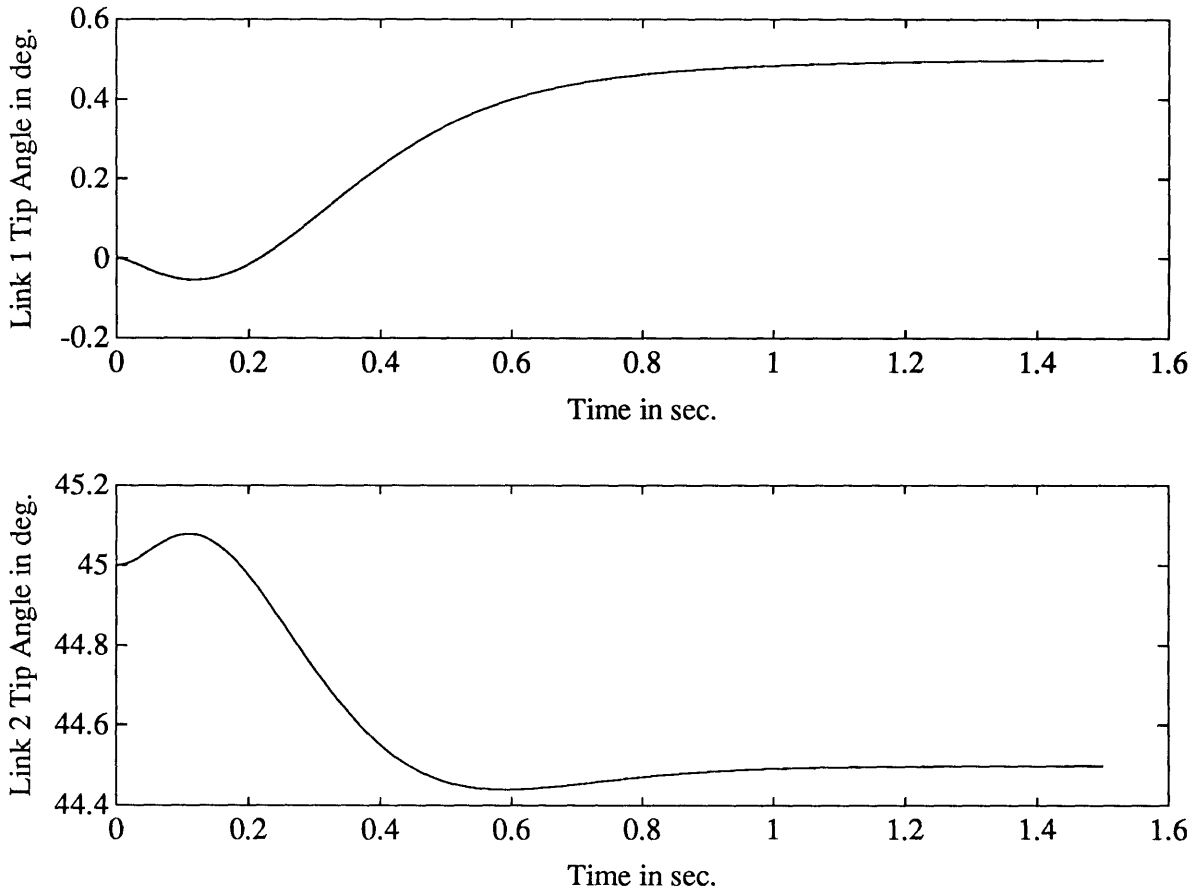


Figure 7.3: Output of Two-flexible-link Arm: Set-point Regulation; $\mu = 1 \times 10^{-4}$.

The following results are true for any number of modes and before any simplifying assumptions are necessary. They arise from the simpler form of the inverted equations:

$$\begin{aligned} \pi_1(\mathbf{w}) &= w_1, & \pi_{3+n+m}(\mathbf{w}) &= \omega_1 w_2, & c_1(\mathbf{w}) &= -\omega_1^2 w_1 \\ \pi_2(\mathbf{w}) &= w_3, & \pi_{4+n+m}(\mathbf{w}) &= \omega_2 w_4, & c_2(\mathbf{w}) &= -\omega_2^2 w_3 \end{aligned}$$

To obtain the steady state manifold coordinates corresponding to the flexible degrees of freedom, we assume only one mode per link and use two sets of simplified equations of motion. In the first set we actually linearize the equations of motion about the equilibrium configuration. This yields the equivalent linear regulator solution mentioned in Chapter 5.

For the second set of simplified equations we maintain all nonlinear terms in the rigid body coordinates and rates but ignore all nonlinear terms that involve the small

elastic deformation coordinates and rates. We remark that this simplified version of the equations of motion has been dubbed the ruthless equations and has been investigated in the context of flexible manipulator equations by the author [71,69,70].

The details of the calculations for the steady state manifold flexible coordinates using these simplified models are presented in Appendix D.

The resulting control law is similar in form to the one obtained for the one-link case:

$$\tau = c(\mathbf{w}(t)) + K_{reg} \begin{bmatrix} \pi_\theta - C_1 \pi_{\dot{\mathbf{q}}} \\ \pi_{\mathbf{q}} \\ \pi_{\dot{\theta}} - C_1 \pi_{\dot{\mathbf{q}}} \\ \pi_{\dot{\mathbf{q}}} \end{bmatrix} - \mathbf{x}(t). \quad (7.10)$$

The matrix of gains K_{reg} is obtained as in the set-point regulation case through the solution of a linear quadratic regulator problem with control weighting $\mu = 1 \times 10^{-4}$ and state weighting Q as before.

In the following we will present the results of using either set of simplified solutions to the regulator equations in the controller implementation.

Linearized Solutions

Starting from the equilibrium configuration (with $\beta(0) = 45^\circ$), desired sinusoidal trajectories are specified for the inboard link's inertial tip angular position and the outboard link's relative tip angular position. The amplitude of the sinusoids is 0.1° about the corresponding rest (equilibrium) positions and the frequencies are chosen to be approximately one tenth of the linearized system frequencies that correspond to bending of each beam, respectively $\omega_1 = 5.89445, \omega_2 = 1.65066$. We point out that this maneuver is kept relatively mild in order that the approximate solution of the regulator equations be close to the actual solution. The simulation results are presented in Figs. 7.4 and 7.5.

From the figures we see that the results are extremely good, even for a linear implementation of the regulator solutions. In terms of transient performance, we see as expected that we are limited locally by the nonminimum phase character of the

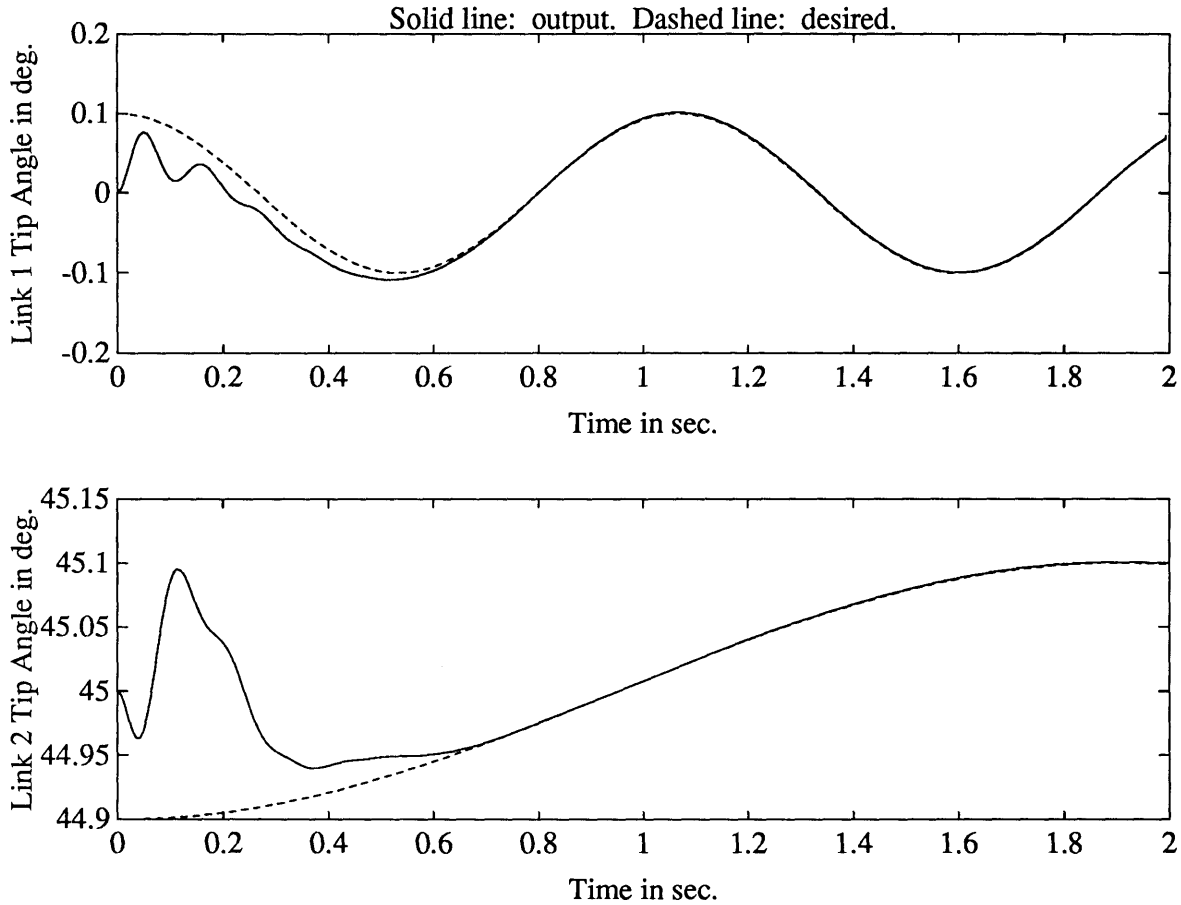


Figure 7.4: Output of Two-flexible-link Arm: Sinusoidal Regulation; $\mu = 1 \times 10^{-4}$.

linear approximation to the equations of motion. In particular, we see that neither of the outputs can have a faster settling time than about 0.9 sec., consistent with a dominant pole at the mirror image location in the left-half plane to a nonminimum phase zero at z_1 (see Table 7.3).

In Fig. 7.6 we show the results of requiring the outputs to follow faster sinusoids. In this case the sinusoidal frequency required of each output is, respectively, $\omega_1 = 18.6399, \omega_2 = 5.21985$. We see that the results are very good. A steady-state error in the tracking of the outboard link's tip is doubtless due to the use of the simple linear model in calculating the solution to the nonlinear output regulation equations. These results of nonetheless show excellent robustness of the output regulator to small uncertainties.

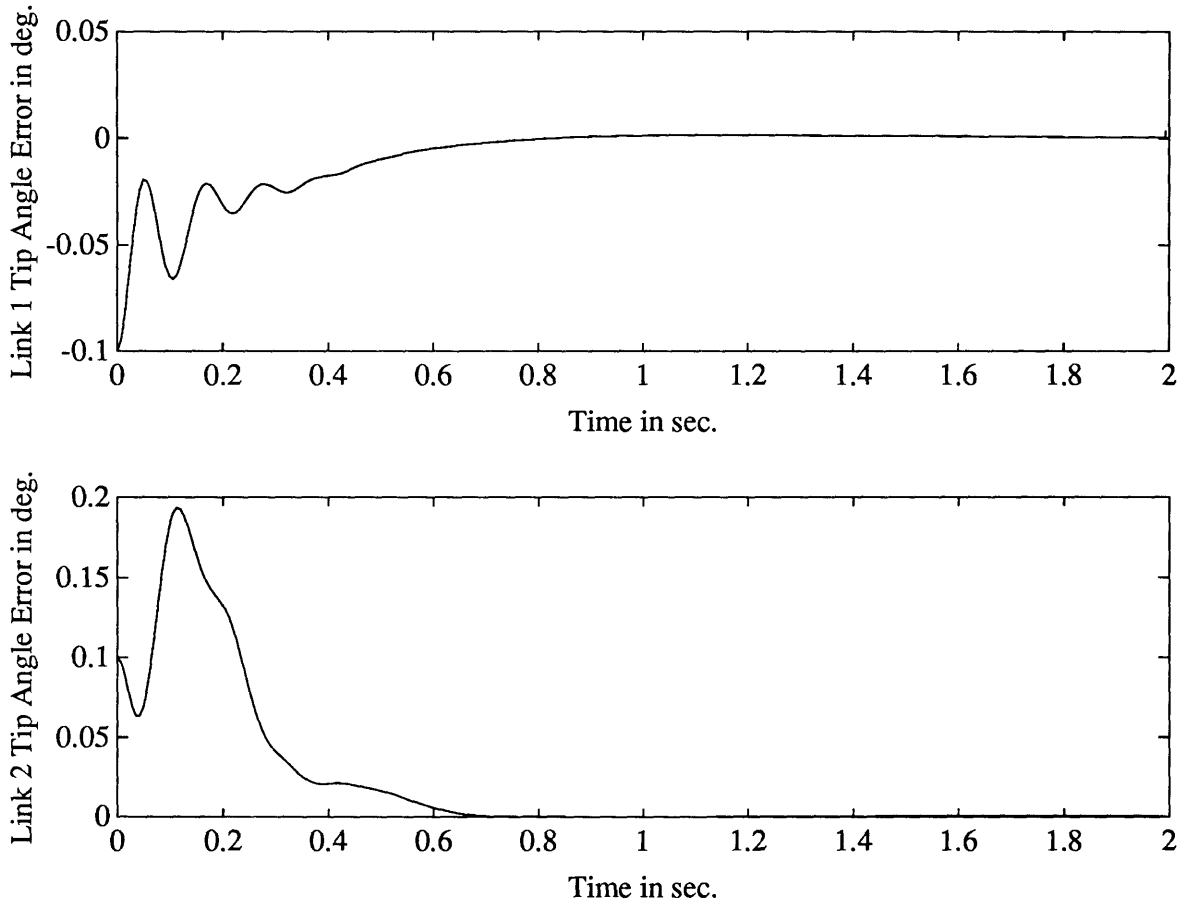


Figure 7.5: Output of Two-flexible-link Arm: Sinusoidal Regulation; $\mu = 1 \times 10^{-4}$.

Finally, in Fig. 7.7 we reduce the control weighting on the LQR solution of the feedback controller gains and we slow down the desired sinusoids. This is done so that larger amplitude sinusoids can be commanded and the validity of the nonlinear output regulation-based feedforward-feedback control scheme presented above be shown for large nonlinear motions of the system. Both commanded sinusoids are chosen to have amplitudes of 45° and frequencies of 0.5 rad/sec.

From the figure it is apparent that even at this large level of motion, and still using just a linear model to solve the feedforward control equations, the results are very good. In this case when the commanded angles are large and the rigid body coordinates tend to be much larger than the flexible deformations, it is expected that a ruthless model will help improve on the steady state error.

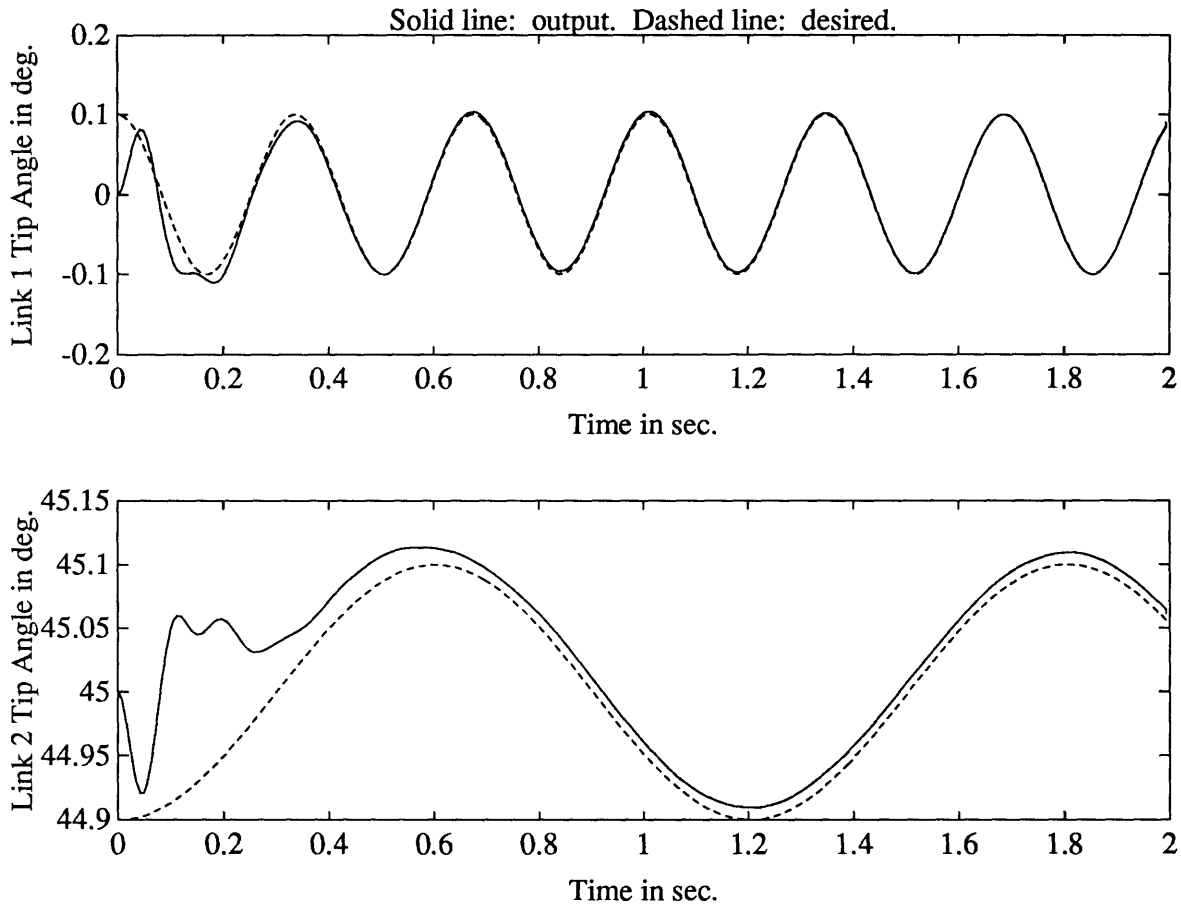


Figure 7.6: Output of Two-flexible-link Arm: Sinusoidal Regulation; $\mu = 1 \times 10^{-4}$.

Ruthless Solutions

In this section we require the system outputs to follow the same sinusoidal trajectories specified above, but in this case we use for the approximate solution to the steady state manifold and feedforward term the second set of simplified equations of motion. Specifically, we solve the nonlinear regulator equations 5.25–5.26 using the equations of motion nonlinear in rigid body coordinates and rates but linear in flexible deformation coordinates and rates (i.e., the *ruthless* equations).

As in the previous section, we use as feedback control the LQR-based set of gains K_{reg} obtained by setting $\mu = 1 \times 10^{-4}$ and using state weighting Q as defined previously. Since such good results were obtained in the previous section for the low

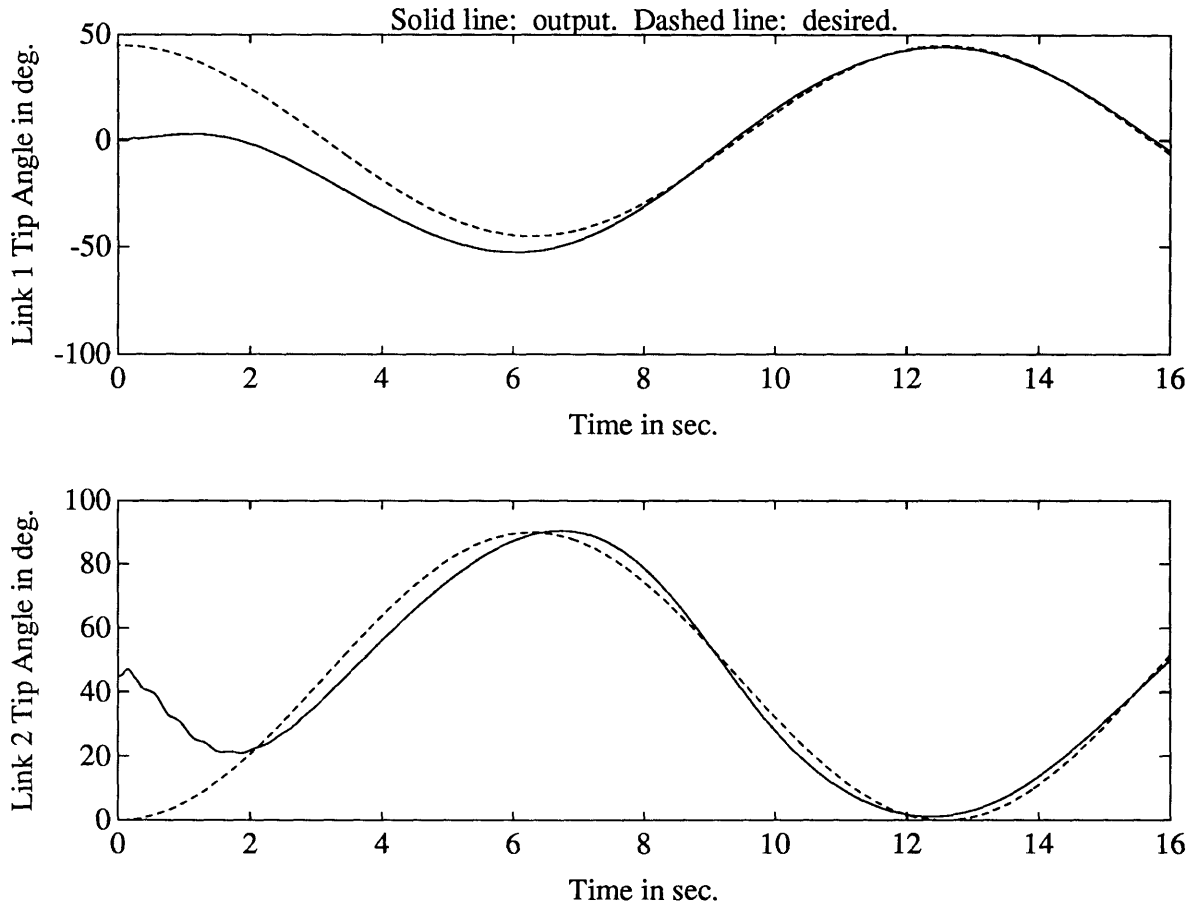


Figure 7.7: Output of Two-flexible-link Arm: Sinusoidal Regulation; $\mu = 0.1$.

frequency commanded sinusoids using the linear version of the equations, we study here only the higher frequency sinusoids, where we stand to gain something by increasing the complexity of our design model.

The results shown in Fig. 7.8 are remarkable even though the commanded sinusoids are of much higher frequency and one of them in fact exceeds the first linearized system frequency. These results are to be compared to Fig. 7.6. We remark that this solution has been obtained by using the ruthless model equations to solve the non-linear regulator equations. These results are almost indistinguishable from those of Fig. 7.6. The small steady state error in the tracking of the outboard link's tip angle remains. This is probably due to the fact that, at the low commanded angles, the neglected flexible coordinate terms in the ruthless model simplification are of mag-

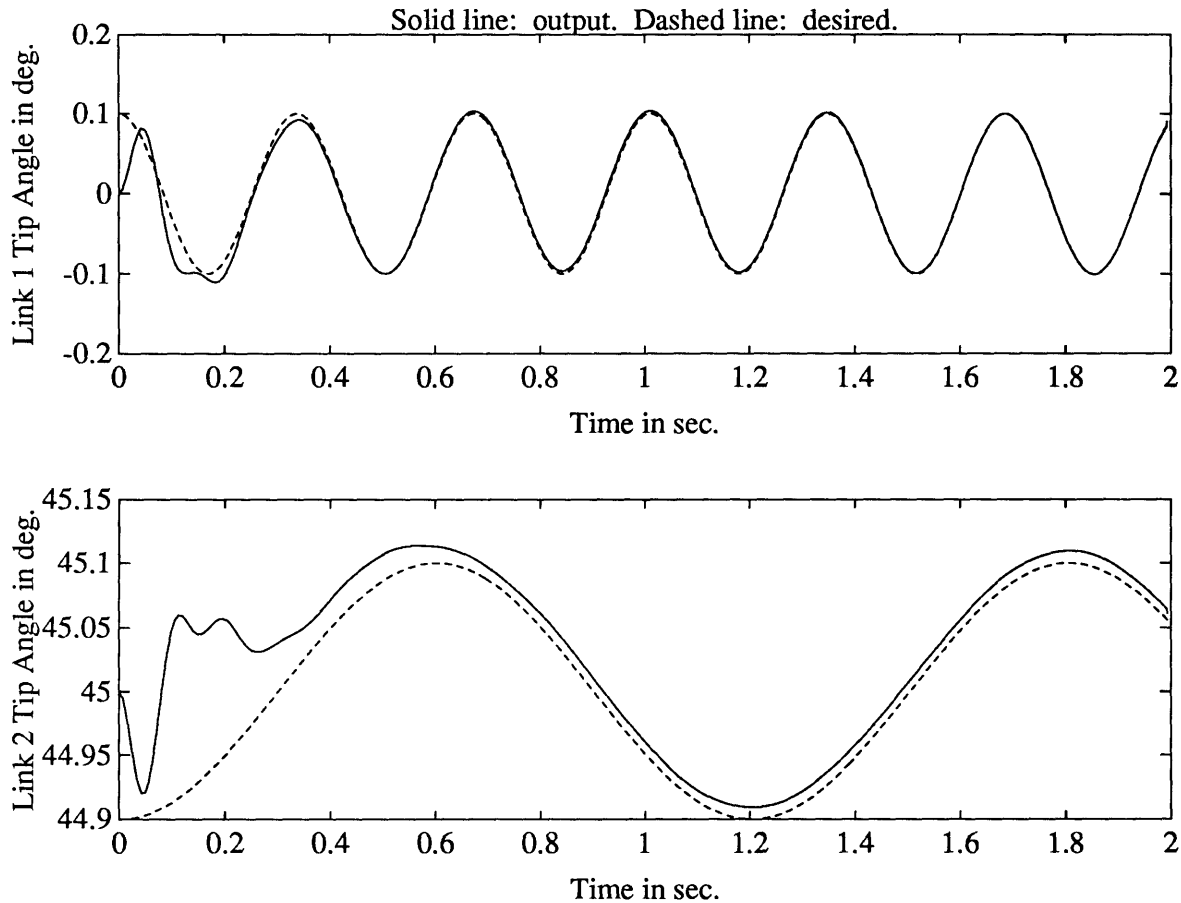


Figure 7.8: Output of Two-flexible-link Arm: Sinusoidal Regulation; $\mu = 1 \times 10^{-4}$.

nitudes comparable to the retained terms. This results in a small but nonnegligible steady state error.

7.2 MIMO Sensitivity Analysis

Let us now consider the performance limits of the two-flexible link manipulator in the context of linear sensitivity theory. For this purpose we will look at the MIMO sensitivity of the linearization of our system about equilibrium. In the MIMO context, it is necessary to carefully define the locations at which a loop is broken to determine a transfer function. In our case we are interested in the disturbance to output transfer function where the disturbance is assumed to occur at the output. See Fig. 7.9. We

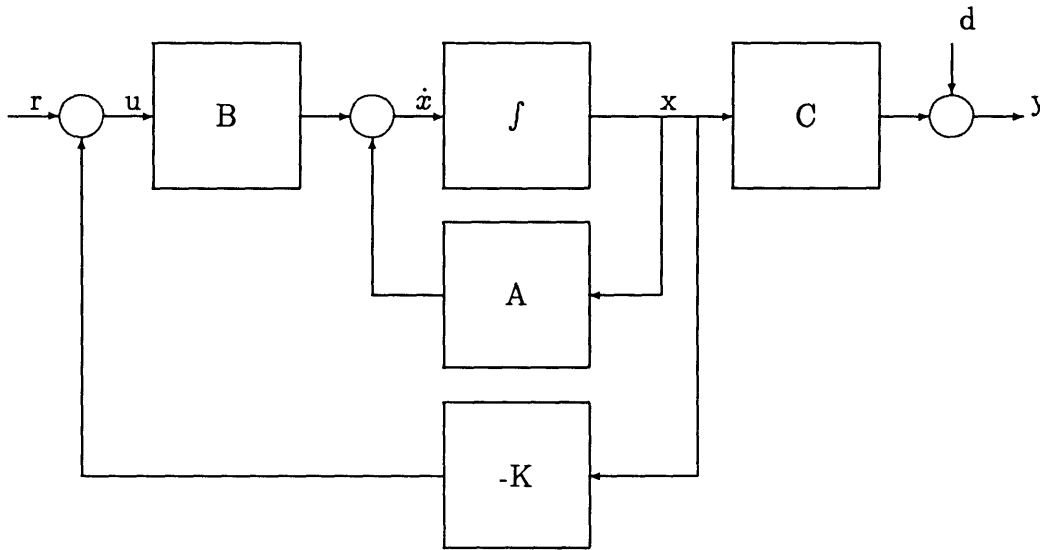


Figure 7.9: Definition of MIMO Sensitivity Transfer Function

will call this the sensitivity transfer function in analogy with the SISO case.

Recall from the discussion in Chapter 3 that in the SISO case the sensitivity transfer function as defined in Fig. 7.9 also gives a measure of sensitivity to small parameter variations.

For a system in state space form

$$\dot{x} = Ax + Bu \tag{7.11}$$

$$y = Cx \tag{7.12}$$

with an LQR-based controller $u = -Kx$, the sensitivity transfer function defined above is given by

$$\dot{x} = (A - BK)x - BK C^T (C C^T)^{-1} d \tag{7.13}$$

$$y = Cx + d. \tag{7.14}$$

For this study we consider a feedback controller designed by solving the LQR problem on the linearized equations of motion, as in section 7.1.1, and setting the control weighting to $\mu = 1 \times 10^{-4}$. This results in a MIMO bandwidth of about 10 rad/sec, obtained by examining the singular value plot of the closed-loop transfer matrix.

We inject sinusoidal output disturbances to our system in order to examine the system response to both low and high frequency excitation. Specifically, we will use

two sinusoidal frequencies: 1 rad/sec, and 20 rad/sec. In a typical SISO design problem, the controller would have shaped the sensitivity function such that it would be small at low frequencies, and thus it would reject disturbances well. At some high frequency we would have an increase in the sensitivity due usually to actuator bandwidth constraints or to nonminimum phase considerations (see Chapter 3). In the case of flexible link manipulators with joint actuators, the system from actuators to tip angles is nonminimum phase. Thus we expect sensitivity to peak if our bandwidth is “close” to the nonminimum phase zero location.

Figure 7.10 shows the two sensitivity plots obtained by considering combinations of corresponding input-output pairs, i.e., shoulder torque to shoulder angle and elbow torque to elbow angle. In the figure, S_{ii} is the sensitivity function from input i to output i . In Fig. 7.11 we show the actual MIMO sensitivity in terms of the singular values of the transfer matrix of the system given by Eqs. 7.13–7.14.

In Fig. 7.12 we show for comparison the MIMO singular value plot for the sensitivity transfer function matrix obtained using an LQR-based controller with control weighting $\mu = 1 \times 10^{-8}$. This controller results in a closed-loop bandwidth of about 100 rad/sec. As expected from the results of Chapter 3 the sensitivity characteristics become worse as the bandwidth approaches the nonminimum phase zero location. In particular we note a much higher peak around the crossover region compared to Fig. 7.11 and increased sensitivity overall in the lower frequency regions.

Returning now to our lower bandwidth controller (i.e., with $\mu = 1 \times 10^{-4}$), we see from Fig. 7.11 that we can expect good disturbance rejection at low frequencies (say below about 2 rad/sec) but will get amplification at frequencies between about 2 rad/sec and 100 rad/sec. We already saw in section 7.1.2 that for sinusoids with frequencies of about one tenth the link bending frequencies the response of the system was very good.

For the following simulations we require both output channels to follow the same frequency sinusoid but with possibly varying amplitudes and phases. In Fig. 7.13 we see the system response when the disturbance frequency is required to be 1 rad/sec for each output.

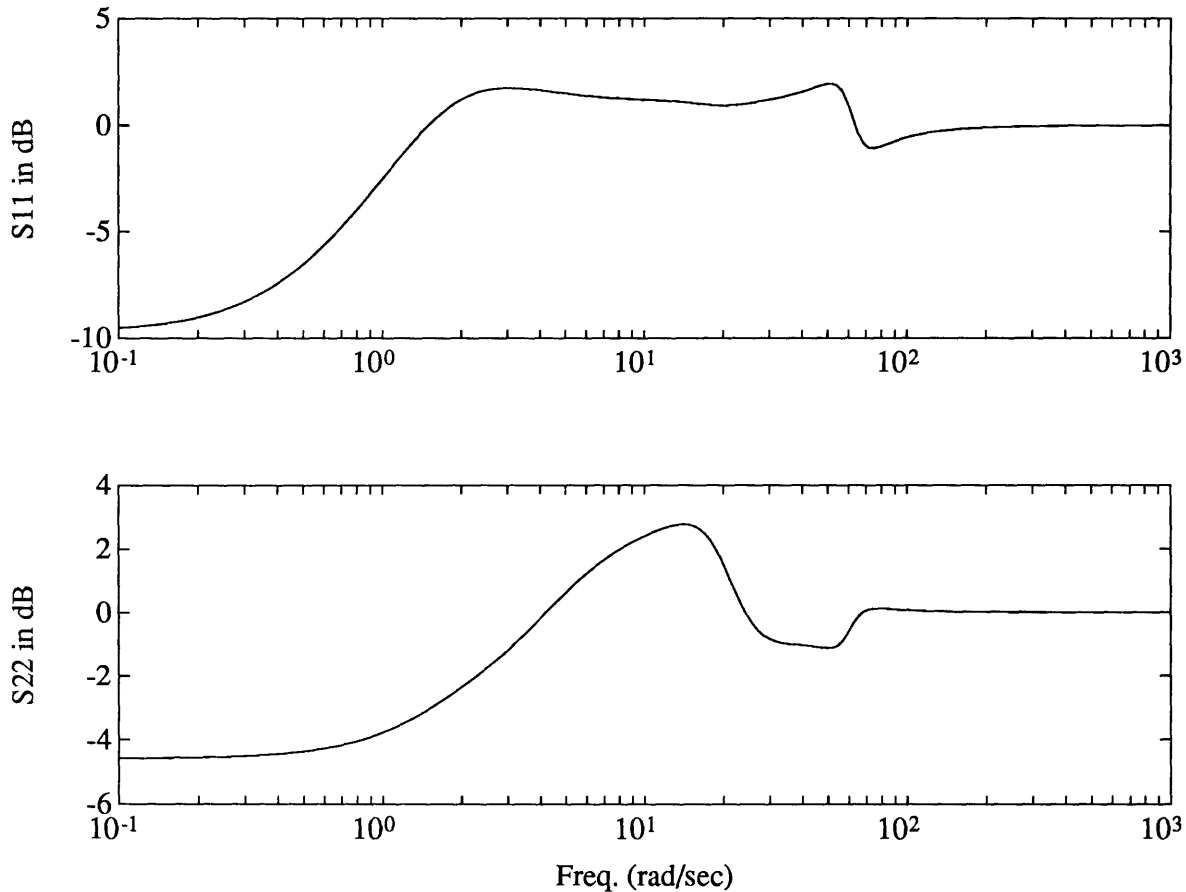


Figure 7.10: SISO Sensitivity Plots: $\mu = 1 \times 10^{-4}$.

As expected, we see from the figure that the disturbance is attenuated by the feedback controller. In Fig. 7.14 we see the response of the system to higher frequency disturbance sinusoids at the outputs: $\omega_1 = \omega_2 = 20$ rad/sec. In this case we see the disturbance is amplified and we would be better off in open loop. It is interesting to look at the open loop response to the higher frequency disturbance. Figure 7.15 shows this response. The resulting drift evidences the nonlinear nature of our plant.

From the MIMO sensitivity plot of Fig. 7.11 we see that the frequency of the commanded output sinusoids in this case is well into the amplification range, so that in this case the use of feedback is actually deleterious.

Figure 7.16 shows the MIMO sensitivity plot for another LQR-based feedback controller. In this case the control weighting has been increased to $\mu = 0.01$. This

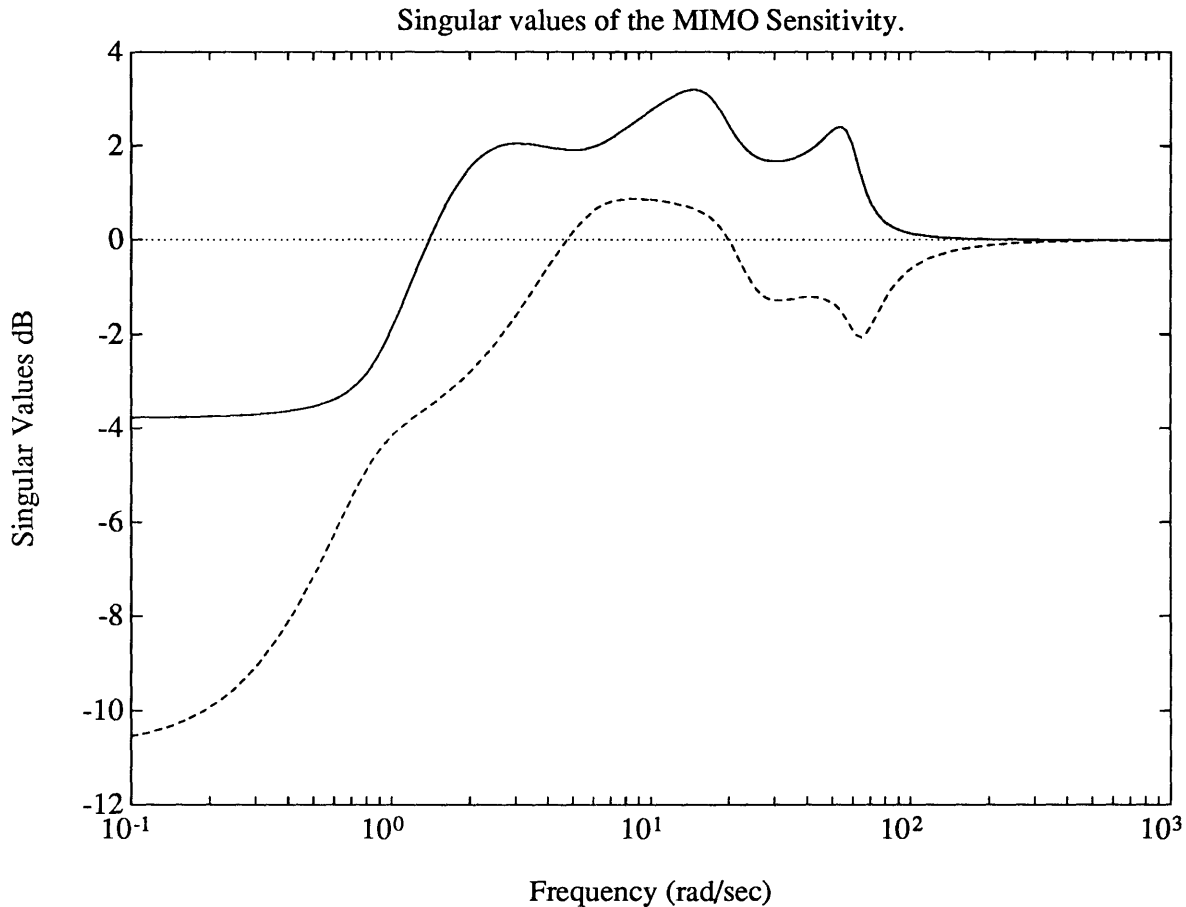


Figure 7.11: MIMO Sensitivity Plot: $\mu = 1 \times 10^{-4}$.

results in a lower bandwidth controller and thus a smaller region of sensitivity reduction. On the other hand, the peaking of the sensitivity function is seen to subside somewhat. The result of applying output disturbances of frequency 0.1 rad/sec is shown in Fig. 7.17. This is included to show that the conclusions arrived at above are not limited to very small angular motions. As can be seen from the figure, the disturbance signals have very large amplitudes (45°). As predicted by the linear theory, the nonlinear system exhibits significant disturbance attenuation at the given frequency.

7.3 Some Practical Considerations

The complexity of the nonlinear output regulator equations make their solution difficult even when a polynomial expansion is used to obtain approximate answers.

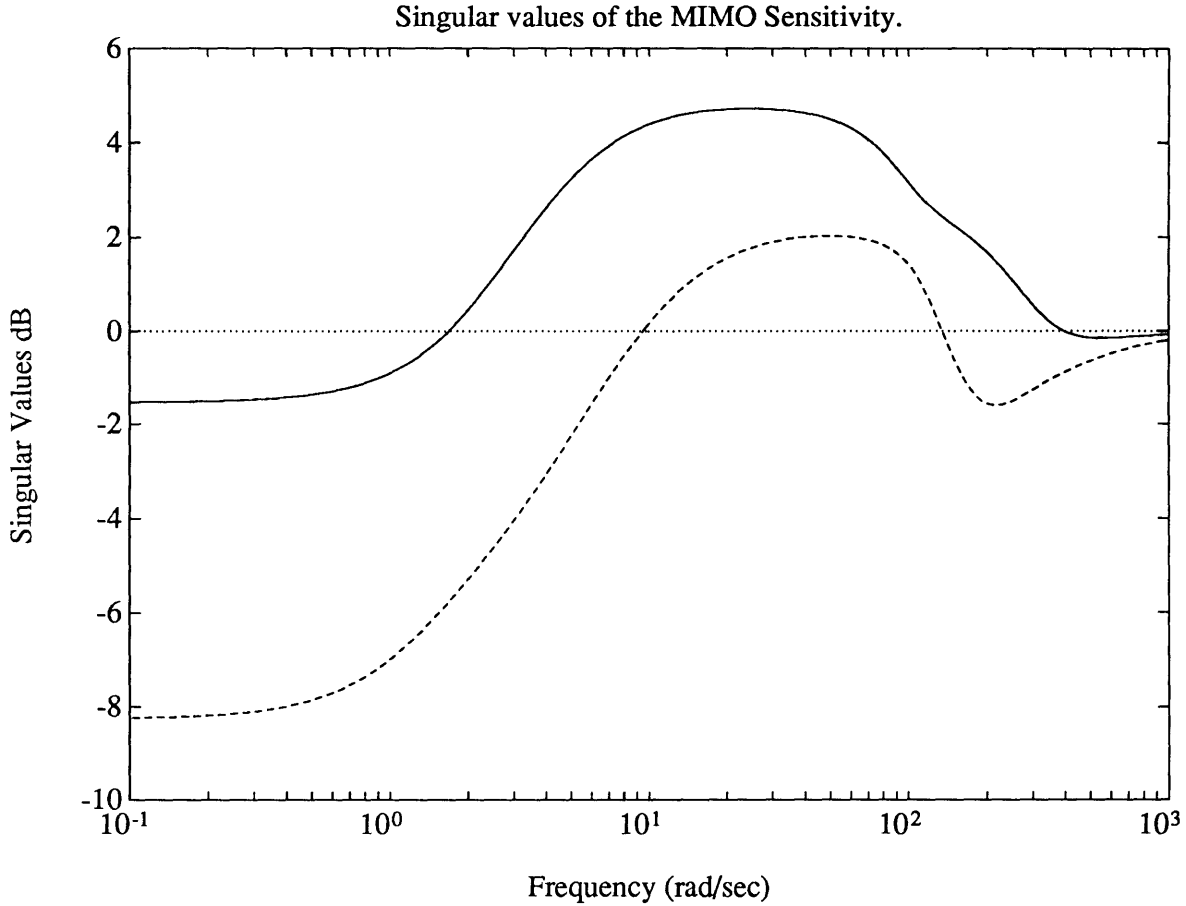


Figure 7.12: MIMO Sensitivity Plot: $\mu = 1 \times 10^{-8}$.

However, the results presented in this chapter show that, even for a broad range of maneuvers of different amplitudes and frequencies, using the linearized equations to solve the regulator equations yields very good results. The solution in the linear case can be reduced to the solution of a linear equation of the type $Ax = b$ by the use of Kronecker products (see Ref. [53]).

For nonlinear equations, even simplified ones such as the ruthless model used above, the complexity of the solution increases very fast with the number of modes retained in the modelling transverse deformations of the links. In the face of limitations to computing power, it would be of interest to develop fast, smart solution algorithms that take advantage of the fact that the solution of the equations at any order does not depend on higher order terms. This is a subject for future research.

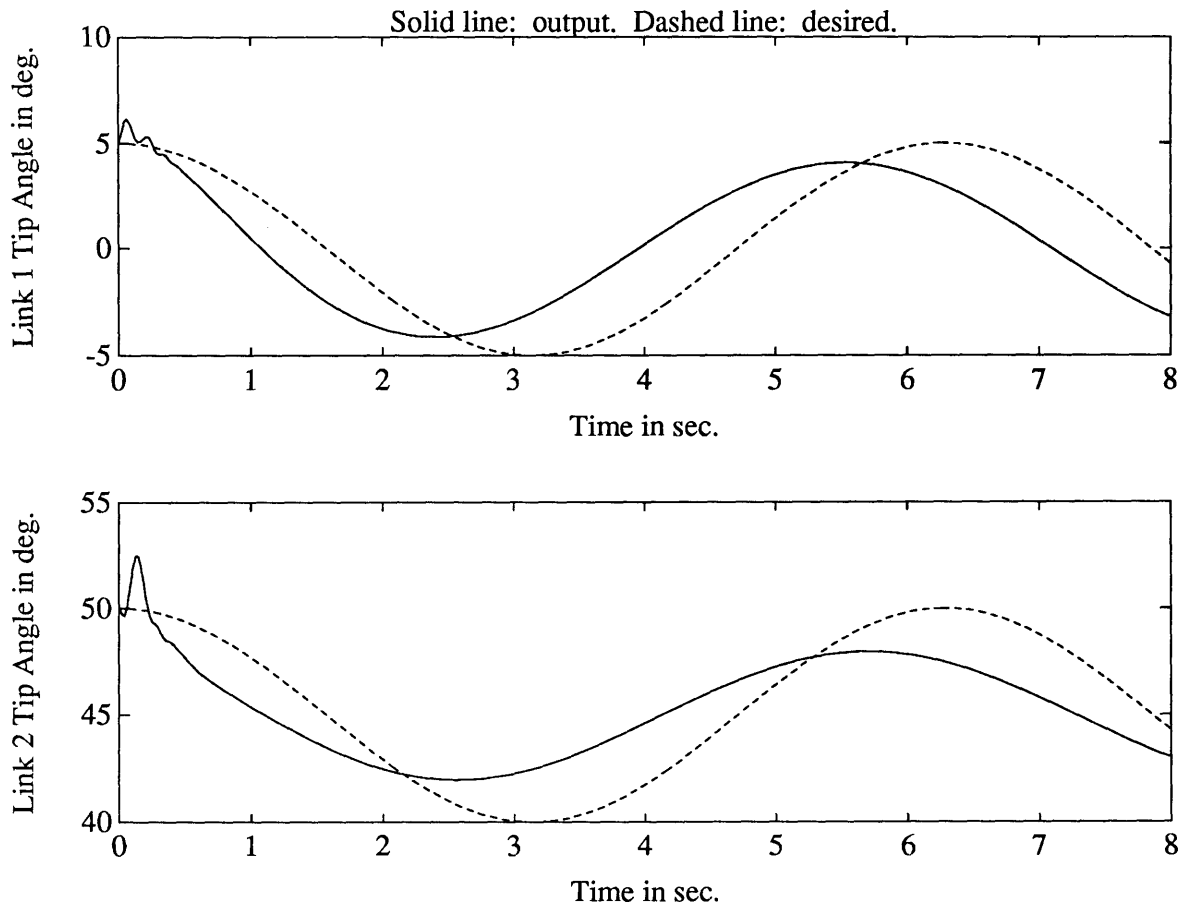


Figure 7.13: Sinusoidal Output Disturbance: $\mu = 1 \times 10^{-4}$.

The practicality of using the output regulation theory to determine the feedforward control for manipulator systems is evidenced by the fact that many basic trajectories of interest can be generated by exosystems which satisfy the sufficient conditions for solvability of the regulator equations. In particular, steps, ramps, p -times differentiable maneuvers in general, and sinusoids are among the trajectories that can be generated. A common way of generating smooth joint-space trajectories for rigid manipulators is through the use of high order (e.g., fifth) polynomial splines. Since these are trajectories that are that many times differentiable, they can be generated by exosystems.

Finally, we point out that the framework presented by the output regulation theory for the feedforward-feedback control of flexible manipulators does not preclude

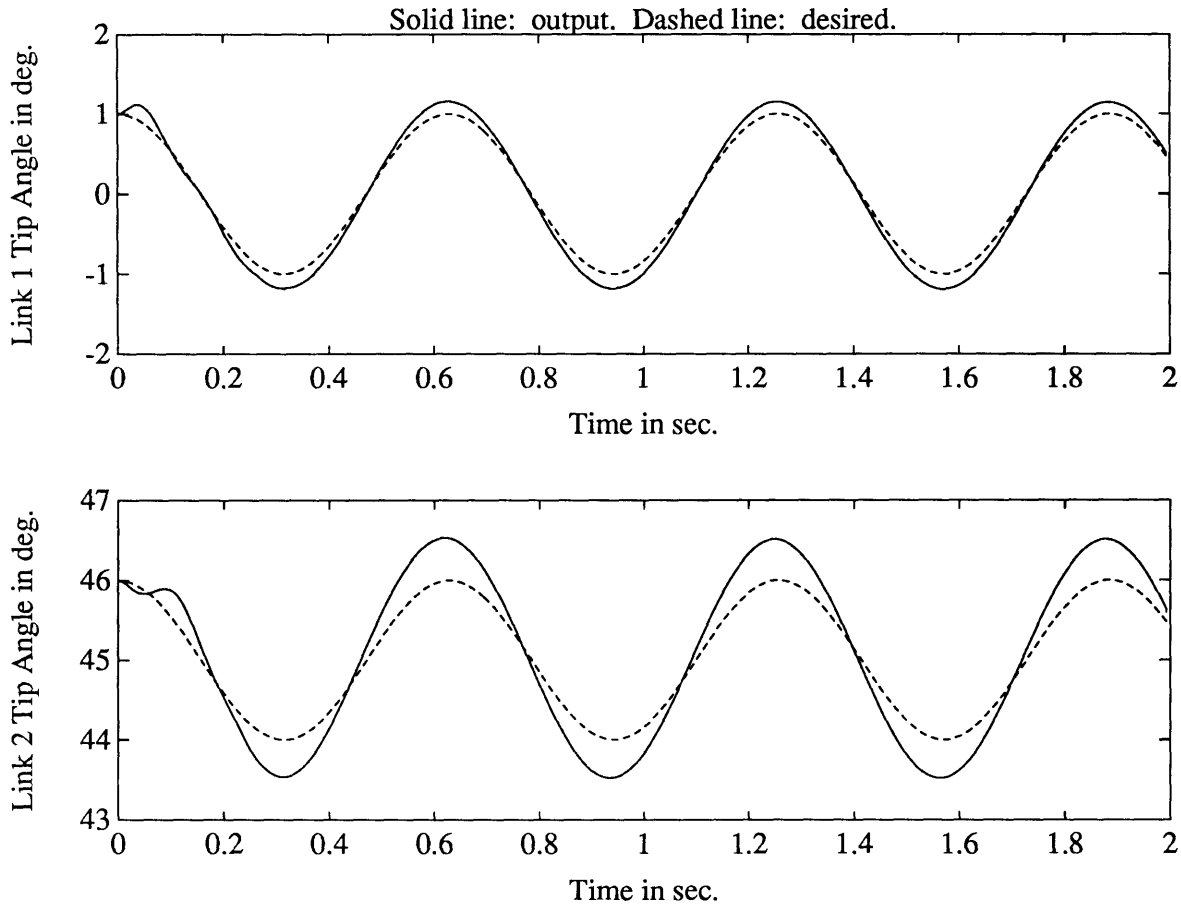


Figure 7.14: Sinusoidal Output Disturbance: $\mu = 1 \times 10^{-4}$.

the use of practical “fixes” to account for model uncertainty, neglected dynamics, etc. In particular, the feedback design question has been left open in the above developments. By using full state feedback LQR-based controllers we have avoided considerations of output feedback and estimators. Because the nonlinear output regulation theory also solves the output error feedback regulator problem, there is no difficulty in considering controllers that do not assume full state feedback. Furthermore, any feedback controller that locally exponentially stabilizes the system can be used in the feedback part of our composite controller. This means that controllers designed to take into account parameter uncertainty, disturbance rejection, or any other relevant considerations can be used as long as they exponentially stabilize the linearized system.

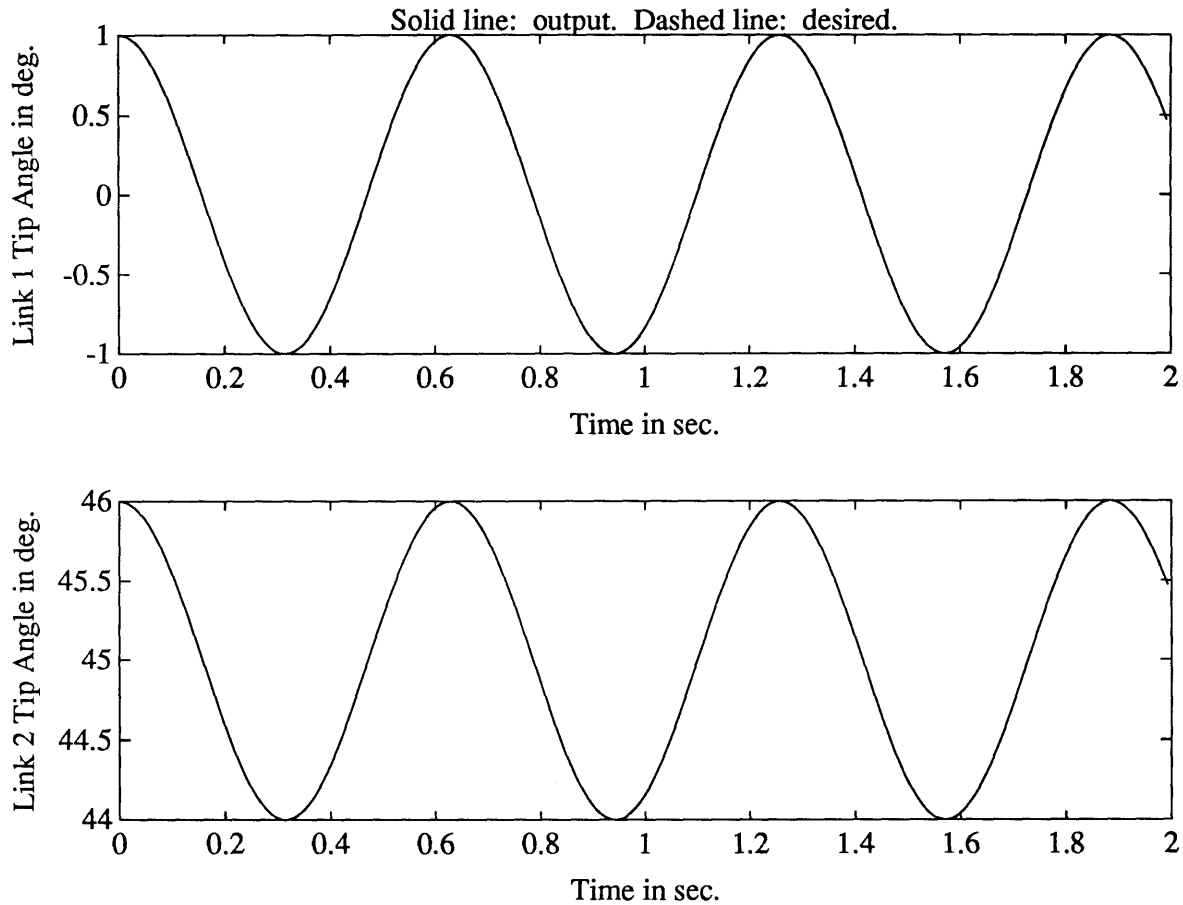


Figure 7.15: Open Loop Sinusoidal Output Disturbance: $\mu = 1 \times 10^{-4}$.

The same considerations apply to the feedforward part of the composite control. For example, pre-filters can be used to smoothen the command signal into the plant so as not to excite higher unmodelled modes that have not been taken into account in the solution of the nonlinear output regulation equations.

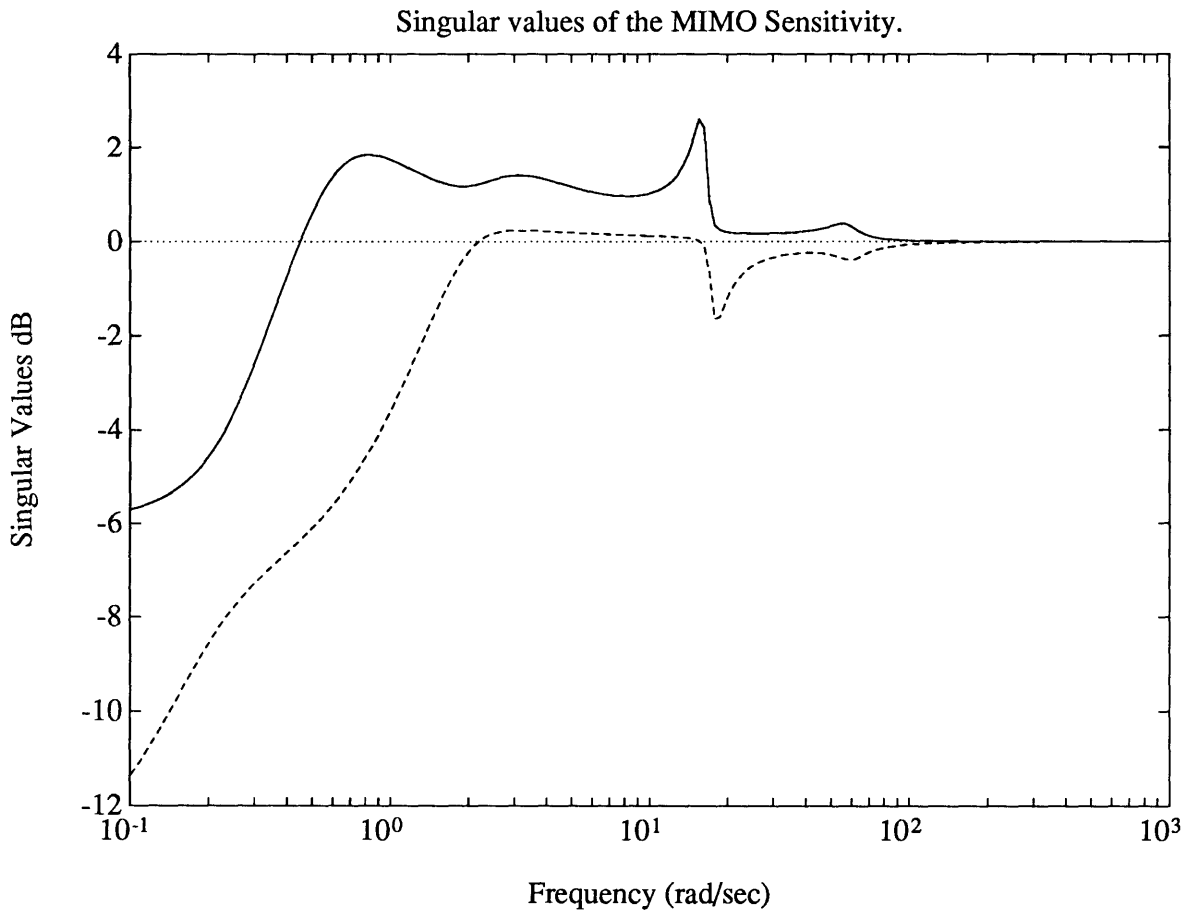


Figure 7.16: MIMO Sensitivity Plot: $\mu = 1 \times 10^{-2}$.

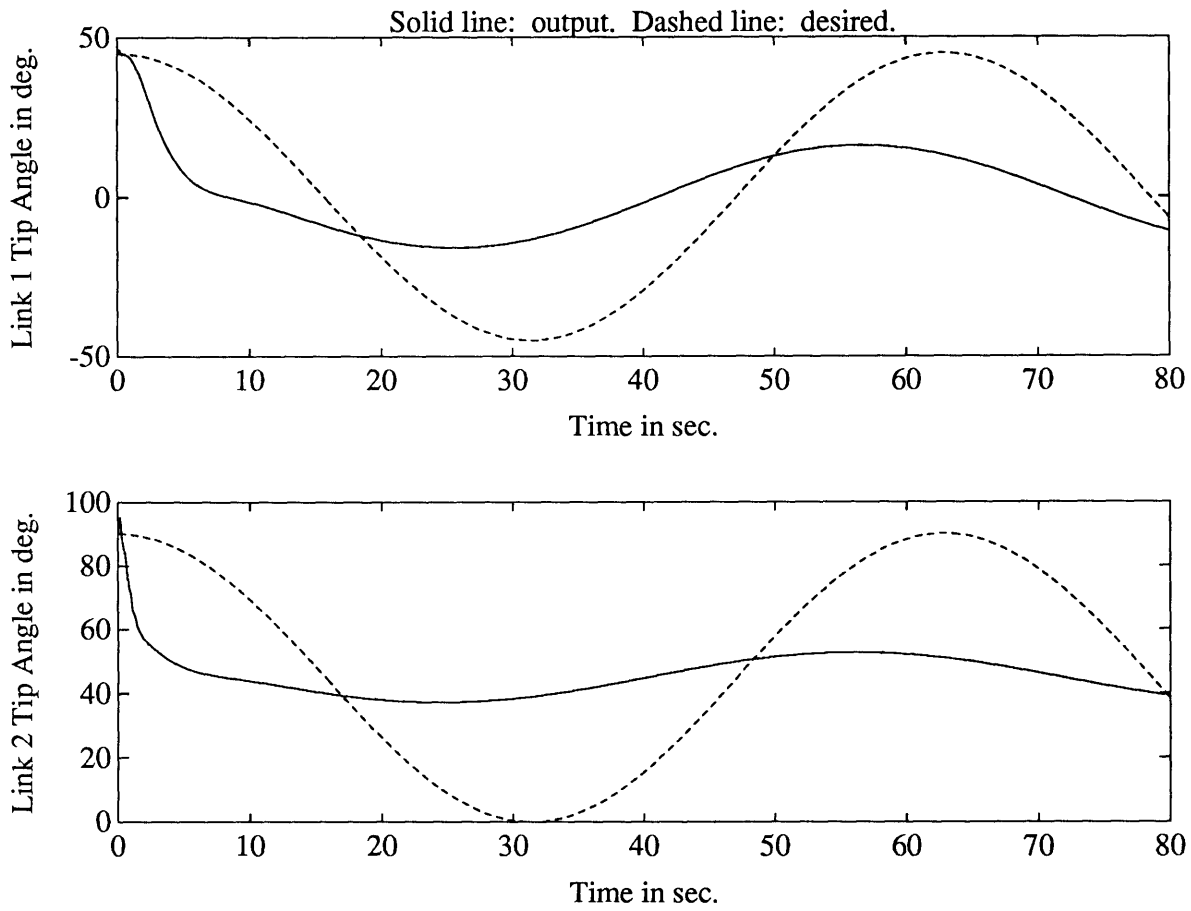


Figure 7.17: Sinusoidal Output Disturbance: $\mu = 1 \times 10^{-2}$.

Chapter 8

Conclusions

The objective of this thesis has been to investigate the fundamental principles and tradeoffs involved in the control of flexible manipulators. In the process, we have succeeded in bringing flexible manipulator control within the grasp of the classical theories for an important class of systems in which flexible deformations remain small. We have endeavored to marry theory and practice. In particular, we wanted to address both achievable performance and the extension of robust control designs for rigid manipulators to flexible link manipulator systems.

In pursuance of this program, in early chapters we presented the dynamics of the systems under consideration in both “exact” infinite dimensional representation and approximate finite dimensional form. A form of the partial differential equations of motion was presented which included the effects of foreshortening and which to the author’s knowledge have not been presented in the literature before.

It is well documented in the literature that linear systems of the type under consideration, specifically, links modelled using beam theory where actuator and sensors are non-collocated, exhibit nonminimum phase behavior. For this reason, and from a practical standpoint, we investigated the nature of linear nonminimum phase systems in depth. The main result is that the achievable performance due to the benefits of feedback control is severely and fundamentally limited by the nonminimum phase character of a system. We then proceeded to point out the extension to a nonlinear setting of the concept of a nonminimum phase system through the definition of zero

dynamics. It is one of the most important contributions of this work that we have extended the fundamental limits of performance due to nonminimum phase nature of a system to the nonlinear setting through the use of a *transient performance measure* that we have defined using center manifold theory and within the context of nonlinear output regulation theory.

Within the nonlinear output regulator theory, we have further clarified the distinction between steady state and transient performance and have brought these useful concepts from the linear realm to the fully nonlinear setting. In the sense that the identified performance measure is locally defined we see that the limits of performance of nonlinear nonminimum phase systems are fundamental, since an asymptotically stable system will eventually reach any neighborhood of the equilibrium point. While the development of a performance measure was carried out for finite dimensional systems, it can easily be extended to certain useful infinite dimensional systems. The extension is made trivial by the fact that center manifold theory applies to the same class of infinite dimensional systems. It is a further contribution of this work that as a result of the definition of a performance measure, the concept of local results is quantitatively defined.

It also becomes clear from the definitions of our performance measure that transient performance depends largely on the feedback portion of the controller, while steady state performance is driven mostly by the feedforward control. In Chapter 4 we investigated the state of the art in inverse dynamics and feedforward control for manipulators with flexibility. Inverse dynamics control, which results in the computed torques of rigid link robots, is impossible for flexible link manipulators when the outputs of interest are the tip (angular) positions. This is due to the nonminimum phase character of the system which results in unstable zero dynamics which in turn locally characterize the unobservable dynamics in the inverted system. When carried out with joint angles as outputs, the inverse dynamics algorithm yields a stable internal dynamics. Because our performance variables are still the tip (angular) positions, this inverse has value only in a stabilization role, and as such represents a particularly complicated and computationally taxing full state feedback stabilizer.

Of the feedforward schemes presented in the literature, some of which exhibit feedback to varying degrees through, for example, partial joint I/O linearizations, the most noteworthy from a practical viewpoint are those that involve simplifying assumptions on the dynamics equations. Other than that, most are found to be not as effective as control schemes because they require the forcing of certain variables to follow a trajectory while trying to coerce others to, e.g., decay to zero. When more actuators are allowed into the problem (such as the tip torques of section 5.3.2) this can be achieved. For the systems under consideration, however, this results in degraded performance to a degree that is not even quantifiable.

A notable exception is the nonlinear output regulation theory, within which our performance measure was defined. In this theory, only the desired performance variables are forced to follow the desired trajectory. Because this is implemented as a feedforward control, we circumvent the problems due to unstable zero dynamics. Furthermore, part of the solution to the regulator problem is the so-called steady state manifold, which in effect is a determination of what all the states want to do if the outputs follow the desired trajectory. Using results from center manifold theory, it is shown that any feedback controller that exponentially stabilizes the system will have its state converging to the steady state manifold. Thus steady state performance is achieved, while benefits of feedback including robustness and performance issues are neatly relegated to the choice of feedback control for the original system with the feedforward disconnected.

It is one of the main conclusions of this thesis that nonlinear output regulation should be heralded as the “computed torques” approach for flexible manipulators, without the problems associated with the full state feedback inversion. The thesis concludes with such an implementation on a two link manipulator where from the practical standpoint we consider simplifications to the nonlinear output regulation equation solutions based on sound engineering judgement. It is concluded that linearized equations yield very effective feedforward control even when high frequency end-point trajectories are commanded. This bespeaks the robustness of the scheme and its usefulness as a practical control scheme.

In the implementation of the nonlinear output regulation controller, the choice feedback controller remains an open question. In Chapter 6 we considered the extension to flexible links of classical feedback controller for rigid links, and analyzed robustness, globality, and practical implementation issues. Most of the results were presented for the one link arm, and where possible infinite dimensional equations were used to obviate the problem of spillover due to truncation. Suggestions for the extension of results to multiple links were presented.

One of the main theoretical contributions in this chapter is the proof of the global asymptotic stability of the nonlinear one-flexible-link arm under the action of joint PD controllers. This intuitive result has been bandied about in the literature but no proofs for the infinite dimensional, nonlinear equations have been presented. The main difficulty arises from the fact that for dynamical systems in infinite dimensional spaces LaSalle's invariance theorem does not hold in general. This is circumvented by the use of a more general invariance principle due to Hale, and the Sobolev imbedding theorems. The proof does not require structural damping to be present, thanks to the fact that all system modes are observable at the hub.

The major practical contributions in this chapter arise from the investigation of the tradeoff between globally stable, robust controllers, such as the joint PD, and the locally defined, higher performance full state feedback controllers, which are shown to locally induce exponential stability.

As mentioned earlier in this conclusion, the developments of all previous chapters are brought to bear in the final chapter where a two link flexible manipulator is controlled in simulation. In the first part of the chapter, a nonlinear output regulation-based controller was implemented. For the solution of the feedforward control we used two simplified models of the equations of motion: linearized about the equilibrium configuration of interest; and nonlinear in rigid body states but linear in flexible deformation states (i.e., *ruthlessly linearized*). For the feedback control we used a simple independent joint PD control and an LQR-based controller obtained using the system's linearization about equilibrium. As expected, transient performance is better with the LQR than with the PD controller.

Using the LQR-based controller, we obtain excellent tracking results when implementing the nonlinear output regulation control for a desired sinusoidal output trajectory. For both low and high frequency sinusoids, the linear solution to the regulator equations is shown to yield excellent results, thus showing not only robustness of the controller, but also suggesting that for certain maneuvers the system is nearly linear, while for still others, even a roughly determined feedforward control signal goes a long way towards increasing system performance. We notice that throughout we are limited to mild enough maneuvers (in terms of the amplitudes of the motions) so that the flexible deflections remain small.

In the last part of the chapter, we return to an investigation of limits to the achievable benefits of feedback (i.e., performance measure). Here we demonstrated that for the class of manipulators under consideration, the frequency domain limits of performance of linear nonminimum phase systems carry over as well into the feedback control of flexible manipulators. By studying the MIMO sensitivity of the system linearized about equilibrium, we correctly predict how output disturbances to the nonlinear system are rejected at low frequencies and magnified near crossover. Considering this sensitivity transfer function as a measure of sensitivity to small parameter variations, in analogy to the linear case, we propose that, at least locally, appropriate conclusions about the robustness of feedback schemes for nonlinear systems can be inferred as well.

8.1 Recommendations for Future Work

Much remains to be done in the theoretical arena when considering continuum models of chains of flexible bodies. Besides formally extending the results presented in this thesis to the multiple link case, it remains to extend passivity results to even the one-link case. In particular, it appears that proving the global stability of passive feedback controllers that measure the joint angle and angular rates and derive a torque command should be a relatively straightforward endeavor.

Of more practical interest is the derivation of rate of decay estimates when using

a passive controller at the joint and when material damping is assumed. Also of great interest is studying what is possible with distributed actuators and sensors such as piezoelectric films. If full actuation is achievable in this way, it might be possible to extend feedback input-output linearization schemes to the flexible link case. This would open the way for adaptive controllers of the type used for rigid robots.

The development of a transient *performance measure* for nonlinear systems brought into evidence how the ultimate performance limits are determined by the system linearization. This prompted the conjecture that a similar phenomenon would be true in the frequency domain. While simulation results presented in this thesis seem to support this conjecture, it remains to be shown analytically that this is indeed the case. While this task promises to be very mathematically involved, it could nonetheless result in some precious insights into the frequency domain nature of nonlinear systems and could possibly be the gateway to practical nonlinear feedback control synthesis.

An area of much practical importance is the selection of system mode shapes for the spatial discretization of nonlinear continuum models. The field of component mode synthesis offers some promise in this respect. The work of Oakley [64] presents some guidelines that seem to be sufficient for local maneuvers about equilibrium, and which we have independently and implicitly adopted in this work.

Finally, the use of feedforward controllers derived from simplified versions of the equations of motion should be investigated from the practical controls point of view. The results presented in previous chapters concerning the nonlinear output regulation theory and the use of very simple models suggest the advantages of such an approach. In particular, it would be useful to derive guidelines in terms of allowable maneuvers that would help in the selection of the simplest model that would yield desired results for various accuracy requirements.

Appendix A

Some Results from Center Manifold Theory

In this Appendix we summarize the relevant results from the Center Manifold Theory. These results are taken from the book by Carr [20] and from the Appendix in the paper by Isidori and Byrnes [44].

A.1 Preliminaries

Definition A.1 *Given a nonlinear system of the form*

$$\dot{x} = f(x) \tag{A.1}$$

where f is a C^r , $r \geq 2$, vector field defined on an open subset U of \mathbb{R}^n , a C^r submanifold S of U is said to be a locally invariant manifold for Eq. A.1 if for $x_0 \in S$, the solution $x(t)$ of Eq. A.1 with $x(0) = x_0$ is in S for $|t| < T, T > 0$. If it is always possible to choose $T = \infty$, then we say that S is an invariant manifold.

Let $x = 0$ be an equilibrium point of Eq. A.1 ($f(0) = 0$), and denote by

$$F = \left[\frac{\partial f}{\partial x} \right]_{x=0}$$

the Jacobian matrix of f in Eq. A.1 at $x = 0$. It is possible to decompose the domain of the linear mapping F into the direct sum of three invariant subspaces, denoted

E^0, E^-, E^+ , whose dimensions (n^0, n^-, n^+) correspond to the number of eigenvalues of F with zero, negative, and positive real parts, respectively. If we now view F as the differential of the nonlinear mapping $f : x \in U \rightarrow f(x) \in R^n$ at $x = 0$, then its domain is the tangent space T_0U to U at $x = 0$, and the three subspaces defined above are subspaces of T_0U satisfying

$$T_0U = E^0 \oplus E^- \oplus E^+.$$

Definition A.2 *Let $x = 0$ be an equilibrium of Eq. A.1. A manifold S , passing through $x = 0$, is said to be a center manifold for Eq. A.1 at $x = 0$, if it is locally invariant and the tangent space to S at 0 is exactly E^0 .*

Consider the system

$$\dot{x} = Ax + f(x, y) \tag{A.2}$$

$$\dot{y} = By + g(x, y) \tag{A.3}$$

where $x \in R^n, y \in R^m$ and A and B are constant matrices such that all the eigenvalues of A have zero real parts while all the eigenvalues of B have negative real parts. The functions f and g are $C^r, r \geq 2$, with $f(0, 0) = 0, f'(0, 0) = 0, g(0, 0) = 0, g'(0, 0) = 0$, and f' represents the Jacobian matrix of f .

Notice that if we consider F as above, i.e., as the Jacobian of f in Eq. A.1 at $x = 0$, and if F has no positive eigenvalues, then it is possible to choose coordinates in U such that the system of Eq. A.1 can be represented in the form of Eqs. A.2–A.3.

A.2 Existence of a Center Manifold

Theorem A.3 *There exist a neighborhood $V \subset R^{n^0}$ of $x = 0$ and a C^{r-1} mapping $\pi : V \rightarrow R^{n^-}$ such that*

$$S = \{(x, y) \in V \times (R^{n^-})\} : y = \pi(x)$$

is a center manifold for the system of Eqs. A.2–A.3.

By definition, a center manifold for the system of Eqs. A.2–A.3 passes through the origin and is tangent to the subset of points whose y coordinate is equal to zero, such that

$$\pi(0) = 0, \quad \frac{\partial \pi}{\partial x}(0) = 0. \quad (\text{A.4})$$

Because the center manifold is also locally invariant for Eqs. A.2–A.3, the mapping π must satisfy the constraint

$$\frac{\partial \pi}{\partial x}(Ax + f(x, \pi(x))) = B\pi(x) + g(x, \pi(x)) \quad (\text{A.5})$$

Equations A.4 and A.5 together show that a center manifold for Eqs. A.3–A.3 can be described as the graph of a mapping $y = \pi(x)$ satisfying the partial differential equation A.5 subject to the constraints specified by Eq. A.4.

A center manifold is not necessarily unique. Further, even if f and g are C^∞ functions, π is only guaranteed to be C^k , $k \geq 2$.

A.3 Stability of the Center Manifold

The prove of existence of the center manifold (see [20]) is carried out for a modified set of equations that is identical with Eqs. A.2–A.3 in a neighborhood of the origin. Let $\psi : \mathbb{R}^n \rightarrow [0, 1]$ be a C^∞ function with $\psi(x) = 1$ when $\|x\| \leq 1$ and $\psi(x) = 0$ when $\|x\| \geq 2$. For $\epsilon > 0$ define F and G by

$$F(x, y) = f(x\psi\left(\frac{x}{\epsilon}\right), y), \quad G(x, y) = g(x\psi\left(\frac{x}{\epsilon}\right), y).$$

Notice that the cut-off function ψ is only a function of x . This is so because*

... the proof of the existence of a centre manifold generalizes in an obvious way to infinite dimensional problems.

With the above definitions, the following equations denote a system which is identical to that of Eqs. A.2–A.3 in a neighborhood of the origin:

$$\dot{x} = Ax + F(x, y) \quad (\text{A.6})$$

$$\dot{y} = By + G(x, y). \quad (\text{A.7})$$

*J.Carr, *Applications of Centre Manifold Theory*, Springer-Verlag, 1981, p. 17.

Lemma A.4 *Let $(x(t), y(t))$ be a solution of Eqs. A.6–A.7 with $\|(x(0), y(0))\|$ sufficiently small. Then there exist positive constants C_1 and μ such that*

$$\|y(t) - \pi(x(t))\| \leq C_1 e^{-\mu t} \|y(0) - \pi(x(0))\|$$

for all $t \geq 0$.

The proof of this lemma is detailed in section 5.2.1.

A.4 Reduction Principle

The results summarized in this section allow us to relate the asymptotic behavior of small solutions of Eqs. A.2–A.3 to solutions of the n-dimensional system

$$\dot{u} = Au + f(u, \pi(u)) \tag{A.8}$$

which governs the flow on the center manifold.

Theorem A.5 a *Suppose that the zero solution of Eq. A.8 is (asymptotically) stable (unstable). Then the zero solution of Eqs. A.2–A.3 is (asymptotically) stable (unstable).*

b *Suppose that the zero solution of Eqs. A.2–A.3 is stable. Let $(x(t), y(t))$ be a solution of Eqs. A.2–A.3 with $(x(0), y(0))$ sufficiently small. Then there exists a solution $u(t)$ of Eq. A.8 such that as $t \rightarrow \infty$,*

$$x(t) = u(t) + O(e^{-\gamma t}) \tag{A.9}$$

$$y(t) = h(u(t)) + O(e^{-\gamma t}) \tag{A.10}$$

where $\gamma > 0$ is a constant depending on B .

A.5 Approximation of the Center Manifold

We note that in general the solution of Eqs. A.4–A.5 for the center manifold is as difficult as solving the original system equations, Eqs. A.2–A.3. Because of this,

the following result has profound consequences for the applicability of the nonlinear regulator theory presented in Chapter 5. It shows that the center manifold can be approximated to any degree of accuracy.

For functions $\phi : R^n \rightarrow R^m$ which are C^1 in a neighborhood of the origin define

$$(M\phi)(x) = \phi'(x)[Ax + f(x, \phi(x))] - B\phi(x) - g(x, \phi(x)).$$

Theorem A.6 *Suppose that $\phi(0) = 0$, $\phi'(0) = 0$ and that $(M\phi)(x) = O(\|x\|^q)$ as $x \rightarrow 0$ where $q > 1$. Then as $x \rightarrow 0$,*

$$\|\pi(x) - \phi(x)\| = O(\|x\|^q).$$

Appendix B

Gronwall's Inequality

Also called the Bellman-Gronwall Inequality (see Ref. [90]).

Theorem B.1 *Suppose $c \geq 0$, $r(\cdot)$ and $k(\cdot)$ are nonnegative valued continuous functions. Let*

$$r(t) \leq c + \int_0^t k(\tau)r(\tau)d\tau, \quad \forall t \in [0, T].$$

Then

$$r(t) \leq c \exp \left[\int_0^t k(\tau)d\tau \right], \quad \forall t \in [0, T]$$

Appendix C

Cantilevered-Loaded Mode Shapes

In this Appendix we derive the natural (unforced) vibration mode shapes for a cantilevered beam loaded with a tip mass and inertia (see Fig. C.1). The center of mass of the tip body is offset from the end of the link by a distance a measured along the undeformed neutral axis of the beam.

Assuming a Bernoulli-Euler beam, the equation for the transverse motion of the beam is given by the partial differential equation

$$\rho \ddot{\eta}_y(x, t) + EI \eta_y''''(x, t) = 0 \quad (\text{C.1})$$

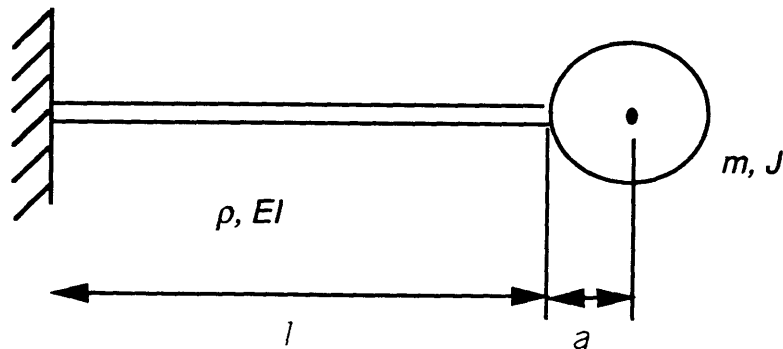


Figure C.1: Cantilevered-Loaded Beam

with the geometric boundary conditions

$$\eta_{\mathbf{y}}(0, t) = 0$$

$$\eta'_{\mathbf{y}}(0, t) = 0$$

and the natural boundary conditions

$$V(l) = m\ddot{\eta}_{\mathbf{y}}(l, t) + ma\ddot{\eta}'_{\mathbf{y}}(l, t)$$

$$M(l) = -ma\ddot{\eta}_{\mathbf{y}}(l, t) - (J + ma^2)\ddot{\eta}'_{\mathbf{y}}(l, t).$$

Using the separation of variables principle, assume a solution of the form $\eta_{\mathbf{y}}(x, t) = \phi(x)q(t)$. Then defining

$$\beta^4 = \frac{\rho\omega^2}{EI}$$

we obtain from Eq. C.1

$$\phi(x)'''' - \beta^4\phi(x) = 0 \tag{C.2}$$

$$\ddot{q}(t) + \omega^2q(t) = 0. \tag{C.3}$$

Solutions of Eq. C.2 are of the form

$$\phi(x) = A \sin(\beta x) + B \sinh(\beta x) + C \cos(\beta x) + D \cosh(\beta x) \tag{C.4}$$

where $\phi(x)$ must satisfy the boundary conditions

$$\phi(0) = 0$$

$$\phi'(0) = 0$$

$$EI\phi'''(l) + m\omega^2\phi(l) + ma\omega^2\phi'(l) = 0$$

$$EI\phi''(l) - ma\omega^2\phi(l) - (J + ma^2)\omega^2\phi'(l) = 0.$$

These boundary conditions form a set of linear equations that can be solved for the coefficients of Eq. C.4 as functions of $\lambda = \beta l$. The values of λ are determined by setting the determinant of the linear equations to be equal to zero. This yields a transcendental equation with a denumerable number of solutions.

To each solution λ_i corresponds a set of coefficients that determine the mode shape $\phi_i(x)$. These are determined only up to a multiplicative constant. These solutions to Eq. C.2 satisfy the orthogonality relation

$$\int_0^l \rho \phi_r(x) \phi_s(x) dx + m \phi_r(l) \phi_s(l) + ma[\phi_r'(l) \phi_s(l) + \phi_r(l) \phi_s'(l)] + (J + ma^2) \phi_r'(l) \phi_s'(l) = 0 \quad (r \neq s). \quad (\text{C.5})$$

If $r = s$ we normalize the mode shapes by equating the above expression to the total mass of the beam, i.e., $\rho l + m$.

C.1 Code Listing

In this section we list some Matlab [59] code that determines the values of λ and the mode shape coefficients for given beam and tip body parameters.

```

Program modes.m
%
% This program calculates the frequencies and modal shapes
% for a cantilever beam with a payload on the end by assuming
% a beam shape of the form:
% phi(x) = A sin(beta*x) + B sinh(beta*x) + C cos(beta*x) + D cosh(beta*x)
% applying boundary conditions to "y" to get four equations with unknowns
% A, B, C, and D, then using a root solver to find the appropriate
% lambda = beta*lb which causes the determinant of the 4x4 to be zero.
%
% Reset variables.
%
%
% User inputs.
%
mb = input('enter mass of beam (kg): ');
lb = input('enter length of beam (m): ');
ei = input('enter stiffness of beam (Nm^2): ');
mp = input('enter payload mass (kg): ');
ip = input('enter payload inertia (kgm^2): ');
a = input('enter payload offset from beam tip (m): ');
nmode = input('enter number of modes to be calculated (<=10): ');
init = input('enter initial guesses for lambda (0 - default): ');
%
% Initial guesses for lambda.
%
```

```

if init == 0,
    lam0 = 0;
    lamin = [1 3 6 9 12 15 18 21 24 27];
else,
    lam0 = init;
    lamin = init;
end
rho = mb/lb;
itot = ip + mp*a*a;
mor = mp/rho;
ior = itot/rho;
maor = mp*a/rho;
mat = 0.*ones(2,2);
lam = 0.*ones(1,nmode);
om = 0.*ones(1,nmode);
coef = 0.*ones(4,nmode);
%
% Declaration of global variables.
%
global mor ior maor lb mat rho la abcd
%
fact = sqrt(ei/rho)/lb/lb;
%
% Solve for nmode modeshapes.
%
for i=1:nmode,
    lam(i) = fzero('zdet_cl',lam0);
%
% Check for a repeated root.
%
    if i>1,
        for j=i-1:-1:1,
            while abs(lam(i)-lam(j))<.1,
                lam0 = lam0+0.1
                lam(i) = fzero('zdet_cl',lam0);
            end
        end
        for j=1:i-1,
            while abs(lam(i)-lam(j))<.1,
                lam0 = lam0+0.5
                lam(i) = fzero('zdet_cl',lam0);
            end
        end
    end
end
om(i) = lam(i)*lam(i)*fact/2/pi;

```

```

% solve for un-normalized coefficients
c = -mat(1,1)/mat(1,2);
abcd = [1 -1 c -c]';
la = lam(i);
%
% calculate integrals:
%   intph2 = integral of phi(x)*phi(x)
%   intphi = integral of phi(x)
%   intxph = integral of x*phi(x)
%
[xout,yout] = ode45('intmod_cl',0,lb,[0 0 0],1e-6);
nptn=length(xout);
intph2(i,i)=yout(nptn,1);
iph(i) = yout(nptn,2);
ixph(i) = yout(nptn,3);
be = lam(i)/lb;
cl = cos(la); chl = cosh(la); sl = sin(la); shl = sinh(la);
phl(i) = abcd'*[sl shl cl chl]';
dphl(i) = be*abcd'*[cl chl -sl shl]';
phil=phl(i);
dphil=dphl(i);
%
% Normalize mode shapes so that first orthogonality relation is equal
% to the total mass.
%
mtot = mb + mp;
iphtot = intph2(i,i) + mp*phil*phil + 2*mp*a*dphil*phil + itot*dphil*dphil;
abig = sqrt(mtot/iphtot);
%
% Calculate normalized coefficients, and integrals.
%
coef(1:4,i) = abig*abcd;
intph2(i,i) = abig*abig*intph2(i,i);
iph(i) = abig*iph(i);
ixph(i) = abig*ixph(i);
phl(i) = abig*phl(i);
dphl(i) = abig*dphl(i);
end
%
% Calculate int(rho*phi(i)*phi(j)) from modal constants.
%
for i=1:nmode,
    for j=1:i-1,
        intph2(i,j)=-mp*phl(i)*phl(j);
        intph2(i,j)=intph2(i,j)-mp*a*(dphl(i)*phl(j)+phl(i)*dphl(j));
    end
end

```

```

        intph2(i,j)=intph2(i,j)-itot*dphl(i)*dphl(j);
        intph2(j,i)=intph2(i,j);
    end
end
%
% Calculate int(EI*ddphi(i)*ddphi(j)) from second orthog. relation.
%
for i=1:nmode,
    intei(i,i)=4*pi*pi*mtot*om(i)*om(i);
    for j=1:i-1,
        intei(i,j)=0;
        intei(j,i)=0;
    end
end
end

disp(' ')
disp('frequencies in Hz are: ');om
disp('lambdas are: ');lam
disp('hit ENTER to continue')
pause
disp(' ')
disp('the coefficients (transpose[ A(i) B(i) C(i) D(i) ]) for modes i=1,nmode are:
i = 0;
%
% calculate the mode shapes as a function of x/lb
%
for x = 0:.04:1,
    i = i + 1;
    bx = x*lam';
    phimat = [sin(bx) sinh(bx) cos(bx) cosh(bx)]';
    lam4 = [lam' lam' lam' lam']';
    phi(i,1:nmode) = sum(coef.*phimat);
    dphmat = lam4.*[cos(bx) cosh(bx) -sin(bx) sinh(bx)]';
    dphi(i,1:nmode) = sum(coef.*dphmat);
    xol(i) = x;
end
disp(' ')
disp('The mode shapes are contained in the matrix phi')
disp('versus the dimensionless position xol=x/lb')
disp('Hit ENTER for a plot of the mode shapes:')
pause
plot(xol,phi)
pause
disp(' ')
disp('The calculated variables are:')

```

```

disp('om: natural frequencies in Hz')
disp('lam: the lambdas')
disp('phi: the mode shapes as a function of xol=x/L')
disp('iph: the integral of rho*phi(i)')
disp('ixph: the integral of rho*x*phi(i)')
disp('intph2: the integral of rho*phi(i)*phi(j) for each mode')
disp('inteI: the integral of EI*ddphi(i)*ddphi(j)')
disp('coef: the coefficients of the mode shapes:')

function y=zdet(lam)
%
% This function is used by modes.m to calculate the determinant of
% the matrix of the modal coefficients.
%
s1 = sin(lam);
sh1 = sinh(lam);
c1 = cos(lam);
ch1 = cosh(lam);
be = lam/lb;
be2 = be*be;
be3 = be*be2;
m11 = -(c1+ch1)+mor*be*(s1-sh1)+maor*be2*(c1-ch1);
m12 = (s1-sh1)+mor*be*(c1-ch1)-maor*be2*(s1+sh1);
m21 = -(s1+sh1)-maor*be2*(s1-sh1)-ior*be3*(c1-ch1);
m22 = -(c1+ch1)-maor*be2*(c1-ch1)+ior*be3*(s1+sh1);
mat = [ m11 m12
        m21 m22 ];
y = det(mat);

function yp=intmod(x,y)
%
% This function is used in lmodes.m to compute the modal integrals
% needed for normalization of the mode shapes and for the two-link
% flexible arm simulation.
%
be = la/lb;
bx = be*x;
phi = abcd'*[sin(bx) sinh(bx) cos(bx) cosh(bx)]';
yp(1) = rho*phi*phi;
yp(2) = rho*phi;
yp(3) = rho*x*phi;
yp = yp';

```


Appendix D

Solution of the Nonlinear Regulator Equations via Polynomial Expansion

In this appendix we include a listing of the MATHEMATICA [95] code developed to solve the nonlinear regulator equations presented in Chapter 5. The equations are solved for the two-flexible link manipulator, assuming one mode per link, and assuming the exosystem generates two sinusoids of frequencies ω_1 and ω_2 that are to be tracked by the inboard and outboard link tip angles, respectively.

D.1 Code Listing

```
Case 1: Two-flexible link system
Share[]
<<simplify.m
Sinusoidal Exosystem.
Define pi2q. -- Note: I am assuming 1 mode per link for now.
Clear[a]
Clear[b]
comba1 = x_Integer a[m_]a[n_] -> a[m,n]
(x_Integer)*a[m_]a[n_] -> a[m, n]
(x_Integer) a[m_] a[n_] -> a[m, n]
comba2 = a[m_]a[n_] -> a[m,n]
```

```

a[m_]*a[n_] -> a[m, n]
combb = a[n_]a[n_] -> a[n, n]
a[n_]^2 -> a[n, n]
combc = x_Integer a[n_]a[r_, s_] -> a[n, r, s]
(x_Integer)*a[n_]a[r_, s_] -> a[n, r, s]
(x_Integer) a[n_] a[r_, s_] -> a[n, r, s]
combd = a[n_]^3 -> a[n, n, n]
a[n_]^3 -> a[n, n, n]
pi2q1 = a[1]w[1] + a[2]w[2] + a[3]w[3] + a[4]w[4];
pi2q2 = Expand[pi2q1^2] //. comba1;
pi2q2 = pi2q2 //. combb;
pi2q3 = Expand[pi2q1^3] //. combb;
pi2q3 = pi2q3 //. comba2;
pi2q3 = pi2q3 //. combc;
pi2q3 = pi2q3 //. combd;
pi2q = pi2q1 + pi2q2 + pi2q3;
pi2q = Collect[pi2q, {w[1], w[2], w[3], w[4]}];
Define pi2p.
comca1 = x_Integer b[m_]b[n_] -> b[m, n];
comca2 = b[m_]b[n_] -> b[m, n];
comcb = b[n_]b[n_] -> b[n, n];
comcc = x_Integer b[n_]b[r_, s_] -> b[n, r, s];

comcd = b[n_]^3 -> b[n, n, n];
pi2p1 = b[1]w[1] + b[2]w[2] + b[3]w[3] + b[4]w[4];
pi2p2 = Expand[pi2p1^2] //. comca1;
pi2p2 = pi2p2 //. comcb;
pi2p3 = Expand[pi2p1^3] //. comca2;
pi2p3 = pi2p3 //. comcb;
pi2p3 = pi2p3 //. comcc;
pi2p3 = pi2p3 //. comcd;
pi2p = pi2p1 + pi2p2 + pi2p3;
pi2p = Collect[pi2p, {w[1], w[2], w[3], w[4]}];
Determine pi4q and pi4p by doing partial differentiations.
pi4q = D[pi2q, w[1]]om[1]w[2] - D[pi2q, w[2]]om[1]w[1] +
      D[pi2q, w[3]]om[2]w[4] - D[pi2q, w[4]]om[2]w[3];
pi4p = D[pi2p, w[1]]om[1]w[2] - D[pi2p, w[2]]om[1]w[1] +
      D[pi2p, w[3]]om[2]w[4] - D[pi2p, w[4]]om[2]w[3];
pi4q1 = D[pi2q1, w[1]]om[1]w[2] - D[pi2q1, w[2]]om[1]w[1] +
      D[pi2q1, w[3]]om[2]w[4] - D[pi2q1, w[4]]om[2]w[3];
pi4p1 = D[pi2p1, w[1]]om[1]w[2] - D[pi2p1, w[2]]om[1]w[1] +
      D[pi2p1, w[3]]om[2]w[4] - D[pi2p1, w[4]]om[2]w[3];
pi4q2 = D[pi2q2, w[1]]om[1]w[2] - D[pi2q2, w[2]]om[1]w[1] +
      D[pi2q2, w[3]]om[2]w[4] - D[pi2q2, w[4]]om[2]w[3];
pi4p2 = D[pi2p2, w[1]]om[1]w[2] - D[pi2p2, w[2]]om[1]w[1] +

```

```

    D[pi2p2,w[3]]om[2]w[4] - D[pi2p2,w[4]]om[2]w[3];
pi4q3 = D[pi2q3,w[1]]om[1]w[2] - D[pi2q3,w[2]]om[1]w[1] +
    D[pi2q3,w[3]]om[2]w[4] - D[pi2q3,w[4]]om[2]w[3];
pi4p3 = D[pi2p3,w[1]]om[1]w[2] - D[pi2p3,w[2]]om[1]w[1] +
    D[pi2p3,w[3]]om[2]w[4] - D[pi2p3,w[4]]om[2]w[3];
pi4p = Collect[pi4p,{w[1],w[2],w[3],w[4]}];
Determine the coefficient for the left-hand side (lhs) equation.
-- Note: Now need to deal with matrices, and will need to approximate sine and cosine
phi = 1.138084;psi = 1.8963692;
C1 = {{phi,0},{0,psi}};
ang45 = 45*Pi/180 //N;
Expand sine and cosine:
beta1 = w[3]-psi pi2p1;
beta2 = -psi pi2p2;
sb = Sin[ang45] + Cos[ang45] (beta1 + beta2)
    - 0.5 Sin[ang45] (beta1^2);
cb = Cos[ang45] - Sin[ang45] (beta1 + beta2)
    - 0.5 Cos[ang45] (beta1^2);
Reevaluate M3 using numerical values from simulation: linearization about the origin
Matrix of constant terms in M3.
Mcons3 = {{10.746617, 5.0356943},{5.0356943, 4.9197}};
Matrix of coefficients of cos(beta) in M3.
Mcos3 = {{5.707913, 2.3992472},{2.3992472, 0}};
Matrix of coefficients of sin(beta) in M3.
Msin3 = {{0, 0},{0, 0}};
M3 = Mcons3 + cb*Mcos3 + sb*Msin3;
M3 = {{14.782721,6.7322182},{6.7322182,4.9197}}
{{14.782721, 6.7322182}, {6.7322182, 4.9197}}
{{14.782721, 6.7322182}, {6.7322182, 4.9197}}
Form and simplify products of the form: sine*q, cosine*q, sine*p. Use function: simplify
--Note: When using more than one mode per link, must remember that p and q appear
Reevaluate M2 using numerical values from simulation: linearization about the origin
Matrix of constant terms in M2.
Mcons2 = {{13.48022, 4.8215191},{4.4247123, 4.4247124}};
Matrix of coefficients of cos(beta) in M2.
Mcos2 = {{7.1952732, 2.5076853},{3.9407335, 0}};
Matrix of coefficients of sin(beta) in M2.
Msin2 = {{0, 0},{0, 0}};
M2 = Mcons2 + cb*Mcos2 + sb*Msin2;
M2 = {{18.568047,6.5947204},{7.2112318,4.4247124}}
{{18.568047, 6.5947204}, {7.2112318, 4.4247124}}
{{18.568047, 6.5947204}, {7.2112318, 4.4247124}}
Del = M3 - M2 . C1;
Del[[1,1]] = Collect[Del[[1,1]],[w[1],w[2],w[3],w[4]]];
Del110 = simplify[Del[[1,1]],0];

```

```

Del111 = simplify[Del[[1,1]]-Del110,1];
Del112 = simplify[Del[[1,1]]-Del111-Del110,2];
Del[[1,2]] = Collect[Del[[1,2]],{w[1],w[2],w[3],w[4]}];
Del120 = simplify[Del[[1,2]],0];
Del121 = simplify[Del[[1,2]]-Del120,1];
Del122 = simplify[Del[[1,2]]-Del121-Del120,2];
Del[[2,1]] = Collect[Del[[2,1]],{w[1],w[2],w[3],w[4]}];
Del210 = simplify[Del[[2,1]],0];
Del211 = simplify[Del[[2,1]]-Del210,1];
Del212 = simplify[Del[[2,1]]-Del211-Del210,2];
Del[[2,2]] = Collect[Del[[2,2]],{w[1],w[2],w[3],w[4]}];
Del220 = simplify[Del[[2,2]],0];
Del221 = simplify[Del[[2,2]]-Del220,1];
Del222 = simplify[Del[[2,2]]-Del221-Del220,2];
Complete lhs through partial differentiations and matrix multiplication.
Determine values of frequency of forcing.
om[1] = 1;
om[2] = 1;
lhs1 = {D[pi4q1,w[1]]om[1]w[2] - D[pi4q1,w[2]]om[1]w[1] +
        D[pi4q1,w[3]]om[2]w[4] - D[pi4q1,w[4]]om[2]w[3],
        D[pi4p1,w[1]]om[1]w[2] - D[pi4p1,w[2]]om[1]w[1] +
        D[pi4p1,w[3]]om[2]w[4] - D[pi4p1,w[4]]om[2]w[3]};
lhs2 = {D[pi4q2,w[1]]om[1]w[2] - D[pi4q2,w[2]]om[1]w[1] +
        D[pi4q2,w[3]]om[2]w[4] - D[pi4q2,w[4]]om[2]w[3],
        D[pi4p2,w[1]]om[1]w[2] - D[pi4p2,w[2]]om[1]w[1] +
        D[pi4p2,w[3]]om[2]w[4] - D[pi4p2,w[4]]om[2]w[3]};
lhs3 = {D[pi4q3,w[1]]om[1]w[2] - D[pi4q3,w[2]]om[1]w[1] +
        D[pi4q3,w[3]]om[2]w[4] - D[pi4q3,w[4]]om[2]w[3],
        D[pi4p3,w[1]]om[1]w[2] - D[pi4p3,w[2]]om[1]w[1] +
        D[pi4p3,w[3]]om[2]w[4] - D[pi4p3,w[4]]om[2]w[3]};
lhs11 = Del110 (lhs1[[1]]+lhs2[[1]]+lhs3[[1]]) +
        Del111 (lhs1[[1]]+lhs2[[1]]) +
        Del112 lhs1[[1]];
lhs12 = Del120 (lhs1[[2]]+lhs2[[2]]+lhs3[[2]]) +
        Del121 (lhs1[[2]]+lhs2[[2]]) +
        Del122 lhs1[[2]];
lhs21 = Del210 (lhs1[[1]]+lhs2[[1]]+lhs3[[1]]) +
        Del211 (lhs1[[1]]+lhs2[[1]]) +
        Del212 lhs1[[1]];
lhs22 = Del220 (lhs1[[2]]+lhs2[[2]]+lhs3[[2]]) +
        Del221 (lhs1[[2]]+lhs2[[2]]) +
        Del222 lhs1[[2]];
lhs1 = lhs11 + lhs12;
lhs2 = lhs21 + lhs22;
Determine now the coefficients of the right-hand side (rhs).

```

```

Kee = {{228.43573,0},{0,79.889449}};
Dee = {{0.99094121,0},{0,0.39650075}};
nomb1 = om[1] w[2] - phi pi4q1 +
        om[2] w[4] - psi pi4p1;
nomb2 = -phi pi4q2 -psi pi4p2;
nomb21 = 0;
nomb22 = nomb1^2;
nomb23 = 2 nomb1 nomb2;
nombt2 = nomb21 + nomb22 + nomb23;
ome1 = om[1] w[2] - phi pi4q1;
ome2 = -phi pi4q2;
ome21 = 0;
ome22 = ome1^2;
ome23 = 2 ome1 ome2;
omet2 = ome21 + ome22 + ome23;
Ceeom = (1.2840395 10^-11 + 9.0647807 10^-17 cb
        + -4.6875879 sb);
Ceenom = (-1.7478598 10^-8
        + 1.7478598 10^-8 cb + 2.5076853 sb);
Ceetom = -3.9407335 sb;
Cee10 = simplify[Ceeom,0];
Cee11 = simplify[Ceeom-Cee10,1];
Cee12 = simplify[Ceeom-Cee11-Cee10,2];
Cee20 = simplify[Ceenom,0];
Cee21 = simplify[Ceenom-Cee20,1];
Cee22 = simplify[Ceenom-Cee21-Cee20,2];
Cee30 = simplify[Ceetom,0];
Cee31 = simplify[Ceetom-Cee30,1];
Cee32 = simplify[Ceetom-Cee31-Cee30,2];
Ceet1 = Cee10 omet2 + Cee11 (ome21 + ome22)
        Cee12 ome21 + Cee20 nombt2 + Cee21 (nomb21
        + nomb22) + Cee22 nomb21;
Ceet2 = Cee30 omet2 + Cee31 (ome21 + ome22)
        Cee32 ome21;
rhs = Kee . {pi2q,pi2p} + Dee . {pi4q,pi4p} -
        {Ceet1,Ceet2} +
        M2 . {-om[1]^2 w[1],-om[2]^2 w[3]};
rhs1 = rhs[[1]];
rhs2 = rhs[[2]];
sol1 = lhs1 + rhs1;
sol2 = lhs2 + rhs2;
Skip to second order terms.
sol1 = Collect[sol1,{w[1],w[2],w[3],w[4]};
sol2 = Collect[sol2,{w[1],w[2],w[3],w[4]};
lq1 = Coefficient[sol1,w[1]];

```

```

lq1 = Coefficient[lq1,w[2],0];
lq1 = Coefficient[lq1,w[3],0];
lq1 = Coefficient[lq1,w[4],0];
lq2 = Coefficient[sol1,w[2]];
lq2 = Coefficient[lq2,w[1],0];
lq2 = Coefficient[lq2,w[3],0];
lq2 = Coefficient[lq2,w[4],0];
lq3 = Coefficient[sol1,w[3]];
lq3 = Coefficient[lq3,w[1],0];
lq3 = Coefficient[lq3,w[2],0];
lq3 = Coefficient[lq3,w[4],0];
lq4 = Coefficient[sol1,w[4]];
lq4 = Coefficient[lq4,w[1],0];
lq4 = Coefficient[lq4,w[2],0];
lq4 = Coefficient[lq4,w[3],0];
lp1 = Coefficient[sol2,w[1]];
lp1 = Coefficient[lp1,w[2],0];
lp1 = Coefficient[lp1,w[3],0];
lp1 = Coefficient[lp1,w[4],0];
lp2 = Coefficient[sol2,w[2]];
lp2 = Coefficient[lp2,w[1],0];
lp2 = Coefficient[lp2,w[3],0];
lp2 = Coefficient[lp2,w[4],0];
lp3 = Coefficient[sol2,w[3]];
lp3 = Coefficient[lp3,w[1],0];
lp3 = Coefficient[lp3,w[2],0];
lp3 = Coefficient[lp3,w[4],0];
lp4 = Coefficient[sol2,w[4]];
lp4 = Coefficient[lp4,w[1],0];
lp4 = Coefficient[lp4,w[2],0];
lp4 = Coefficient[lp4,w[3],0];
ar1 = Solve[{lq1==0,lq2==0,lq3==0,lq4==0,lp1==0,lp2==0,lp3==0,lp4==0},
            {a[1],a[2],a[3],a[4],b[1],b[2],b[3],b[4]}]
ar1s=ar1[[1]];
Now solve for second order term coefficients.
sol1 = sol1 /. ar1s;
sol1 = Collect[sol1,{w[1],w[2],w[3],w[4]}];
lq11 = Coefficient[sol1,w[1],2];
lq11 = Coefficient[lq11,w[2],0];
lq11 = Coefficient[lq11,w[3],0];
lq11 = Coefficient[lq11,w[4],0];
lq22 = Coefficient[sol1,w[2],2];
lq22 = Coefficient[lq22,w[1],0];
lq22 = Coefficient[lq22,w[3],0];
lq22 = Coefficient[lq22,w[4],0];

```

```

lq33 = Coefficient[sol1,w[3],2];
lq33 = Coefficient[lq33,w[2],0];
lq33 = Coefficient[lq33,w[1],0];
lq33 = Coefficient[lq33,w[4],0];
lq44 = Coefficient[sol1,w[4],2];
lq44 = Coefficient[lq44,w[2],0];
lq44 = Coefficient[lq44,w[3],0];
lq44 = Coefficient[lq44,w[1],0];
lq12 = Coefficient[sol1,w[1]w[2]];
lq12 = Coefficient[lq12,w[3],0];
lq12 = Coefficient[lq12,w[4],0];
lq13 = Coefficient[sol1,w[1]w[3]];
lq13 = Coefficient[lq13,w[2],0];
lq13 = Coefficient[lq13,w[4],0];
lq14 = Coefficient[sol1,w[1]w[4]];
lq14 = Coefficient[lq14,w[3],0];
lq14 = Coefficient[lq14,w[2],0];
lq23 = Coefficient[sol1,w[2]w[3]];
lq23 = Coefficient[lq23,w[1],0];
lq23 = Coefficient[lq23,w[4],0];
lq34 = Coefficient[sol1,w[3]w[4]];
lq34 = Coefficient[lq34,w[1],0];
lq34 = Coefficient[lq34,w[2],0];
lq24 = Coefficient[sol1,w[2]w[4]];
lq24 = Coefficient[lq24,w[1],0];
lq24 = Coefficient[lq24,w[3],0];
sol2 = sol2 /. ar1s;
sol2 = Collect[sol2,{w[1],w[2],w[3],w[4]}];
lp11 = Coefficient[sol2,w[1],2];
lp11 = Coefficient[lp11,w[2],0];
lp11 = Coefficient[lp11,w[3],0];
lp11 = Coefficient[lp11,w[4],0];
lp22 = Coefficient[sol2,w[2],2];
lp22 = Coefficient[lp22,w[1],0];
lp22 = Coefficient[lp22,w[3],0];
lp22 = Coefficient[lp22,w[4],0];
lp33 = Coefficient[sol2,w[3],2];
lp33 = Coefficient[lp33,w[2],0];
lp33 = Coefficient[lp33,w[1],0];
lp33 = Coefficient[lp33,w[4],0];
lp44 = Coefficient[sol2,w[4],2];
lp44 = Coefficient[lp44,w[2],0];
lp44 = Coefficient[lp44,w[3],0];
lp44 = Coefficient[lp44,w[1],0];
lp12 = Coefficient[sol2,w[1]w[2]];

```

```

lp12 = Coefficient[lp12,w[3],0];
lp12 = Coefficient[lp12,w[4],0];
lp13 = Coefficient[sol2,w[1]w[3]];
lp13 = Coefficient[lp13,w[2],0];
lp13 = Coefficient[lp13,w[4],0];
lp14 = Coefficient[sol2,w[1]w[4]];
lp14 = Coefficient[lp14,w[3],0];
lp14 = Coefficient[lp14,w[2],0];
lp23 = Coefficient[sol2,w[2]w[3]];
lp23 = Coefficient[lp23,w[1],0];
lp23 = Coefficient[lp23,w[4],0];
lp34 = Coefficient[sol2,w[3]w[4]];
lp34 = Coefficient[lp34,w[1],0];
lp34 = Coefficient[lp34,w[2],0];
lp24 = Coefficient[sol2,w[2]w[4]];
lp24 = Coefficient[lp24,w[1],0];
lp24 = Coefficient[lp24,w[3],0];
ar2 = Solve[{lq11==0,lq22==0,lq33==0,lq44==0,lq12==0,lq13==0,lq14==0,
  lq23==0,lq34==0,lq24==0,lp11==0,lp22==0,lp33==0,lp44==0,
  lp12==0,lp13==0,lp14==0,lp23==0,lp34==0,lp24==0},
  {a[1,1],a[2,2],a[3,3],a[4,4],a[1,2],a[1,3],a[1,4],a[2,3],
  a[3,4],a[2,4],b[1,1],b[2,2],b[3,3],b[4,4],b[1,2],b[1,3],
  b[1,4],b[2,3],b[3,4],b[2,4]}]

```

Finally, third order terms.

```

ar2s = ar2[[1]];
sol1 = sol1 /. ar2s;
lq111 = Coefficient[sol1,w[1],3];
lq222 = Coefficient[sol1,w[2],3];
lq333 = Coefficient[sol1,w[3],3];
lq444 = Coefficient[sol1,w[4],3];
lq112 = Coefficient[sol1,w[1]^2 w[2]];
lq122 = Coefficient[sol1,w[1] w[2]^2];
lq113 = Coefficient[sol1,w[1]^2 w[3]];
lq133 = Coefficient[sol1,w[1] w[3]^2];
lq114 = Coefficient[sol1,w[1]^2 w[4]];
lq144 = Coefficient[sol1,w[4]^2 w[1]];
lq123 = Coefficient[sol1,w[1] w[2] w[3]];
lq124 = Coefficient[sol1,w[1] w[2] w[4]];
lq134 = Coefficient[sol1,w[1] w[3] w[4]];
lq223 = Coefficient[sol1,w[2]^2 w[3]];
lq224 = Coefficient[sol1,w[2]^2 w[4]];
lq233 = Coefficient[sol1,w[3]^2 w[2]];
lq234 = Coefficient[sol1,w[2] w[3] w[4]];
lq244 = Coefficient[sol1,w[4]^2 w[2]];
lq334 = Coefficient[sol1,w[3]^2 w[4]];

```



```

lq344 = Coefficient[sol1,w[4]^2 w[3]];
sol2 = sol2 /. ar2s;
lp111 = Coefficient[sol2,w[1],3];
lp222 = Coefficient[sol2,w[2],3];
lp333 = Coefficient[sol2,w[3],3];
lp444 = Coefficient[sol2,w[4],3];
lp112 = Coefficient[sol2,w[1]^2 w[2]];
lp122 = Coefficient[sol2,w[1] w[2]^2];
lp113 = Coefficient[sol2,w[1]^2 w[3]];
lp133 = Coefficient[sol2,w[1] w[3]^2];
lp114 = Coefficient[sol2,w[1]^2 w[4]];
lp144 = Coefficient[sol2,w[4]^2 w[1]];
lp123 = Coefficient[sol2,w[1] w[2] w[3]];
lp124 = Coefficient[sol2,w[1] w[2] w[4]];
lp134 = Coefficient[sol2,w[1] w[3] w[4]];
lp223 = Coefficient[sol2,w[2]^2 w[3]];
lq224 = Coefficient[sol2,w[2]^2 w[4]];
lp233 = Coefficient[sol2,w[3]^2 w[2]];
lp234 = Coefficient[sol2,w[2] w[3] w[4]];
lp244 = Coefficient[sol2,w[4]^2 w[2]];
lp334 = Coefficient[sol2,w[3]^2 w[4]];
lp344 = Coefficient[sol2,w[4]^2 w[3]];
bigeq1 = {lq111,lq222,lq333,lq444,lq112,lq122,lq113,
          lq133,lq114,lq144,lq123,lq124,lq134,lq223,
          lq224,lq233,lq234,lq244,lq334,lq344};
ar31 = Solve[bigeq1 == {0,0,0,0,0,0,0,0,0,0,0,0,0,0,0,
                       0,0,0,0,0,0},{a[1,1,1],a[2,2,2],a[3,3,3],a[4,4,4],a[2,1,1],
                       a[1,2,2],a[3,1,1],
                       a[1,3,3],a[4,1,1],a[1,4,4],a[3,1,2],a[4,1,2],a[4,1,3],a[3,2,2],
                       a[4,2,2],a[2,3,3],a[4,2,3],a[2,4,4],a[4,3,3],a[3,4,4]}}];
ar31s = ar31[[1]]
bigeq2 = {lp111,lp222,
          lp333,lp444,lp112,lp122,lp113,
          lp133,lp114,lp144,lp123,lp124,lp134,lp223,
          lp224,lp233,lp234,lp244,lp334,lp344} /. ar31s;
ar32 = Solve[bigeq2 == {0,0,0,0,0,0,0,0,0,0,0,0,0,0,0,
                       0,0,0,0,0,0},{b[1,1,1],
                       b[2,2,2],b[3,3,3],b[4,4,4],b[2,1,1],b[1,2,2],b[3,1,1],
                       b[1,3,3],b[4,1,1],b[1,4,4],b[3,1,2],b[4,1,2],b[4,1,3],b[3,2,2],
                       b[4,2,2],b[2,3,3],b[4,2,3],b[2,4,4],b[4,3,3],b[3,4,4]}}];
ar32s=ar32[[1]]

simplify[expr_,o_] :=
  Block[{i, j, rest = 0, count1, test, next, e, t0, f = 100},
    test = Expand[expr];

```

```
count1 = Length[test]; Print[count1];
Do[
  t0 = test[[i]];
  Do[
    e[j] = Exponent[t0, w[j]],
    {j,4}];
  next = If[Sum[e[n], {n,4}] > 0, 0, t0];
  rest = rest + next;
  If[i == f, Print[i]; f = f + 100],
  {i, count1}]; Print[Length[rest]]; Return[rest]]
```

References

- [1] R. A. Adams. *Sobolev Spaces*. Academic Press, New York, 1975.
- [2] H. Asada and Z.-D. Ma. Inverse dynamics of flexible robots. *Transactions of the ASME Journal of Dynamic Systems, Measurement and Control*, 1989.
- [3] H. Asada, Z.-D. Ma, and H. Tokumaru. Inverse dynamics of flexible robot arms for trajectory control. In *Proceedings of the 1987 ASME Winter Annual Meeting, Modeling and Control of Robotic Manipulators and Manufacturing Processes*, pages 329–336, 1987.
- [4] C. D. Bailey. A new look at Hamilton’s principle. *Foundations of Physics*, 5(3):433–451, September 1975.
- [5] A. V. Balakrishnan. *Applied Functional Analysis*. Springer-Verlag, New York, 1976.
- [6] A. V. Balakrishnan. Compensator design for stability enhancement with collocated controllers. *IEEE Transactions on Automatic Control*, 36(9):994–1007, September 1991.
- [7] E. Barbieri. On transfer functions and control of a flexible slewing link. In *Proceedings of the 1991 American Control Conference*, pages 1431–1432, Piscataway, NJ, June 1991. IEEE, Institute of Electrical and Electronics Engineers.
- [8] E. Bayo. A finite-element approach to control the end-point motion of a single-link flexible robot. *Journal of Robotic Systems*, 4(1):63–75, 1987.
- [9] E. Bayo. Computed torque for the position control of open-chain flexible robots. In *Proceedings of the 1988 IEEE International Conference on Robotics and Automation*, pages 316–321, Philadelphia, PA, April 1988.
- [10] E. Bayo, R. Movaghar, and M. Medus. Inverse dynamics of a single-link flexible robot. analytical and experimental results. *International Journal of Robotics and Automation*, 3(3):150–157, 1988.
- [11] E. Bayo, P. Papadopoulos, J. Stubbe, and M. A. Serna. Inverse dynamics and kinematics of multi-link elastic robots: An iterative frequency domain approach. *The International Journal of Robotics Research*, 8(6):49–62, 1989.

- [12] L. Bers, F. John, and M. Schechter. *Partial Differential Equations*, volume 3 of *Lectures in Applied Mathematics*. Wiley (Interscience), New York, 1964.
- [13] S. P. Bhattacharyya and J. B. Pearson. On error systems and the servomechanism problem. *International Journal of Control*, 15(6):1041–1062, 1972.
- [14] H. W. Bode. *Network Analysis and Feedback Amplifier Design*. D. Van Nostrand Company, Inc., Princeton, New Jersey, December 1959.
- [15] S. Boyd and C. A. Desoer. Subharmonic functions and performance bounds on linear time-invariant feedback systems. *IMA Journal of Mathematical Control and Information*, 2:153–170, 1985.
- [16] C. I. Byrnes and A. Isidori. Local stabilization of minimum-phase nonlinear systems. *Systems and Control Letters*, 11:9–17, 1988.
- [17] C. I. Byrnes and A. Isidori. Passivity, feedback equivalence, and the global stabilization of minimum phase nonlinear systems. *IEEE Transactions on Automatic Control*, 36(11):1228–1240, November 1991.
- [18] F. M. Callier and C. A. Desoer. Stabilization, tracking, and disturbance rejection in multivariable convolution systems. *Annale de la Societ e Scientifique de Bruxelles*, 94:7–51, 1980.
- [19] R. H. Cannon and E. Schmitz. Initial experiments on the end-point control of a one link experimental manipulator. *International Journal of Robotics Research*, 3(3), 1984.
- [20] J. Carr. *Applications of Centre Manifold Theory*, volume 35 of *Applied Mathematical Sciences*. Springer-Verlag, New York, 1981.
- [21] V. H. L. Cheng and C. A. Desoer. Limitations on the closed-loop transfer function due to right-half plane transmission zeros of the plant. *IEEE Transactions on Automatic Control*, AC-25(6):1218–1220, December 1980.
- [22] R. V. Churchill and J. W. Brown. *Complex Variables and Applications*. McGraw-Hill Book Company, New York, fourth edition, 1984.
- [23] S. A. Collins, D. W. Miller, and A. H. von Flotow. Distributed sensors as spatial filters in active structural control. Submitted to the *Journal of Sound and Vibration*, November 1991.
- [24] C. M. Dafermos and W. J. Hrusa. Energy methods for quasilinear hyperbolic initial-boundary value problems. Applications to elastodynamics. In C. M. Dafermos, D. D. Joseph, and F. M. Leslie, editors, *The Breadth and Depth of Continuum Mechanics*, pages 609–634. Springer-Verlag, Berlin, 1986.
- [25] E. J. Davison and S. H. Wang. Properties and calculation of transmission zeros of linear multivariable systems. *Automatica*, 10:643–658, 1974.

- [26] A. De Luca. Nonlinear regulation of robot motion. Communicated by J. T. Wen, January 1992.
- [27] A. De Luca, L. Lanari, and G. Ulivi. Output regulation of a flexible robot arm. In A. Bensoussan and J. L. Lions, editors, *Analysis and Optimization of Systems, Proceedings of the 9th International Conference, Antibes*, pages 833–842, Berlin, June 12–15 1990. INRIA, Springer-Verlag.
- [28] C. A. Desoer and M. Vidyasagar. *Feedback Systems: Input/Output Properties*. Academic Press, New York, 1975.
- [29] H. Elmali and N. Olgac. Robust output tracking of nonlinear mimo systems via sliding mode technique. In *Proceedings of the 1991 American Control Conference*, pages 56–57, Boston, MA, May 1991. IEEE, Institute of Electrical and Electronics Engineers.
- [30] F. M. Fleming and E. F. Crawley. The zeroes of controlled structures: Sensor/actuator attributes and structural modelling. In *Proceedings of the Structures, Structural Dynamics, and Materials Conference*, pages 1806–1816. AIAA/ASME/ASCE/ASC, April 1991.
- [31] B. A. Francis. The linear multivariable regulator problem. *SIAM Journal of Control and Optimization*, 15(3):486–505, May 1977.
- [32] B. A. Francis and W. M. Wonham. The internal model principle for linear multivariable regulators. *Journal of Applied Mathematics and Optimization*, 2:170–194, 1975.
- [33] J. S. Freudenberg and D. P. Looze. Right half plane poles and zeros and design tradeoffs in feedback systems. *IEEE Transactions on Automatic Control*, AC-30(6):555–565, June 1985.
- [34] B. Gebler. Feed-forward control strategy for an industrial robot with elastic links and joints, 1987.
- [35] W. Hahn. *Stability of Motion*, volume 138 of *Die Grundlehren der mathematischen Wissenschaften in Einzeldarstellungen*. Springer-Verlag, New York, 1967.
- [36] J. K. Hale. Dynamical systems and stability. *Journal of Mathematical Analysis and Applications*, 26:39–59, 1969.
- [37] M. Hautus. Linear matrix equations with applications to the regulator problem. In I. D. Landau, editor, *Outils et Modèles Mathématiques pour l'Automatique*, pages 399–412. C.N.R.S., Paris, 1983.
- [38] R. M. Hirschorn. Invertibility of multivariable nonlinear control systems. *IEEE Transactions on Automatic Control*, AC-24(6):855–865, December 1979.
- [39] R. M. Hirschorn. Output tracking in multivariable nonlinear systems. *IEEE Transactions on Automatic Control*, AC-26(2):593–595, April 1981.

- [40] M. G. Hollars. Experiments in end-point control of manipulators with elastic drives. SUDAAR 568, Stanford University Guidance and Control Laboratory, Stanford, California 94305, May 1988.
- [41] I. M. Horowitz. *Synthesis of Feedback Systems*. Academic Press, New York, 1963.
- [42] P. C. Hughes and G. B. Sincarsin. Dynamics of an elastic multibody chain: Part A—Body motion equations, and Part B—Global dynamics. *Dynamics and Stability of Systems*, 4(3 & 4):209–244, 1989.
- [43] A. Isidori. *Nonlinear Control Systems*. Springer-Verlag, Berlin, second edition, 1989.
- [44] A. Isidori and C. I. Byrnes. Output regulation of nonlinear systems. *IEEE Transactions on Automatic Control*, 35(2):131–140, February 1990.
- [45] A. Isidori and C. Moog. On the nonlinear equivalent of the notion of transmission zeros. In C. I. Byrnes and K. H. Kurzhanski, editors, *Modeling and Adaptive Control*. Springer-Verlag, 1987.
- [46] K. Jürgen Bathe. *Finite Element Procedures in Engineering Analysis*. Civil Engineering and Engineering Mechanics Series. Prentice-Hall, Inc., Englewood Cliffs, New Jersey 07632, 1982.
- [47] T. R. Kane and D. A. Levinson. *Dynamics: Theory and Applications*. McGraw-Hill, New York, 1985.
- [48] T. R. Kane, P. W. Likins, and D. A. Levinson. *Spacecraft Dynamics*. McGraw-Hill Book Company, New York, 1983.
- [49] T. R. Kane, R. R. Ryan, and A. K. Banerjee. Dynamics of a cantilever beam attached to a moving base. *AIAA Journal of Guidance, Control, and Dynamics*, 10(2):139–151, March-April 1987.
- [50] C. K. Kao and A. Sinha. Sliding mode control of vibration in flexible structures using estimated states. In *Proceedings of the 1991 American Control Conference*, pages 2467–2474, Boston, MA, May 1991. IEEE, Institute of Electrical and Electronics Engineers.
- [51] P. Kumar, P. Truss, and C. G. Wagner-Bartak. System design features of the space shuttle remote manipulator. In *Proceedings of the Fifth World Congress on Theory of Machines and Mechanisms*, pages 839–842. American Society of Mechanical Engineers, 1979.
- [52] H. Kwakernaak and R. Sivan. *Linear Optimal Control Systems*. Wiley-Interscience, a Division of John Wiley & Sons, Inc., New York, 1972.
- [53] L. Lanari and J. Wen. A family of asymptotically stable control laws for flexible robots based on a passivity approach. CIRSSE 85, Rensselaer Polytechnic Institute, February 1991.

- [54] J. P. LaSalle. Stability theory for ordinary differential equations. *Journal of Differential Equations*, 4:57–65, 1968.
- [55] R. Lozano-Leal and B. Brogliato. Adaptive control of robot manipulators with flexible joints. In *Proceedings of the 1991 American Control Conference*, pages 938–943, Boston, MA, May 1991. IEEE, Institute of Electrical and Electronics Engineers.
- [56] A. D. Luca. Dynamic control of robots with joint elasticity. In *Proceedings of the IEEE International Conference on Robotics and Automation*, pages 152–158, Philadelphia, PA, April 1988.
- [57] D. G. Luenberger. *Optimization by Vector Space Methods*. Decision and Control. John Wiley & Sons, Inc., New York, 1969.
- [58] S. K. Madhavan and S. N. Singh. Inverse trajectory control and zero dynamics sensitivity of an elastic manipulator. In *Proceedings of the 1991 American Control Conference*, pages 1879–1884, Piscataway, NJ, June 1991. Institute of Electrical and Electronics Engineers.
- [59] The MathWorks, Inc., 21 Eliot Street, South Natick, MA 01760. *PRO-MATLAB for Sun Workstations*, January 1990.
- [60] L. Meirovitch. *Analytical Methods in Vibrations*. Macmillan Publishing Co., Inc., New York, 1967.
- [61] K. A. Morris and M. Vidyasagar. A comparison of different models for beam vibrations from the standpoint of control design. *Transactions of the ASME Journal of Dynamic Systems, Measurement, and Control*, 112:349–356, September 1990.
- [62] H. C. Moulin, E. Bayo, and B. Paden. Existence and uniqueness of solutions of the inverse dynamics of multi-link flexible arms. to appear in *Journal of Robotic Systems*.
- [63] P. K. Nguyen, R. Ravindran, R. Carr, and D. M. Gossain. Structural flexibility of the shuttle remote manipulator system mechanical arm. In *Proceedings of the AIAA Guidance, Navigation, and Control Conference*, pages 246–256, San Diego, California, August 1982. AIAA.
- [64] C. M. Oakley. Experiments in modelling and end-point control of two-link flexible manipulators. SUDAAR 603, Stanford University Guidance and Control Laboratory, Stanford, California 94305, April 1991.
- [65] C. M. Oakley and J. Robert H. Cannon. Theory and experiments in selecting mode shapes for two-link flexible manipulators. In *First International Symposium on Experimental Robotics*, Montréal, Canada, June 1989.

- [66] K. Ogata. *Modern Control Engineering*. Prentice-Hall, Inc., Englewood Cliffs, New Jersey, 1970.
- [67] B. Paden, B. Riedle, and E. Bayo. Exponentially stable tracking control for multi-joint flexible-link manipulators. In *Proceedings of the 1990 American Control Conference*, pages 680–684, Piscataway, NJ, May 1990. Institute of Electrical and Electronics Engineers.
- [68] C. E. Padilla and A. H. von Flotow. Nonlinear strain-displacement relations in the dynamics of a two-link flexible manipulator. Space Systems Laboratory Report 6-89, Massachusetts Institute of Technology, Cambridge, Massachusetts 02139, May 1989.
- [69] C. E. Padilla and A. H. von Flotow. Sdm 91 paper. *sdm*, April 1991.
- [70] C. E. Padilla and A. H. von Flotow. Jgcd 2. *AIAA Journal of Guidance, Control, and Dynamics*, March-April 1992.
- [71] C. E. Padilla and A. H. von Flotow. Nonlinear strain-displacement relations and flexible multibody dynamics. *AIAA Journal of Guidance, Control, and Dynamics*, 15(1):128–136, January-February 1992.
- [72] J.-H. Park and H. Asada. Dynamic analysis of noncollocated flexible arms and design of torque transmission mechanisms. In *Proceedings of the 1991 American Control Conference*, pages 1885–1890, Boston, MA, May 1991. IEEE, Institute of Electrical and Electronics Engineers.
- [73] L. A. Pars. *A Treatise on Analytical Dynamics*. Ox Bow Press, Woodbridge, Connecticut 06525, 1979. Reprint. First published 1965.
- [74] R. Ravindran and R. H. Doetsen. Design aspects of the shuttle remote manipulator control. In *Proceedings of the AIAA Guidance, Navigation, and Control Conference*, pages 456–465, San Diego, California, August 1982. AIAA.
- [75] A. A. Rogdriguez and M. A. Dahleh. Wiener-hopf control of stable infinite dimensional systems. In *Proceedings of the 1991 American Control Conference*, pages 2160–2165, Boston, MA, May 1991. IEEE, Institute of Electrical and Electronics Engineers.
- [76] W. Rudin. *Functional Analysis*. Higher Mathematics. McGraw-Hill, New York, 1973.
- [77] M. G. Safonov and M. Athans. Robustness and computational aspects of nonlinear stochastic estimators and regulators. *IEEE Transactions on Automatic Control*, AC-23(4):717–725, 1978.
- [78] E. Schmitz. Experiments on the end-point position control of a very flexible one-link manipulator. SUDAAR 548, Stanford University Guidance and Control Laboratory, Stanford, California 94305, June 1985.

- [79] B. Siciliano and W. J. Book. A singular perturbation approach to control of lightweight flexible manipulators. *The International Journal of Robotics Research*, 7(4):79–90, August 1988.
- [80] B. Siciliano, W. J. Book, and G. De Maria. An integral manifold approach to control of a one link flexible arm. In *Proceedings of the 25th Conference on Decision and Control*, pages 1131–1134, Athens, Greece, December 1986.
- [81] J. Slotine and W. Li. *Applied Nonlinear Control*. Prentice Hall, New Jersey, 1991.
- [82] S. L. Sobolev. *Some Applications of Functional Analysis in Mathematical Physics*, volume 90 of *Translations of Mathematical Monographs*. American Mathematical Society, Providence, Rhode Island, third edition, 1991.
- [83] V. A. Spector and H. Flashner. Modeling of non-collocated structural control systems. In *Proceedings of the AIAA Guidance, Navigation, and Control Conference*, pages 74–83, Minneapolis, Minnesota, August 15–17 1988. AIAA.
- [84] V. A. Spector and H. Flashner. Sensitivity of structural models for noncollocated control systems. *Transactions of the ASME Journal of Dynamic Systems, Measurement, and Control*, 111:646–655, December 1989.
- [85] V. A. Spector and H. Flashner. Modeling and design implications of noncollocated control in flexible systems. *Transactions of the ASME Journal of Dynamic Systems, Measurement, and Control*, 112:186–193, June 1990.
- [86] M. W. Spong, K. Khorasani, and P. V. Kokotovic. An integral manifold approach to the feedback control of flexible joint robots. *IEEE Journal of Robotics and Automation*, RA-4(4):291–300, August 1987.
- [87] S. P. Timoshenko, D. H. Young, and W. Weaver. *Vibration Problems in Engineering*. Wiley and Sons, New York, 4th edition, 1974.
- [88] M. Uchiyama and Z. H. Jiang. Compensability of end-effector position errors for flexible robot manipulators. In *Proceedings of the 1991 American Control Conference*, pages 1873–1878, Piscataway, NJ, June 1991. Institute of Electrical and Electronics Engineers.
- [89] C. R. Uhlik. Experiments in high-performance nonlinear and adaptive control of a two-link, flexible-drive-train manipulator. SUDAAR 592, Stanford University Guidance and Control Laboratory, Stanford, California 94305, May 1990.
- [90] M. Vidyasagar. *Nonlinear Systems Analysis*. Electrical Engineering Series. Prentice-Hall, Inc., Englewood Cliffs, New Jersey 07632, 1978.
- [91] M. Vidyasagar. System theory and robotics. *IEEE Control Systems Magazine*, pages 16–17, April 1987.

- [92] D. Wang and M. Vidyasagar. Transfer functions for a single flexible link. In *International Conference on Robotics and Automation*, pages 1042–1047, Piscataway, NJ, June 1989. IEEE, Institute of Electrical and Electronics Engineers.
- [93] J. T.-Y. Wen. Robustness analysis for evolution systems in hilbert space: A passivity approach. CIRSSE 13, Rensselaer Polytechnic Institute, Troy, New York 12180-3590, 1989.
- [94] T. Williams. Transmission zero bounds for large space structures, with applications. *AIAA Journal of Guidance, Control, and Dynamics*, 12(1):33–38, January-February 1989.
- [95] S. Wolfram. *Mathematica: A System for Doing Mathematics by Computer*. Addison-Wesley Publishing Company, Redwood City, CA, 1988.
- [96] W. M. Wonham. *Linear Multivariable Control: A Geometric Approach*. Springer-Verlag, New York, second edition, 1979.
- [97] P. C. Young and J. C. Willems. An approach to the linear multivariable servomechanism problem. *International Journal of Control*, 15(5):961–979, 1972.
- [98] V. I. Zubov. *Methods of A. M. Lyapunov and their Application*. P. Noordhoff Ltd., Groningen, The Netherlands, 1964.